Molecular Mechanisms Regulating Dendritic Spine Morphology

by

Lei Zhou

Department of Neurology and Neurosurgery
McGill University
Montreal, Quebec, Canada

August 2010

A thesis submitted to McGill University in partial fulfillment of the requirements of the degree of Doctor of Philosophy

Table of Contents

List of abbreviations

ADF	actin depolymerizing factor
AMPA	α-amino-3-hydroxy-5-methyl-4-isoxazolepropionic acid
AMPAR	AMPA receptor
ANOVA	analysis of variance
Arp2/3	actin-related protein 2 and 3
BDNF	brain derived neurotrophic factor
Cdk5	cyclin-dependent kinase 5
CAS	Crk-associated substrate
DAG	diacylglycerol
EGF	epidermal growth factor
EGFP-f	farnesylated enhanced green fluorescent protein
EM	electron microscopy
EPSCs	excitatory postsynaptic currents
F-actin	filamentous actin
FAK	focal adhesion kinase
FRET	fluorescent-resonance energy transfer
FRAP	fluorescence recovery after photobleaching
G-actin	globular actin
GABA	gamma-aminobutyric acid
GAP	GTPase activating protein
GEF	guanine nucleotide exchange factor
GFP	green fluorescent protein
GPI	glycosylphosphatidylinositol
GRIP	glutamate receptor-interacting protein
HAD	haloacid dehalogenase
IP_3	inositol 1,4,5-triphosphate
LK1	LIM-kinase 1

LK2	LIM-kinase 2
LRRs	leucine-rich repeats
LTD	long-term depression
LTP	long-term potentiation
NMDA	N-methyl-D-aspartate
NMDAR	NMDA receptor
PAK	p21-activated kinase
PDZ	PSD-95/Dlg/ZO-1
PH	pleckstrin-homology
PI3K	phosphatidylinositol 3-kinase
PICK1	protein interacting with C-kinase 1
PIP_2	phosphatidylinositol 4,5-bisphosphate
PKC	protein kinase C
PKD	protein kinase D
PLCγ1	phospholipase C gamma 1
PP2B	protein phosphatase 2B
PSD	postsynaptic density
PTPs	protein tyrosine phosphatases
Pyk2	proline-rich tyrosine kinase 2
RNAi	RNA interference
ROCK	Rho-associated kinase
RTK	receptor tyrosine kinase
SAM	sterile-α-motif
SER	smooth endoplasmic reticulum
SEM	serial electron microscopy
SH2	Src homology 2
SH3	Src homology 3
SSH	slingshot phosphatase
SFV	Semliki Forest Virus
SPAR	spine associated RapGAP
SynGAP	synaptic Ras GAP

TBS	theta-burst stimulation or Tris-buffered saline
TESKs	testicular protein kinases
TfR	transferring receptor
TRP	transient receptor potential

List of figures

Acknowledgements

I would like to give my greatest gratitude to my supervisor, Dr. Keith Murai, who has supported me throughout my graduate study with his knowledge and patience. I was fortunate enough to meet Keith when I first came to McGill University. He has taught me a lot for the past six years. Without his guidance and support, I would have never accomplished my graduate study and research.

I am also grateful to members of my advisory committee Drs. Salvatore Carbonetto, Alyson Fournier, and Yong Rao for their perceptive suggestions and valuable comments. Also thanks to Dr. Don van Meyel for helpful discussion.

I am lucky to have a chance to work with so many nice and smart people in the lab, who have helped to make the lab an excellent environment for research. Many thanks to Emma Jones, Denise Cook, Sabrina Chirezi, Yann Bernardinelli, William Todd Farmer, and Chris Salmon for their discussions, intelligent suggestions and unhesitant help in the lab. Also thanks to Alexandra Iliescu and Edith Hanna for lab assistance. I also want to thank people who have left the lab. Special thanks to Sarah Martinez, who has done tremendous and excellent work on the PLC project. Also to our "software expert", Dr. Mike Haber, for his great assistance on data analysis.

I also want to thank my friends outside the lab, Li Yu, Qiuxia Liang, Wentzu Chang, Lei Shi, Songting Cheng, who bring me so much fun outside work. Life is boring without you guys.

I am in debt to my parents for their endless care, help and support throughout my entire life. Also thanks to my husband, Xuxu Yan, who gives me one hundred percent support with whatever I want to do. Special thanks to my daughter, Avril Yan, who brings me a lot of joy.

Abstract

In the central nervous system, chemical synapses are highly specialized junctions that are known to be critical for communication between neurons. The ability of synapses to change their physiological and structural properties, known as synaptic plasticity, is important for storing information in neural connections. Dendritic spines are small protrusions on dendrites where the majority of glutamatergic synapses form in the brain. In general, a dendritic spine has an enlarged head region that is connected to the dendritic shaft by a narrow neck. This geometry allows spines to function as individual biochemical compartments and control postsynaptic signaling events. Recent evidence indicates that structural remodeling of spines and the formation of new synaptic contacts may lead to long-term changes in synaptic function including long-term potentiation (LTP) and long-term depression (LTD). These forms of synaptic plasticity are believed to contribute to cognitive processes such as learning and memory. Interestingly, the actin cytoskeleton is enriched in dendritic spines and its turnover contributes to spine shape and motility. A variety of signaling proteins associate with the actin cytoskeleton and are likely critical for controlling the morphological plasticity of spines. However, the molecular mechanisms that regulate actin-based spine dynamics remain unclear. My studies revealed novel pathways downstream of the EphA class of receptor tyrosine kinases that are important for regulating spine plasticity. I showed that PLCγ1 physically interacts with the EphA4 receptor tyrosine kinase and links EphA4 to the downstream actin depolymerizing/severing protein, cofilin. PLCγ1 signaling is critical for maintaining spine morphology and PLC activity is required for spine retraction caused by ephrin ligand binding to EphA4. Remarkably, the amount of cofilin associated with the cell membrane is regulated by PLC and EphA4 activity. Furthermore, I found that ephrin binding to EphA receptors cause the dephosphorylation and activation of cofilin through the phosphatases slingshot

(SSH) and calcineurin. Both of the phosphatases are needed for EphA-mediated reorganization of actin filaments and dendritic spine remodeling. These studies contribute new insight into the intricate signaling mechanisms downstream of EphA receptors that control the local remodeling of the actin cytoskeleton in dendritic spines and structural plasticity of excitatory synapses in the central nervous system.

Résumé

Les synapses chimiques sont des jonctions hautement spécialisées du système nerveux central ayant un rôle déterminant pour la communication entre les neurones. Ces dernières sont capables de changer leurs propriétés structurales et physiologiques. Ce phénomène, appelé la plasticité synaptique, est important pour le stockage de l'information. Les épines dendritiques sont de petites saillies sur les dendrites des neurones où la majorité des synapses glutamatergiques du cerveau se forment. De manière générale, une épine dendritique se compose d'une large tête connectée à l'arbre dendritique par une structure plus étroite appelée cou. Cette géométrie permet le fonctionnement des épines comme des compartiments biochimiques indépendant, pouvant ainsi contrôler les événements de transmission synaptique localement, soit au niveau postsynaptique. De récentes évidences expérimentales indiquent que les réarrangements structurels des épines et la formation de nouvelles synapses qui en découle pourraient induire des changements persistant du fonctionnement de la synapse. Ces changements sont de deux types : la potentialisation à long terme (PLT) et la dépression à long terme (DLT). Ce sont deux formes de plasticité synaptique connues pour contribuer aux processus cérébraux de la cognition tels que l'apprentissage et la mémoire. Il est intéressant de noter que le cytosquelette d'actine est très dense dans les épines dendritiques et que son turnover contribue à la morphologie ainsi qu'à la motilité de ces dernières. Une grande variété de protéines de signalisation sont connues pour s'associer avec le cytosquelette d'actine et ont donc probablement un rôle crucial pour le contrôle de la plasticité morphologique des épines. Néanmoins, les mécanismes moléculaires qui régulent la dynamique des épines basée sur le cytosquelette d'actine restent obscurs à ce jour. La présente étude révèle de nouvelles voies de signalisation moléculaire en aval de la classe EphA des récepteurs à la tyrosine kinase ayant un rôle dans la régulation de la plasticité des épines dendritiques. Cette étude montre que la PLCγ1 interagit physiquement

avec le récepteur EphA4 tyrosine kinase et relie, en aval, EphA4 à la cofiline, une protéine ayant un pouvoir polymérisant ou dépolymérisant sur les filaments d'actine. De plus, elle démontre que la PLCγ1 est essentielle pour le maintien de la morphologie des épines car la rétraction de celles-ci observée lors de la liaison de l'ephrine à son récepteur EphA4 nécessite une activité des PLC. La quantité de cofiline s'associant à la membrane cellulaire est apparue comme étant régulée de façon remarquable par l'activité de la PLC et du EphA4. Finalement, la démonstration que la liaison de l'ephrine à son récepteur EphA cause la déphosphorylation et l'activation de la cofiline par la phosphatase slingshot (SSH) et la calcineurine a été effectuée. Ces deux phosphatases sont apparues essentielles pour la réorganisation des filaments d'actines et des modifications morphologiques des épines dendritiques induites par EphA. Cette étude contribue donc à la compréhension des mécanismes de signalisation complexes prenant place en aval des récepteurs EphA lors des modifications structurales des épines observées lors des phénomènes de plasticité des synapses excitatrices du système nerveux central.

Chapter 1 Introduction

1.1 Purpose of the thesis

In the brain, neurons communicate through complex sites of interaction called synapses. A typical synapse is a structure composed of three main components: the presynaptic bouton, the synaptic cleft, and the postsynaptic terminal. Neurotransmitter is released from the presynaptic bouton and crosses the synaptic cleft to activate neurotransmitter receptors on the postsynaptic terminal. Interestingly, studies have shown that the postsynaptic terminal is not a static structure but can show remarkable structural plasticity in the developing and adult central nervous system. This has opened up an exciting and active area of research investigating how morphological changes at synapses may be related to information processing and storage in the brain.

Much research on this topic is focused on understanding how structural modifications in postsynaptic compartments of synapses, known as dendritic spines, relate to brain plasticity. Dendritic spines are micrometer-sized structures attached to the main dendritic shaft that are enriched with cell surface receptors, signaling proteins, and cytoskeletal elements. However, exactly how these molecules are networked together to regulate the properties of spines remains unclear. Understanding how cell surface receptors on spines transduce extracellular signals to alter spine morphology will likely offer insights into mechanisms underlying brain development, learning and memory, and neurological disorders.

This dissertation investigated the role of a specific family receptors (Eph receptors) and their downstream signaling pathways in regulating dendritic spine morphology. In the Chapter 1, I will review background literature related to the development and plasticity of dendritic spines. In Chapter 2, I will provide an overview of the molecular mechanisms of spine plasticity that are related to the studies in Chapters 3 and 4. Chapter 5 summarizes the thesis, suggests overall implications of the findings, and discusses potential future directions.

1.2 Models of Spinogenesis

There are several different models on the origin of dendritic spines (Ethell & Pasquale 2005). The first model is that spines form from dendritic filopodia. Filopodia are highly dynamic structures that rapidly extend and retract from dendrites, especially during early stages of brain development (Dailey & Smith 1996; Korkotian & Segal 2001). Live imaging of developing neurons in the hippocampus and neocortex has shown that many filopodia are replaced by dendritic spines, supporting the hypothesis that filopodia transform into spines (Dailey & Smith 1996; Maletic-Savatic et al 1999; Marrs et al 2001; Okabe et al 2001; Trachtenberg et al 2002). A more recent study using electron microscopy in the adult barrel cortex has shown that newly formed filopodial-type spines lack synapses. However, new protrusion that persists for several days form synapses on existing presynaptic boutons, suggesting that spines form before actual synapses have been established (Knott et al 2006). A second model suggests that spines arise from synapses that form on dendritic shafts (Miller & Peters 1981). This model arose because of the observation that the majority of synapses on 15-day-old hippocampal neurons are located on dendritic shafts (Harris et al 1992). Consistent with this, live imaging has recorded the emergence of mature spines from dendritic shaft synapses in hippocampal neurons (Dailey & Smith 1996; Marrs et al 2001). A combination of the first two models has also been suggested, where filopodia retract after contacting an axon. This generates a shaft synapses from which a dendritic spines arises (Fiala et al 1998; Marrs et al 2001). A final model is that spines form through an intrinsic mechanism in neurons and in the absence of axonal contact. Cerebellar Purkinje cells are known to form immature-looking spines prior to the establishment of contact with presynaptic parallel fibers from granule cells (Sotelo et al 1990; Takacs et al 1997). The models presented here are probably not mutually exclusive. Neuronal type and experimental context (i.e. brain region and developmental stage being analyzed) likely play a major role in determining the cellular events involved in dendritic spine formation.

1.3 Morphology of dendritic spines

More than a century ago, by using early light microscopic techniques, Ramon y Cajal discovered small thorn-like structures projecting from dendrites which he called “espinas” (Ramon y Cajal 1893). Later he described dendritic spines with different shapes and sizes. This discovery was confirmed by more modern-day studies with serial electron microscopy (SEM). Using SEM, Harris and colleagues have shown that dendritic spines have diverse morphologies even along the same dendrite, and especially across different neuron types in the brain (Bartlett & Banker 1984; Chicurel & Harris 1992; Harris & Stevens 1989). “Mushroom”, “stubby”, “thin”, and “branched” spines have been described based upon the size of their heads and degrees of constriction of the neck region (Harris et al 1992; Hayashi & Majewska 2005; Parnass et al 2000; Sorra & Harris 2000). In general, a “mushroom” spine is characterized by a large head that is connected to a narrow neck. “Thin” spines are similar to mushroom spines but have smaller heads. “Stubby” spines lack a constriction in the neck region. “Filopodia” are considered relatively long and thin spines without bulbous heads, representing a group of motile protrusions that may become spines or not and potentially serve as spine precursors. Consistent with this, filopodia-like spines are abundant in early development when synapses are formed (Hering & Sheng 2001; Zuo et al 2005). Although more rare, other types of spines including “branched” spines with two or more heads have also been described (Comery et al 1996). Some studies using *in vivo* repeated imaging techniques have supported the concept that spines initially grow as filopodia-like protrusions and progressively mature into mushroom-shaped spines (Knott et al 2006; Mattila & Lappalainen 2008).

1.4 Intracellular components of spines

The special architecture of spines enables them to compartmentalize biochemical signals at synapses. The dendritic spine neck, in particular, is an important barrier for small molecules and ions (such as calcium), preventing

unregulated dissipation from the spine head to the dendritic shafts (Hayashi & Majewska 2005; Kennedy & Ehlers 2006). The ability of spines to confine signals is believed to help store the activation history of synapses and allow for the expression of synaptic plasticity (Alvarez & Sabatini 2007; Bloodgood & Sabatini 2005; Kennedy & Ehlers 2006; Tada & Sheng 2006).

Inside a dendritic spine is a complex network of cytoskeleton and organelles (Spacek & Harris 1997). Actin serves as the primary structural scaffold of dendritic spines and provides a core for the assembly of many protein complexes at synapses. Smooth endoplasmic reticulum (SER) functions as an internal calcium store in some spines (Berridge 2002). More than 80% of large mushroom spines contain stacks of SER (Nimchinsky et al 2002; Spacek & Harris 1997), suggesting a function role of the SER in maintaining the function of mature synapses. Interestingly, less than 50% of small spines, regardless of age, contain SER, suggesting that other mechanisms (such as cytoplasmic buffers) regulate calcium fluxes within their small volumes (Spacek & Harris 1997). Polyribosomes have been found at the base of spines, suggesting local protein translation occurs near some synapses (Steward & Levy 1982). Local protein synthesis is believed to modify the protein composition at synapses, and contribute to processes such as long-term potentiation (LTP) consolidation (Bramham 2008).

1.5 Functional implications of spine remodeling

Accumulating evidence suggests a strong correlation between the size of the spine head and synaptic strength. Ultrastructural analysis has shown that the surface area of the postsynaptic density (PSD), which provides a structural framework for localizing neurotransmitter receptors and ion channels at synapses, correlates well with the volume of the spine head. Furthermore, PSD size is also directly proportion to the amount of AMPA-type glutamate receptors at synapses (Harris & Stevens 1989; Lisman & Harris 1993; Schikorski & Stevens 1997; Takumi et al 1999). Two-photon uncaging of glutamate at individual synapses further demonstrates that AMPA and NMDA receptor currents correlate linearly

with spine head size. Thus, larger spines pass more current after synaptic activation (Beique et al 2006; Matsuzaki et al 2001; Noguchi et al 2005). These studies show a close structure-function relationship at spines.

1.6 Spine remodeling

1.6.1 Spines in activity/experience-dependent plasticity *in vivo*

Dendritic spines are highly dynamic structures. Imaging studies on green fluorescent protein (GFP)-labelled neurons show that spines undergo various changes in shape, including elongation, 'morphing' of the head region, retraction, splitting and merging with other spines over several minutes (Dunaevsky et al 1999). The observed spine motility is highly dependent on the reorganization of actin content in spines as drugs that disrupt actin polymerization rapidly arrest spine motility (Fischer et al 1998). Interestingly, spines are highly motile during early development when new synapses are being formed and motility is reduced in mature neurons. However, a significant number of spines retain their ability to show dynamic changes over short time periods (Dunaevsky et al 1999; Lippman & Dunaevsky 2005).

Studies also show that dendritic spines undergo rapid and extensive changes in shape and number in response to environmental challenges such as sensory experience and learning (Bailey & Kandel 1993; Buonomano & Merzenich 1998; Trachtenberg et al 2002; Zuo et al 2005). Long-term repeated imaging studies using 2-photon microscopy in adult barrel cortex demonstrated that about 50% of spines of pyramidal neurons are stable, lasting over a month, whereas ~20% of spines undergo rapid turnover (Trachtenberg et al 2002). Other studies show that some dendritic spines in the cortex enlarge after the animals experience a novel sensation (Holtmaat et al 2006) while other spines remain stable for weeks (Grutzendler et al 2002; Trachtenberg et al 2002). New spines also form after novel experience. However, only ~3% of the newly formed spines remain over weeks. Since changes in spine number and shape potentially lead to modifications

in synaptic connectivity and strength between neurons, spines may provide a structural basis for memory retention throughout the life of an animal (Holtmaat et al 2006; Yang et al 2009).

1.6.2 Alterations in dendritic spine morphology induced by LTP and LTD

Long-term potentiation (LTP) and long-term depression (LTD) are a long lasting increases and decreases in synaptic strength, respectively, and represent the best electrophysiological correlates of learning and memory to date (Bliss & Collingridge 1993; Bliss & Lomo 1973; Bourne & Harris 2007; Malenka & Nicoll 1999). The induction and expression of LTP or LTD require many molecular components including NMDARs, AMPARs, calcium-dependent kinase II (CAMKII), calcineurin, and protein kinase C (PKC) (Byrne 2008). Extensive research suggests a strong link between LTP/LTD and learning/memory (Byrne 2008). For example, blocking LTP induction with NMDAR antagonists impairs spatial learning (Davis et al 1992). Knock-out mice of various protein kinases that cause LTP deficits also block spatial memory (Abeliovich et al 1993; Frankland et al 2004; Grant & Silva 1994; Kang et al 2001; Silva et al 1992a; Silva et al 1992b). Also, forebrain specific calcineurin transgenic mice that have deficit in LTD and LTP have impairments in working, spatial memory (Li et al 2006; Malleret et al 2001; Zeng et al 2001). LTD in the cerebellum is also believed to contribute to motor learning since several lines of knock-out mice, including mGluR1 (metabotrophic GluR1) knock-out mice, have impairments in parallel fiber LTD and motor learning (Aiba et al 1994; Chen & Tonegawa 1997; Whitlock et al 2006).

Recent studies suggest that dendritic spines modify their size during LTP and LTD. Glutamate uncaging studies reveal that high frequency stimulation of synapses (which is known to induce LTP) results in spine enlargement (Matsuzaki et al 2004). This spine enlargement is associated with an increased in AMPA receptor-mediated currents and is NMDA receptor-dependent (Matsuzaki et al 2004). Other studies using quanta-like release of glutamate induce a transient

increase in the size of large spines and a persistent enlargement of small spines. This suggests that small spines may be 'learning spines', whereas large spines represent 'memory spines' and contain physical traces of long-term memory (Alvarez & Sabatini 2007; Kasai et al 2003; Matsuzaki et al 2004). In contrast, induction of LTD has been shown to cause spine retraction (Nagerl et al 2004; Okamoto et al 2004). Remarkably, the reduction in spine size can be reversed by subsequent high frequency stimulation (Zhou et al 2004). These studies provide a link between physiological function and spine morphology.

It needs to be mentioned that some studies have failed to link LTP/LTD with changes in spine size. Bagal et al. reported that LTP induction by glutamate uncaging is not accompanied by spine expansion (Bagal et al 2005). Another study examining parallel fiber-Purkinje cell synapses in the cerebellum showed that LTD is not associated with spine shrinkage or elimination (Sdrulla & Linden 2007). The discrepancies between these studies and those described above may be related to different experimental set-ups and procedures. Complicating this issue is the possibility that LTP/LTD-associated changes in synapse morphology might not occur at all spines.

1.7 Spine morphology and diseases

Many studies suggest that disrupted spine size and shape lead to abnormal properties of excitatory synapses (Fiala et al 2002). Indeed, a number of neurological diseases are associated with substantial alterations in either spine morphology or density, including Down's and Fragile-X syndromes, schizophrenia, Parkinson's disease, autism, and Alzheimer's disease (Blanpied & Ehlers 2004; Irwin et al 2000; Kaufmann & Moser 2000; Sawa & Snyder 2002; van Spronsen & Hoogenraad 2010). Patients with Fragile X syndrome have an abundance of abnormally long, thin, and immature filopodia-like spines (Pfeiffer & Huber 2009). Interestingly, spine loss is also found to accompany many psychiatric diseases including schizophrenia (Fiala et al 2002) and addiction (Robinson & Kolb 1999). Thus abnormal spine structure is highly correlated with diseases where patients experience impaired cognitive function. However, it

remains to be determined if spine alterations directly cause abnormal cognitive function or are a consequence of diseases.

Chapter 2 Signaling pathways that regulate dendritic spine morphogenesis

2.1 Actin cytoskeleton in spines

Spines are highly actin-rich structures that are almost devoid of microtubules and intermediate filaments (Matus 2000; Peters et al 1991). EM analysis has shown that actin filaments are organized into a meshwork in the dendritic spine head, whereas they are found in longitudinal bundles within the spine neck (Fifkova & Delay 1982; Hirokawa 1989). The F-actin meshwork in the spine head, composed of highly branched actin filaments, supports the structure of the spine head and helps organize molecules within spines (Cingolani & Goda 2008; Matus 2000; Matus et al 2000). Some actin filaments in the spine head are attached to the PSD, while others some run parallel to the PSD (Fifkova & Delay 1982).

Ultrastructural analysis of dissociated hippocampal neurons extracted with detergent to reveal cytoskeletal components show that actin filament bundles in the spine neck or filopodia are not homogenous but contain branched filaments and linear filaments of variable lengths (Korobova & Svitkina 2010). In the spine base, actin filaments converge from a broad area in the dendrite toward the neck in a delta-shaped organization (Korobova & Svitkina 2010). Unlike traditional filopodial protrusions from the cell membrane which contain F-actin bundles connected by actin crosslinkers, filopodia spines contain branched actin filaments and loosely bundled actin filaments with various length (Korobova & Svitkina 2010). Thus, actin filaments serve as the primary cytoskeletal scaffold of spines.

2.1.1 Actin dynamics in the spine

The actin in spines consists of only β and γ cytoplasmic isoforms (Kaech et al 1997). It exists in two states: monomeric actin (globular, G-actin) or polymerized helical filaments (F-actin). Under steady-state conditions and with a given G-actin concentration, G-actin monomers are added to the barbed ends (plus ends) of actin filaments and dissociated from pointed ends (minus ends). This creates a net flow of newly acquired G-actin through the filament, referred to as actin treadmilling, and results in the turnover of actin filaments while preserving the overall filament

length (Sekino et al 2007; Star et al 2002). Time-lapse imaging of GFP-tagged actin in hippocampal neurons shows that the actin in spines undergoes rapid remodeling over a time scale of minutes (Fischer et al 1998). Indeed, a study using FRAP (fluorescence recovery after photobleaching) analysis shows that the majority of actin subunits in dendritic spines are in a constant state of dynamic equilibrium, cycling between filamentous (F)-actin and globular (G)-actin (Star et al 2002).

More recent work using two-photon microscopy combined with photo-activatable GFP-labelled β-actin suggests that there are two pools of F-actin inside spines. A dynamic pool exists at the spine tip with a turnover time of about 40 seconds, and a more stable pool at the base of the spine head with turnover time of approximately 17 minutes (Honkura et al 2008). The dynamic pool of F-actin located at the spine tip undergoes rapid treadmilling behavior in order to generate an expansive force that supports changes in spine shape. The size of the stable pool of F-actin at spine head base, on the other hand, correlates with spine head volume.

In the neck of mushroom-shaped spines, F-actin forms axial bundles having unique polarity with their barbed growing ends towards the spine head. This suggests that spines grow at their tip (Rao & Craig 2000). A more recent study using GFP-labelled actin showed that the addition of actin monomers to the barbed end of F-actin also occurs at the base of filopodia-like spines, suggesting F-actin bundles in the spine neck have mixed polarity with a smaller fraction of actin filaments with barbed end facing away from the spine tip (Hotulainen et al 2009; Korobova & Svitkina 2010). However, a smaller percentage of mature mushroom spines are believed to have G-actin added to F-actin at the base of spines. Interestingly, in the spine head, F-actin may not be uniformly spread throughout the entire spine head but may be restricted to localized regions near the spine head surface (Hotulainen et al 2009). These results suggest that actin organization and dynamics are highly regulated in the dendritic spines.

2.1.2 Actin remodeling in spines and neural plasticity

Increasing evidence suggests that long-term synaptic plasticity is associated with a rapid and persistent reorganization of the actin cytoskeleton in spines. Electrical stimulation used to induce LTP/LTD has been shown to change reorganization of the actin cytoskeleton and induce changes in spine anatomy. Consistent with this, studies have reported that LTP-inducing stimuli in the hippocampus increase the F-actin content in spines (Fukazawa et al 2003; Lin et al 2005). Synaptic activation through local glutamate uncaging also induces a rapid shift in the actin subunit equilibrium from G-actin toward F-actin in spines. This occurs in parallel with spine enlargement (Okamoto et al 2004). Interestingly, studies using inhibitors of actin polymerization show that LTP relies on actin and its dynamic reorganization. LTP fails to stabilize upon application of latrunculin A, a drug that blocks the incorporation of G-actin into polymerizing actin filaments (Kim & Lisman 1999). Induction of LTD is also associated with spine shrinkage (Nagerl et al 2004; Zhou et al 2004) and loss (Bastrikova et al 2008; Monfils & Teskey 2004). The activity of cofilin, an actin severing/depolymerisation protein, is involved in the spine shrinkage associated with LTD (Zhou et al 2004).

2.2 Actin filament regulatory proteins

There are a variety of actin-binding proteins expressed by neurons that can directly regulate the structure and organization of the actin cytoskeletal network and hence may contribute to the structural plasticity of spines. Actin-binding proteins modify actin structures in different ways including promoting actin filament bundle formation by crosslinking actin filaments (such as alpha-actinin, drebrin, spinophilin, epsin, synaptopodin); inducing nucleation and branching (such as Arp2/3, profilin II, cortactin, neurabin, Abp1) and promoting actin depolymerisation (such as cofilin, gelsolin, profilin I) (Ethell & Pasquale 2005). The functions of several of theses actin-binding proteins in regulating dendritic spine morphology have been recently revealed. For example, over-expression of

alpha-actinin increases the length of dendritic spines and the number of filopodia-like spines (Nakagawa et al 2004). Expression of Arp2/3, which promotes F-actin nucleation and branching, induces spine head expansion (Racz & Weinberg 2008). Cortactin also functions to stabilize F-actin and promotes F-actin branching (Hering & Sheng 2003). Over-expression of cortactin induces spine elongation, whereas knock-down of cortactin protein using RNAi leads to spines loss (Hering & Sheng 2003). Thus, actin-regulatory proteins serve many roles in modulating spine structure.

2.2.1 Cofilin and dendritic spines

Among actin regulator proteins, cofilin/ADF (actin depolymerization factor) family members are enriched in spines (Chen et al 2007; Racz & Weinberg 2006). These proteins mediate rapid turnover of actin filaments in different ways. They can directly depolymerize actin filaments by promoting actin monomer dissociation from the pointed ends and also sever F-actin to promote actin filament disassembly or provide more barbed ends. The ADF/cofilin family proteins have three forms in mammals: ADF (also known as destrin), cofilin-1 (the major form in non-muscle tissue) and cofilin-2 (the major form in muscle). ADF and cofilin-1 have similar activities in actin regulation (Bernstein & Bamburg 2010). The activity of cofilin is negatively regulated by phosphorylation at N-terminal serine-3 in the N-terminus of the protein (Agnew et al 1995; Aizawa et al 2001) by LIM-kinases (Nunoue et al 1995) or testicular protein kinases (TESKs) (Toshima et al 2001). ADF is also negatively regulated by LIMKs (Bernstein & Bamburg 2010). Dephosphorylation of cofilin by Slingshot (SSH) family proteins (Niwa et al 2002) or Chronophin phosphatase (CIN) (Gohla & Bokoch 2002) reactivates cofilin. Cofilin plays key roles in various cellular activities, including in cell division, motility and the formation and maintenance of specialized actin-rich structures (Arber et al 1998; Sidani et al 2007). For example, cofilin is important for maintaining and extending lamellipodial protrusions at the leading edge of migrating cells (Bailly & Jones 2003; Dawe et

al 2003). Complete knock-out of the cofilin-1 gene in mice is embryonic lethal suggesting it plays a critical role in many tissues (Bernstein & Bamburg 2010).

Cofilin is implicated in regulating the development and morphological plasticity of spines (Fedulov et al 2007; Hotulainen et al 2009; Shi et al 2009; Zhou et al 2004). Indeed, direct manipulation of cofilin function perturbs spinogenesis and the maintenance of spines (Hotulainen et al 2009; Shi et al 2009). Reduction of endogenous cofilin expression in dissociated neurons by RNAi results in spines with aberrantly long necks or neurons with abnormal filopodia-like protrusions (Hotulainen et al 2009). These neurons also have a modest reduction in the frequency of miniture excitatory postsynaptic currents (mEPSCs), suggesting a slight decrease in the number of active excitatory synapses (Hotulainen et al 2009). In these spines, the F-actin turnover rate is decreased threefold. Interestingly, over-expression of wild-type cofilin does not affect spine head sizes suggesting that signaling mechanisms exist in spines to suppress cofilin activity. Expressing a non-phosphorylated form (constitutively active form) of cofilin (S3A; serine-3 mutated to alanine) in mature neurons does result in longer, immature-looking spines (Shi et al 2009). Furthermore, over-expression of phosphomimetic form (an inactive form) of cofilin (S3D; serine-3 mutated to aspartic acid to mimic phosphorylation) causes a decrease in spine length, shifting the spine head-to-length ratio toward a more mature spine phenotype. The ability of cofilin S3D to alter the spine head size suggests that it may be acting in a dominant-negative fashion by competing with endogenous regulators of cofilin (Shi et al 2009). These studies suggest that cofilin activity is important in maintaining proper spine morphology.

Cofilin phosphorylation/dephosphorylation are believed to be involved in spine expansion/shrinkage in response to LTP/LTD induction, respectively. Studies suggest that LTP induction in the dentate gyrus of the hippocampus increases cofilin phosphorylation in dendritic spines while blocking phosphorylation of cofilin impairs LTP (Fukazawa et al 2003). More detailed studies show that induction of LTP by theta-burst stimulation (TBS) increases the levels of phospho-PAK (a Rac effector) and phospho-cofilin and this has been

implicated in spine enlargement (Chen et al 2007). Interestingly, rats subjected to learning paradigms have a higher percentage of spines containing phospohorylated cofilin in hippocampal pyramidal neurons (Fedulov et al 2007) and the phospho-cofilin-positive spines are associated with larger synapses (Fedulov et al 2007). In contrast, blocking the dephosphorylation of cofilin by infusing a synthetic peptide into neurons with a patch electrode, which mimics the substrate region of either cofilin or phosphorylated cofilin abolishes the spine shrinkage induced by low frequency stimulation (Zhou et al 2004).

Cofilin can be also be regulated by other mechanisms including the binding to phosphoinositides. In particular, cofilin has been shown to bind to the phosphoinositides PIP_2 (phosphatidylinositol 4,5-bisphosphate) (Bamburg 1999). Cofilin has multiple binding sites for direct binding to PIP_2, which are also binding sites for F-actin (Yonezawa et al 1991a; Yonezawa et al 1990). Binding to PIP_2 inhibits the ability of cofilin to bind to F-actin and cofilin-PIP_2 interactions modulate cofilin activity by tethering non-phosphorylated cofilin to the cell membrane (DesMarais et al 2005; Nagaoka et al 1996; Nagaoka et al 1995).

2.2.2 Enzymes that inhibit cofilin function (LIM and Tes Kinases)

Proteins of the LIM-kinase family (LIM is an acronym for three homeodomain-containing proteins, Lin-11, Isl-1, and Mec-3) include LIM-kinase 1 (LK1) and LIM-Kinase 2 (LK2) (Mizuno et al 1994; Okano et al 1995) and are known to regulate cofilin activity. LIM kinases are composed of two N-terminal LIM domains, an internal PDZ domain, and a C-terminal serine-theronine kinase domain. There are several splice variants of LK1 and LK2 that vary in size and domain composition (Ikebe et al 1997). To date, the only substrate identified for LKs is cofilin (Yang et al 1998). LK1 and LK2 inactive cofilin by phosphorylation at Ser-3 (Arber et al 1998; Sumi et al 2001; Sumi et al 1999), and hence serve as upstream regulators of cofilin function. Interestingly, LK1 and LK2 are downstream of pathways associated with the Rho-family of small GTPases. It has been suggested that LK1 can be activated by PAK, an effector of

the small GTPases Rac, whereas LK2 acts downstream of Rho and Cdc42, but not Rac (Sumi et al 1999). Furthermore, LK2 can be phosphorylated and activated by the RhoA effector Rho-associated kinase, ROCK (Sumi et al 2001).

In situ hybridization for LK1 and LK2 has shown that both proteins are expressed in the brain during development. LK1 mRNA is particularly enriched in the brain as opposed to other tissues in the rodent (Mori et al 1997). LK2 mRNA, in contrast, is more ubiquitous than LK1 and found throughout many tissues during development. LK2 is highly expressed in the hippocampus at postnatal day 7 and only weakly detected in the adult rat brain.

Interestingly, LK1 knock-out mice have reductions in cofilin phosphorylation levels and abnormal dendritic spine morphology. The spine head sizes are reduced and spine necks are thicker (Meng et al 2002). Physiological recordings in LK1 knock-out mice have shown that the basal synaptic transmission is normal, however, the knock-out mice have elevated LTP when compared to control mice. At the behavioural level, LK1 knockout mice have impaired fear conditioning responses and disrupted spatial learning. Remarkably, a mutation in LK1 is associated with Williams syndrome, a neurodevelopmental disorder characterized by mental retardation and visuospatial cognitive defects (Frangiskakis et al 1996; Meng et al 2002). LK2 knockout mice, in contrast, show normal cofilin phosphorylation levels (Meng et al 2004). The normal levels of cofilin phosphorylation in the LK2 knock-out mice are believed to be explained by compensating effects of LK1. Indeed, LK1 and LK2 double knockout mice have more severely reduced endogenous cofilin phosphorylation levels when compared with LK1 knockout mice (Meng et al 2004). To date, spine morphology in LK2 knock-out mice has not been studied. However, LK1/LK2 double knock-out mice show altered basal synaptic transmission and LTP, further suggesting the critical role of both LKs in synaptic regulation (Meng et al 2004). All of these results suggest that LK1 and LK2 are critical players in regulating synaptic plasticity, possibly through the remodeling of the actin cytoskeleton in dendritic spines.

2.2.3 Enzymes that enhance cofilin activity (Slingshot and Chronophin)

To maintain normal levels of cofilin-mediated actin turnover, cofilin needs to be re-activated by dephosphorylation. Slingshot phosphatase composes one major family of phosphatases that serve this role. Slingshot phosphatases were first identified and characterized in *Drosophila*. Slingshot mutant flies show a bristle and hair bifurcation phenotype (Niwa et al 2002). Loss of the *ssh* gene also causes a prominent elevation in phospho-cofilin and F-actin levels. In mammals, three genes encode SSH proteins (SSH-1, -2 and -3). In human, each SSH protein has a long (L) and short (S) isoforms by alternative splicing, whereas in mouse, each SSH has only one isoform whose structure is similar to the long form of SSH in humans (Ohta et al 2003). *In situ* hybridization analysis indicates that all three SSH genes are highly expressed in the hippocampus, cerebellum, and olfactory bulb of the adult mouse brain (Ohta et al 2003). Knock-outs for SSH1 and SSH2 have not been reported. However, SSH3 knock-out mice develop normally, suggesting a possible compensatory mechanisms between different SSH members (Kousaka et al 2008).

All mouse SSH family members contain N-terminal A and B domains and a protein phosphatase domain (P domain) and C-terminal serine-rich domain (S domain)(Ohta et al 2003). The signature motif (H/V)CX5(S/T) in the active-site in the P domain is conserved across protein tyrosine phosphatases (PTPs) in general. The A domain of SSH protein is required for F-actin-induced enhancement of phosphatase activity while the B and P domains are essential for phospho-cofilin substrate recognition and cofilin-phosphatase activity of SSH1 (Kurita et al 2008). A phosphatase-inactive CS mutant of SSH1, in which the catalytic Cys residue is replaced by Ser, forms a stable enzyme-substrate complex with phospho-cofilin, and functions as a dominant-negative protein (Kurita et al 2008). SSH activity is strongly increased by its binding to F-actin (Eiseler et al 2009; Kurita et al 2008) suggesting an important requirement for F-actin for SSH to dephosphorylate cofilin.

Slingshot activity itself is regulated by several mechanisms including phosphorylation/dephosphorylation. Pulldown experiments show that

phosphorylation of SSH1 by PAK4 at serine 978 and serine 937 on the C-terminus decreases its phosphatase activity (Soosairajah et al 2005), and increases the binding of the regulatory protein 14-3-3ζ to the phosphorylation sites (Nagata-Ohashi et al 2004). Protein kinase D (PKD1), a serine/threonine kinase known to regulate cell motility, phosphorylates SSH on serine 978 downstream of RhoA activation (Eiseler et al 2009). This phosphorylation on SSH dissociates it from actin filaments and allows the binding to 14-3-3ζ regulatory proteins. This causes SSH to be sequestered away from actin filaments and active cofilin at the leading edge of a cell. Phosphatidylinositol 3-kinase (PI3K) has also been shown to inhibit SSH activation and cofilin dephosphorylation downstream of insulin signaling (Nagata-Ohashi et al 2004), although it remains unclear if PI3K directly phosphorylates SSH proteins.

SSH1 can be reactivated by calcineurin (PP2B)-mediated dephosphorylation in cell-free assays and HeLa cells, suggesting that Ca2+ signals activate SSH1 and result in cofilin dephosphorylation. The cofilin dephosphorylation can be blocked by calcineurin inhibitors, expression of dominant negative calcineurin, or transfection of SSH1 siRNA (Wang et al 2005). Interestingly, activation of dopamine D4 receptors in GABAergic interneurons in prefrontal cortex causes activation of SSH1 through calcineurin activation. This leads to cofilin activation and actin depolymerization. The disruption of actin filaments interferes with myosin-dependent GluR1 transport and decrease AMPAR current in these neurons (Yuen & Yan 2009).

Besides slingshot, chronophin (CIN) has also been shown to be a phosphatase for cofilin (Gohla et al 2005). CIN is a member of the haloacid dehalogenase (HAD) family of phosphatases, whose involvement in mammalian signal transduction pathways is poorly understood. CIN over-expression decreases basal cofilin phosphorylation levels in HeLa cells, whereas catalytically-inactive CIN or CIN depletion by siRNA causes enhanced phospho-cofilin levels.

2.3 Eph receptors

Dendritic spines contain a variety of cell surface receptors that influence spine properties in response to external signals (Sheng & Hoogenraad 2007; Tada & Sheng 2006). Cell surface receptors regulate spines by modulating cell adhesion and promoting differential signaling events that ultimately control actin dynamics. Some of the cell surface molecules are located at the synaptic cleft and are critical for trans-synaptic signaling process that regulates the development and maintenance of spines. Receptors such as neurexins/neuroligins, the Ig-superfamily protein SynCAM, extracellular leucine-rich repeats (LRRs) containing proteins, and cadherins are known to stabilize points of axon–dendrite contact and induce bi-directional signals that promote pre- and post-synaptic development (Biederer & Stagi 2008; Sheng & Hoogenraad 2007). Many of these adhesion molecules contain PDZ-binding motifs at the intracellular portion, which interacts directly with synaptic scaffolding proteins such as PSD-95, and allows them to facilitate the recruitment of synaptic proteins during development.

In addition to these adhesion-type of molecules, Eph receptors and their ephrin ligands have been shown to play important roles in spine morphogenesis and maintenance as well as modulating synaptic plasticity (Klein 2009; Pasquale 2008). Ephs/ephrins were originally identified as molecular cues involved in axon guidance and topographic map formation in the visual system (McLaughlin & O'Leary 2005; Scicolone et al 2009). Eph receptors typically serve as repulsive cues in growth cone guidance and are important in establishing patterns of connectivity in several regions of the central nervous system (Flanagan & Vanderhaeghen 1998). However, more recent studies show that Eph receptors can both promote and inhibit neurite growth, depending on the level of receptor activation along ephrin gradients (Hansen et al 2004).

2.3.1 The structure of Eph receptors and ephrin ligands

In mammals, Eph receptors comprise a large family of receptor tyrosine kinases (RTKs), including both EphA (EphA1 to A8, and EphA10) and EphB

(EphB1 to B4 and EphB6) receptors based on sequence homology and preference for ephrin ligands (Klein 2004). Although promiscuity exists, EphA class receptors typically bind to A-type ephrins (ephrin-A1 to A5), which are bound to the cell membrane through a GPI (glycosyl phosphatidylinositol) anchor. EphB receptors preferentially bind to B-type ephrins (ephrinB1 to B3), which are transmembrane proteins that have cytoplasmic domains. Both A- and B- type ephrin ligands are localized in lipid raft microdomains and shown to transduce their own "reverse" signals in cells (Kullander & Klein 2002). Eph receptors are composed of an extracellular ligand-binding domain, two fibronectin-like type III repeats, a conserved cytoplasmic juxtamembrane region, tyrosine kinase domain, sterile alpha motif (SAM) domain and a C-terminal PDZ domain binding motif (found in most Eph receptors). In the absence of ligands, the tyrosine kinase domain of the Eph receptor is stabilized and inhibited by the juxtamembrane region in the absence of ephrin binding. Ligand-receptor interactions induce receptor multimerization and phosphorylation of conserved tyrosines in the juxtamembrane region. This allows the receptor to undergo a conformation change that promotes its autophosphorylation ability (Binns et al 2000) and allows for the recruitment of SH2-domain containing proteins through various phosphorylated tyrosine residues in the C-terminus (Wybenga-Groot et al 2001) and promotes its ability to phosphorylate other proteins (Bourgin et al 2007; Fu et al 2007).

2.3.2 Eph receptors and dendritic spines

In the hippocampus, several Eph receptors localize to dendrites and spines. Recent studies point to a critical role of Eph receptors in regulating dendritic spine morphology. EphB2, by phosphorylating the proteoglycan syndecan-2, promotes spine morphogenesis in cultured hippocampal neurons (Ethell et al 2001). EphB2 and ephrinB signaling also induces phosphorylation of the Rho-GEF, Kalirin, and causes its recruitment to the PSD. This, in turn, enhances local activation of Rac and PAK and the Rac1 guanine exchange factor (GEF) Tiam1, and leads to

rearrangement of the actin cytoskeleton and spine morphogenesis (Penzes et al 2003; Tolias et al 2007). Interestingly, activated EphB2 receptors interact with and help to cluster NMDA receptors (NMDARs) at synapses and lead to synaptic specializations in cultured neurons, suggesting that EphB2 could be important for synapse formation in early development (Dalva et al 2000). Moreover, EphB2 activation by ephrinB2-Fc increased NMDAR-dependent calcium influx in primary cortical neurons through Fyn, a Src family tyrosine kinase (Dalva et al 2000; Takasu et al 2002). Other than EphB2, EphB1 and EphB3 may also play roles in spines. There appears to be some redundant function for EphB receptors at dendritic spines as generation of double and triple knock-outs of EphB1, EphB2 and EphB3 are required to detect decreases in spine density and alterations of spine morphology in the brain. Interestingly, filamentous actin (F-actin) is accumulated in dendritic shafts rather than in spines in the triple knock-out mutants, suggesting that EphB receptors may influence the targeting of actin to spines (Henkemeyer et al 2003a).

2.3.3 EphA4 and downstream signals that control spine morphology

To date, the only A class Eph receptor found to play a critical role in modulating spine morphology is EphA4. EphA4 is highly expressed in the developing and adult mouse hippocampus (Murai et al 2003a). One of its ligands, ephrinA3, is concentrated to the tips of astrocytic processes which surrounding synapses. Activation of EphA4 in hippocampal slices by ephrin-A3-Fc leads to spine retraction and loss in hippocampal slices (Murai et al 2003a). However, treating hippocampal slices with EphA4 Fc, which inhibits the interaction between endogenous EphA4 and ephrins results in irregular and disorganized spines, suggesting that EphA receptor signaling is important for maintaining spine morphology and organization (Murai et al 2003a). Consistent with this, EphA4 knock-out mice have abnormal spines that are elongated and distorted in shape (Murai et al 2003a) and ephrin-A3 knock-out mice also have disorganized spines

with significantly longer necks. This results in an increased number in mushroom-shaped spines and a loss of stubby spines (Carmona et al 2009). A transgenic mouse line that over-expresses ephrin-A3 in astrocytes from the GFAP promoter also shows a significant loss of spines (Filosa et al 2009).

EphA4 likely signals through several proteins to alter spine morphology. It is known to interact with Cdk5, a proline-directed serine and threonine kinase, that is highly expressed in postsynaptic densities and activates p35 in a ephrin-dependent manner (Fu & Ip 2007). Ephrin-A1 stimulation (the ephrin ligand with the highest affinity to EphA4) (Flanagan & Vanderhaeghen 1998), leads to activation of Cdk5 and causes a decrease in spine density in hippocampal slices (Fu et al 2007). Cdk5 knockdown blocks the ephrin-A1-induced dendritic spine retraction in dissociated hippocampal neurons, suggesting that Cdk5 mediates the ephrinA-induced effects. Further biochemical studies show that upon EphA4 activation, activated Cdk5 helps Src tyrosine kinase to phosphorylate and activate ephexin1, a Rho GTPase exchange factor. Ephexin-1 activates RhoA and regulates actin reorganization in spines. EphA4 activation also regulates dendritic spine remodeling through inhibiting β1 integrin signaling pathways that stabilize dendritic spines (Bourgin et al 2007).

2.4 PLCγ1

Downstream of receptor tyrosine kinases (RTK) is an array of signaling proteins. Among these are proteins of the phospholipase C family (Patterson et al 2005). Phospholipase C (PLC) is known to be important for phosphoinositide metabolism, cell morphology, and synaptic function (Rebecchi & Pentyala 2000). PLC hydrolyzes phosphatidylinositol 4,5-bisphosphate (PIP_2) to generate inositol 1,4,5-triphosphate (IP_3) and 1,2-diacylglycerol (DAG). Mammalian PLCs contain 12 different isoforms, including β (β1–β4), γ (γ1 and γ2), δ (δ1–δ4), and ε and ζ (Poulin et al 2005). PLCγ1 is a multi-domain signaling protein, containing two tandem Src Homology 2 (SH2) domains, a SH3 domain, a split pleckstrin homology (PH) domain, and a split catalytic lipase domain (Rebecchi & Pentyala

2000). It has been suggested that activation of PLCγ1 by RTKs leads to an association of PLCγ1 protein with the activated receptor, which then phosphorylates PLCγ1 (Rebecchi & Pentyala 2000). The RTK then phosphorylates PLCγ1 on 3 tyrosine residues, Y771, Y783, and Y1253. Phosphorylation on Y783, in particular, has been shown to correlate with the level of activated PLCγ1 protein (Kim et al 1991; Poulin et al 2005).

Previous electrophysiological studies have shown that postsynaptic inhibition of PLC prevents induction of NMDAR-dependent LTD in hippocampus (Reyes-Harde & Stanton 1998). Recent studies demonstrate that stimulation of NMDAR leads to activation of PLC and a rapid decrease in PIP_2 levels in hippocampal neurons (Horne & Dell'Acqua 2007). Inhibition of PLC activation prevents decreased postsynaptic scaffold proteins localization to dendritic spines, decreased AMPAR surface expression, and decreased spine F-actin content during chemical LTD (Horne & Dell'Acqua 2007). Other studies show that hippocampal LTP is supported by TrkB-mediated PLCγ signaling (Gartner et al 2006). Blocking PLCγ produces a significant reduction in LTP that is comparable with the effects seen in TrkB or BDNF knock-out mice. These results together suggest important roles of PLC in synaptic plasticity.

Chapter 3 EphA4 signaling regulates phospholipase Cγ1 activation, cofilin membrane association, and dendritic spine morphology

The text of this chapter is a reprint of the material originally published in the *Journal of Neuroscience* 2007 May 9; 27(19):5127-38.

EphA4 signaling regulates phospholipase Cγ1 activation, cofilin membrane association, and dendritic spine morphology

Lei Zhou[1], Sarah J. Martinez[1], Michael Haber[1], Emma V. Jones[1], David Bouvier[2], Guy Doucet[2], Amadou T. Corera[3], Edward A. Fon[3], Andreas H. Zisch[4], and Keith K. Murai[1*]

[1]Centre for Research in Neuroscience, Department of Neurology and Neurosurgery, The Research Institute of the McGill University Health Centre, Montreal General Hospital, 1650 Cedar Avenue, Montreal, QC, H3G 1A4 Canada, [2]Département de Pathologie et Biologie Cellulaire and Groupe de Recherche sur le Système Nerveux Central, Université de Montréal, Montréal, Québec, H3C 3J7 Canada, [3]Centre for Neuronal Survival and Department of Neurology and Neurosurgery, Montreal Neurological Institute, McGill University, 3801 University Street, Montreal, QC H3A 3B4 Canada, and [4]Department of Obstetrics, University Hospital Zurich, Frauenklinikstr 10, 8091 Zurich, Switzerland; and Zurich Center for Integrative Human Physiology.

Contribution of Authors

I performed the majority of the experiments including PLCγ1 activation studies shown in figure 2, spine morphology analysis shown in figure 5 and 6, cofilin fractionation shown in figure 7, and the RNAi study shown in supplemental figure 1. Sarah J. Martinez produced the PLCγ1 plasmids, performed the *in vitro* kinase activity and GST pulldown assays shown in figure 1 and 3. Michael Haber performed immunostaining of EphA4 and PLCγ1 shown in supplemental figure 2, and helped in data processing of spine morphology analysis. Emma V. Jones performed co-immunoprecipitation of EphA4 and PLCγ1 as shown in figure 3C. David Bouvier, Guy Doucet, Amadou T. Corera, and Edward A. Fon performed the synaptosome preparation analysis. Andreas H.

Zisch performed an initial yeast-2-hybrid experiment and indentified a potential interaction between EphA4 and PLCγ1.

Abstract

Specialized postsynaptic structures known as dendritic spines are the primary sites of glutamatergic innervation at synapses of the central nervous system. Recent studies have shown that spines rapidly remodel their actin cytoskeleton to modify their shape and this has been associated with changes in synaptic physiology. However, the receptors and signaling intermediates that restructure the actin network in spines are only beginning to be identified. We recently reported that the EphA4 receptor tyrosine kinase regulates spine morphology. However, the signaling pathways downstream of EphA4 that induce spine retraction upon ephrin ligand binding remain poorly understood. Here, we demonstrate that ephrin stimulation of EphA4 leads to the recruitment and activation of phospholipase C γ1 (PLCγ1) in heterologous cells and in hippocampal slices. This interaction occurs through an SH2-domain of PLCγ1 and requires the EphA4 juxtamembrane tyrosines. In the brain, PLCγ1 is found in multiple compartments of synaptosomes, and is readily found in postsynaptic density fractions. Consistent with this, PLC activity is required for the maintenance of spine morphology and ephrin-induced spine retraction. Remarkably, EphA4 and PLC activity modulates the association of the actin depolymerizing/severing factor, cofilin, with the plasma membrane. Since cofilin has previously been implicated in the structural plasticity of spines, this signaling may enable cofilin to depolymerize actin filaments and restructure spines at sites of ephrin-EphA4 contact.

Introduction

Dendritic spines are specialized protrusions from the dendritic shaft where excitatory synapses are formed in the brain. The stereotypic spine has an enlarged head that is connected to the dendritic shaft by a constricted neck. This morphology creates a biochemical compartment that accommodates the postsynaptic density (PSD), a dense region of ion channels and receptors that are complexed with scaffolding and other signaling proteins (Kim & Sheng 2004). Remarkably, spines change their morphology within minutes (Dailey & Smith 1996; Dunaevsky et al 1999; Fischer et al 1998) and this may adjust the physiology of synapses during processes such as learning and memory formation (Segal 2005). Recent studies indicate that this structural plasticity relies on the dynamics of actin filaments, which are concentrated in spines and serve as their primary structural scaffold (Matus 2000).

Among molecules that may control actin rearrangements in spines are proteins of the cofilin/ADF (actin depolymerization factor) family (Bamburg 1999; Racz & Weinberg 2006). Cofilin/ADF proteins bind, depolymerize, and sever actin filaments (Bamburg 1999). Cofilin activity is negatively regulated by kinases (Lim Kinase 1/2 and Tes kinase) (Arber et al 1998) and positively regulated by phosphatases (slingshot and chronophin) through phospho-cycling on a serine residue (Huang et al 2006). Cofilin is also modulated by phosphoinositides, especially PIP_2 (phosphatidylinositol 4,5-bisphosphate). Cofilin has multiple binding sites for PIP_2 (Yonezawa et al 1991a; Yonezawa et al 1990) and cofilin-PIP_2 interactions tether cofilin to the cell membrane (DesMarais et al 2005; Nagaoka et al 1996) and modulate cofilin activity (Nagaoka et al 1995). The cofilin-PIP_2 interaction also inhibits the enzyme PLCγ1 from cleaving PIP_2 when PLCγ1 is not tyrosine phosphorylated (Yonezawa et al 1991a). PLCγ1 is activated by receptor tyrosine kinases (RTKs), enabling it to hydrolyze PIP_2 into IP_3 and DAG (Rebecchi & Pentyala 2000). Cofilin and PLCγ1 are important regulators of cell morphology and implicated in synaptic plasticity (Meng et al 2002; Micheva et al 2001; Reyes-Harde & Stanton 1998; Zhou et al 2004).

However, the receptors that control these proteins at synapses remain to be fully described.

Several classes of RTKs may regulate PLCγ1 and cofilin including those of the Eph family. Eph receptors are divided into EphA and EphB subtypes (Kullander & Klein 2002). In general, EphA receptors bind GPI-anchored ephrin-As, whereas EphB receptors respond to transmembrane ephrin-Bs. Eph receptors are important for spine morphogenesis and maintenance *in vitro* and *in vivo* (Ethell & Pasquale 2005). Several signaling mechanisms have been elucidated for EphB receptors in spines, however, those downstream of EphA receptors remain to be described.

Here, we identify an EphA4 signaling pathway that regulates spine morphology. We show that EphA4 triggers PLCγ1 activation through an SH2-domain interaction with the juxtamembrane tyrosines of EphA4. PLC signaling is necessary for maintaining spine morphology and for ephrin-induced spine retraction. Remarkably, EphA4 and PLC signaling alters the membrane association of cofilin. We propose that EphA4 promotes PLCγ1 signaling to allow cofilin translocation away from the cell membrane, enabling it to depolymerize actin filaments in spines at sites of ephrin-A/EphA4 contact.

Materials and Methods

DNA constructs

Full-length mouse PLCγ1 was cloned from an EST vector (IMAGE Clone ID# 6854923; Open Biosystems, Huntsville, AL) through polymerase chain reaction and ligated in-frame into pcDNA3 with a V5 epitope tag (Invitrogen, Carlsbad, CA). The lipase-inactive PLCγ1 mutant (H335Q) (Huang et al 1995; Rong et al 2003; Ronnstrand et al 1999) and EphA4 juxtamembrane tyrosine mutants (Y596E and Y602E) were created using standard PCR-based mutagenesis (Cowan et al 2005; Zisch et al 2000). The EphA4 kinase-dead construct has been described previously (Murai et al 2003a). The N- and C-terminal SH2 domains of PLCγ1 were cloned into pGEX-4T1 (Promega, San Luis Obispo, CA) and used for GST fusion protein production using standard procedures.

For RNAi constructs, a short hairpin sequence directed against mouse PLCγ1 (Patterson et al 2002) was cloned into pSUPER (OligoEngine, Seattle, WA) containing the H1 promoter for driving the expression of a short-hairpin RNA and a PGK promoter for expressing GFP. In order to more thoroughly delineate dendritic spines, the GFP sequence was replaced with membrane-targeted EGFP (EGFPf; BD Biosciences, San Jose, CA). To generate RNAi plasmids, two complementary oligos containing the PLCγ1 shRNA were annealed (Sequence: 5'GATCCCCAAACAACCGGCTCTTCGTCTTCAAGAGAGACGAAGAGCC GGTTGTTTTTTTTA3' and 5'AGCTTAAAAAAAACAACCGGCTCTTCGTCTCTCTTGAAGACGAAGAG CCGGTTGTTTGGG3') and cloned into the BglII and HindIII sites of pSuper. A shRNA vector containing a scrambled sequence of the PLCγ1 shRNA sequence, which did not show homology to the mouse genome, was cloned in a similar fashion and used in control experiments (Sequence: 5'GATCCCCTAGACCTATATCCCTGCGCTTCAAGAGAGCGCAGGGATATA GGTCTATTTTTA3' and 5'AGCTTAAAAATAGACCTATATCCCTGCGCTCTCTTGAAGCGCAGGGAT

ATAGGTCTAGGG3').

Antibodies and Recombinant Proteins

The following antibodies were used in this study: mouse PLCγ1 (mouse monoclonal; Millipore, Upstate Division, Billerica, MA); PLCγ1 (rabbit polyclonal; Cell Signaling Technologies, Danvers, MA); pY783 PLCγ1 (Cell Signaling Technologies, Danvers, MA); pY771 PLCγ1 (Cell Signaling Technologies, Danvers, MA); pS1248 PLCγ1 (Millipore, Upstate Division, Billerica, MA); EphA4 (Murai et al 2003a; Soans et al 1994); pY20 (BD Biosciences, San Jose, CA); SNAP25 (a generous gift from Dr. P. McPherson, Montreal Neurological Institute), synaptophysin (Sigma, St. Louis, MO); PSD95 (BD Biosciences, San Jose, CA); NR1 (BD Biosciences, San Jose, CA); cofilin (Cell Signaling, Danvers, MA and Cytoskeleton, Denver, CO), V5 (Sigma, St. Louis, MO), transferrin receptor (Invitrogen, Carlsbad, CA), GAPDH (Abcam, Cambridge, MA), anti-rabbit and mouse HRP (GE Healthcare, Amersham Biosciences Division, Fairfield, CT), and control mouse IgGs (Jackson Immunochemicals, West Grove, PA). The following recombinant proteins were used: human IgG Fc (Jackson Immunochemicals, West Grove, PA), EphA4 kinase domain (Cell Signaling Technologies, Danvers, MA) and ephrin-A3 and -A5 Fc (R & D Systems, Minneapolis, MN).

Immunoprecipitation and Western Blot Analysis

For COS7 cell experiments, EphA4 and juxtamembrane mutants were transfected with Lipofectamine 2000 (Invitrogen, Carlsbad, CA) and 24 hours later stimulated for 45 minutes with dimeric control Fc, ephrin-A3 Fc or ephrin-A5 Fc. Cells were lysed in modified RIPA buffer (1% Triton X-100; 1% sodium deoxycholate; 0.1% SDS; 20 mM Tris; 150 mM NaCl; 1 mM EDTA) containing protease inhibitors and orthovanadate. Lysates were subjected to immunoprecipitation using 2 mg of mouse anti-PLCγ1 or mouse IgG control and coupled to protein-G sepharose (GE Healthcare, Amersham Biosciences Division,

Fairfield, CT). The degree of phosphorylation was determined using an antibody against pY783 and a protein-A HRP secondary antibody. The amount of immunoprecipitated protein was detected by stripping and reprobing membranes with rabbit anti-PLCγ1. Alternatively, transfected cell lysates were directly probed with anti-pY783, pY771 or pS1248 and stripped and reprobed for PLCγ1. For densitometry, the amount of phosphorylation was quantified using ImageJ and was normalized against the total PLCγ1 levels. Data was collected over three independent experiments.

For biochemistry involving hippocampal tissue, slices (300 μm thick) were prepared as described previously (Murai et al 2003a) and kept *in vitro* for approximately 2–5 min before stimulation with Fc fusion proteins (9.5μg/ml). Following stimulation for 45 min, slices were lysed in RIPA buffer. Lysates were immunoprecipitated with either anti-EphA4 or anti-PLCγ1 antibodies coupled to protein-A or protein-G sepharose, respectively. Phosphorylation of EphA4 was detected using an anti-phosphotyrosine antibody (PY20) coupled to HRP. PLCγ1 phosphorylation was detected with an anti-pY783 and protein-A HRP. Blots were stripped and reprobed by immunoblotting with anti-EphA4 or rabbit anti-PLCγ1 antibodies and anti-rabbit HRP to confirm that equal amounts of protein were immunoprecepitated from each condition.

The following procedure was used to co-immunoprecipitate EphA4 and PLCγ1 from mouse hippocampus. Hippocampi were dissected from the mouse brain at postnatal day 21 and homogenized in Triton lysis buffer (20 mM Tris pH 7.4, 137 mM NaCl, 25 mM β-glycerophosphate, 2 mM EDTA, 1% Triton X-100, 10% glycerol, supplemented with protease inhibitors and sodium orthovanadate) using a dounce homogenizer and lysed on ice for 15 minutes. Lysates were centrifuged at 13,000 rpm for 10 minutes at 4ºC to pellet cell debris. Lysates were precleared for 1 hour with protein-G sepharose, then subjected to immunoprecipitation using 5μg of mouse IgG control or mouse anti-PLCγ1 coupled to protein-G sepharose for 5 hours at 4ºC. Immune complexes were washed three times with lysis buffer, boiled in 40μl 3X SDS sample buffer and resolved by SDS-PAGE. The association of EphA4 and PLCγ1 was detected by

immunoblotting with a rabbit anti-EphA4 antibody.

GST Pulldown Assays

GST fusion proteins were prepared as described in Zisch et al., 1998. GST fusion proteins (GST, N-terminal SH2 PLCγ1, or C-terminal SH2 PLCγ1) coupled to agarose beads were incubated with transfected COS7 cell lysates (EphA4, EphA4 Y596E, or EphA4 Y602E solubilized in 1% Brij97 (Sigma, St. Louis, MO) in PBS with protease inhibitors and orthovanadate) overnight at 4 degrees. The beads were subsequently washed with 1% Brij97/PBS (with protease inhibitors and orthovanadate), diluted with sample buffer, and boiled for 5 minutes. Supernatants were subjected to SDS-PAGE and blotted using anti-EphA4 antibodies and anti-rabbit HRP as described previously.

***In Vitro* Kinase Assay**

For *in vitro* kinase assays, endogenous PLCγ1 from COS7 cells was immunoprecipitated as previously described. PLCγ1 immunoprecipitates were resuspended in kinase buffer containing 25 mM Hepes (pH7.4), 25 mM b-glycerophosphate, 25 mM $MgCl_2$, 0.1 mM Na_3VO_4, 0.5 mM DTT, 1 mM ATP. 0.5µg of recombinant EphA4 kinase domain was used in conditions that included the activated kinase. The reaction mixture was incubated at 30^oC for 30 min with gentle agitation every 10 min. The reaction was stopped by adding 25µl 3X SDS sample buffer and boiled for 5 min. Phosphorylation of PLCγ1 at Y783 was detected by Western blot analysis using pY783 and protein A-HRP. The total amount of PLCγ1 immunoprecipitated was determined by stripping and reprobing membranes with rabbit anti-PLCγ1. Data were collected from three independent experiments and quantified as described previously.

Synaptosome Preparations

Synaptic proteins were purified as described in the Supplemental Data section.

Cell Membrane Preparations

Cell membrane fractionation experiments were performed as described (Cote et al 2005). Briefly, cells were collected in PBS, centrifuged at 800g for 5min, and then resuspended in 300µl of buffer A (20mM Tris-HCl pH 7.5, 150 mM NaCl, 5 mM NaF, 1 mM Na_3VO_4, 10 mg/ml protease inhibitors). The cells were then subjected to a single freeze/thaw cycle in liquid nitrogen and a 37 ºC water bath and the membranes were pelleted using centrifugation at 16,000g for 10 min. The pellet was then washed with 500µl of Buffer A and extracted with buffer B (buffer A + 1% Triton X-100). Equal amounts of proteins were resolved by SDS-PAGE and the levels of membrane-associated cofilin analyzed by immunoblotting with cofilin antibodies. Equal loading between samples was confirmed by blotting for the transferrin receptor. For PLC inhibitor experiments, COS7 cells were seeded at a density of $1x10^6$ cells/ml and the next day were treated with either the PLC inhibitor U73122 (EMD Biosciences, La Jolla, CA) or control compound U73343 (EMD Biosciences, La Jolla, CA) at a final concentration of 10 µM for 3 hours prior to collecting the cells. For ephrin stimulation experiments, cells were seeded at a density of $1x10^5$ cells/ml and the next day transfected with the cDNA for EphA4 using Lipofectamine 2000 (Invitrogen, Carlsbad, CA). 24 hours following the transfection, the cells were treated with 8 µg/ml recombinant control Fc or ephrinA5-Fc fusion proteins for 40 min at 37 ºC. Membranes were then fractionated as described above. For densitometry, the amount of cofilin in each condition was quantified using ImageJ and normalized against the amount of transferrin receptor. Data was collected over three independent experiments.

For membrane fractionation in hippocampal slices following ephrin stimulation, 300µm slices were made from postnatal day 10 mice and placed into stimulation media containing Fc or ephrin-A5 Fc proteins (9.5 µg/ml). After 45min of stimulation, slices were coarsely homogenized, and then subjected to a single freeze/thaw cycle followed by the procedure described above. Data were collected from three independent experiments and quantified as described above.

Immunofluorescence in Heterologous Cells

For immunofluorescence studies in heterologous cells, COS7 cells were plated onto chambered slides (LabTek) and transfected as previously described. Cells were fixed with 4% paraformaldehyde/0.1M phosphate buffer for 30 minutes, rinsed with TBS and incubated for 1 hour in blocking solution (5% goat serum/0.1%Triton X-100 in TBS (Tris-buffered saline)). Cells were then incubated overnight (at 4ºC) with anti-pY783 in blocking solution. The next day, the cells were washed with 0.1%Triton-X100/TBS and incubated with a goat anti-rabbit Alexa 568 secondary (Invitrogen, Carlsbad, CA) for 1 hour at room temperature. After washing cells with 0.1%Triton-X100/TBS, cells were coverslipped for microscopy.

Semliki Forest Virus Plasmid Construction and Virus Preparation

For expressing PLCγ1 constructs and fluorescent proteins in hippocampal slices, Semliki Forest virus (SFV) constructs were created (Ehrengruber et al 1999). PLCγ1 and membrane-targeted farnesylated EGFP (EGFPf; Clontech, Cambridge, UK) genes were each cloned 3' to a viral subgenomic promoter in modified SFV vectors (Lundstrom et al 2003). Viral particles were produced as previously described (Haber et al 2006). SFV particles were injected into hippocampal slices with a Picospritzer (General Valve, Fairfield, NJ).

Hippocampal Slice Preparation

Organotypic hippocampal slices were prepared as described (Murai et al 2003a). Briefly, 300μm slices from postnatal 6-7 day (P6-7) mouse pups were made using a McIllwain tissue chopper (Stoelting, Kiel, WI) and transferred onto semi-porous tissue culture inserts (0.4 μm pore size; Millipore, Bedford, MA) containing media (50% Minimum Essential Medium / 25% Horse Serum/25% Hanks Balanced Salt Solution / 6.5mg/ml D-glucose / 0.5% penicillin / streptomyosin, pH~7.2). Media was replaced every two days and slices were cultured for 1 week before viral gene delivery. 16-20 hours post-infection, slices

were fixed and mounted for confocal imaging.

For imaging hippocampal slices following stimulation, 300μm slices were made from mice approximately 3 months of age and placed into stimulation media containing dimeric Fc or ephrin-A5 Fc and U73122 (PLC-inhibitor) or U73343 for 45 minutes. The slices were then fixed with 4% paraformaldehyde/0.1M phosphate buffer for 30 minutes. CA1 pyramidal cells were labeled using diolistics. Briefly, 1.3μm tungsten particles (BioRad, Hercules, CA) carrying the lipophilic dye, DiI (Invitrogen, Carlsbad, CA), were coated onto the inner portion of plastic tubing, cut into cartridges, loaded into a Helios Gene Gun (BioRad, Hercules, CA), and propelled into hippocampal slices at 120psi using helium gas. The DiI was allowed to transport for 16 hours in fixative before imaging by confocal microscopy.

For RNAi experiments, shRNA plasmids (see DNA constructs section) were delivered using biolistic gene transfer with a Helios Gene Gun (BioRad, Hercules, CA). Briefly, PLCγ1 shRNA and control shRNA plasmids were precipitated onto 1.6μm gold microcarriers and deposited on the inner lining of Tefzel tubing (BioRad, Hercules, CA) to generate bullets. Hippocampal slices were prepared as described above from postnatal day 5 mice and cultured for 9-10 days before propelling gold microcarriers onto hippocampal slices at 100psi using helium gas. To improve the efficiency of CA1 pyramidal cell transfection, a 3.0μm membrane filter (Millipore, Bedford, MA) was placed between the gene gun nozzle and the hippocampal slices. The shRNA constructs were allowed to express for 72 hours before fixation and imaging by confocal microscopy.

Confocal imaging

Confocal imaging was performed with a Yokogawa spinning disk confocal system (Perkin-Elmer, Wellesley, MA) connected to a Nikon Eclipse TE2000 (Nikon, Tokyo, Japan). Z-stacks were collected using Metamorph imaging software (Molecular Devices Inc., Palo Alto, CA).

Image analysis

For analysis of dendritic spine morphology, images of dendrites were taken for each condition (control, PLCγ1 wt, or PLCγ1 lipase inactive mutant (LIM) or PLCγ1 shRNA or control shRNA) from 3 independent experiments. Each image contained a Z-stack maximum projection of a primary apical dendrite from a CA1 pyramidal cell taken approximately 100μm from the cell body (Control = 16 dendritic segments with 568 spines total; PLCγ1 wt = 26 dendritic segments with 886 spines total; PLCγ1 LIM = 22 dendritic segments with 603 spines total). For RNAi experiments, 33 dendritic segments (with 889 spines) were used in the control shRNA condition and 41 dendritic segments (with 918 spines) in the PLCγ1 shRNA condition. All images were normalized for EGFPf signal intensity and thresholded in Photoshop (Adobe Systems, Seattle, WA). Geometric measurements of spine parameters (length, head width, area, and density) were acquired using the Reconstruct computer program (http://synapses.bu.edu/tools/index.htm). Spines were defined as any protrusion from the dendritic shaft that is not a dendrite branch. The dividing line of the spine head and neck was determined subjectively using the contours of the dendritic spine head. For spines without clearly defined head portions (i.e. stubby or elongated spines), the spine head area was considered equal to the total spine area and spine head width equal to the neck width. For each dendritic segment, the spine parameters were combined to generate an average value which was then used for comparisons. All quantifications were performed by an investigator blind to the experimental conditions. Using a computer to sort spines according to the measured parameters, spines were classified into four types (i.e. mushroom, stubby, elongated, or other). The ‘mushroom’ category corresponds to spines that have enlarged head regions with a constricted neck. ‘Stubby’ spines lack neck regions. The ‘elongated’ category includes filopodia-like spines and long spines with small, but well formed head regions. The ‘other’ category includes spines with abnormal dimensions, such as those with large heads and highly branched spines that do not fit into the three other categories. Differences between samples were performed using a t-test or analysis of variance (ANOVA) with a

Student-Newman-Keuls *post-hoc* comparison.

For stimulation experiments, images of dendrites were acquired similar to as described above over three independent experiments. 35 dendritic segments (with 752 spines) were used for the Fc + U73343 condition; 33 segments (with 752 spines) were used for the Fc + U73122 condition; 33 segments (with 686 spines) were used for the ephrin-A + U73343 condition; and 31 segments (with 704 spines) were used for the ephrin-A + U73122 condition. Quantifications were performed by an investigator blind to the experimental conditions and differences between samples were performed using a Kolmogorov-Smirnov test or analysis of variance (ANOVA) with a Student-Newman-Keuls *post-hoc* comparison.

Results

EphA4 activates PLCγ1 in heterologous cells and hippocampal slices

We recently reported that EphA4 activation with ephrin-A ligands induces dendritic spine retraction (Murai et al 2003a). However, the downstream signaling cascades of this receptor remain to be fully described. Using GST pulldown assays from hippocampal lysates, we initially found that EphA4 bound well to an SH2 domain of PLCγ1, a protein known to be important for phosphoinositide metabolism, cell morphology, and synaptic function (Rebecchi & Pentyala 2000). To follow up on this observation, we transfected EphA4 into COS7 cells (which have little endogenous EphA4) while over-expressing PLCγ1 (Figure 1A). EphA4 caused an increase in the phosphorylation of tyrosine 783 of PLCγ1, which is critical for PLCγ1 activity and is an indicator of its level of activation (Kim et al 1991; Poulin et al 2005). This phosphorylation event, however, was not detected after transfection of a kinase-dead form of EphA4, suggesting that kinase-dependent signaling is required for PLCγ1 activation downstream of EphA4.

We next were interested in determining if stimulation of EphA4 transfected COS7 cells with recombinant ephrin-A (versus control Fc) proteins would lead to an elevation in the phosphorylation of endogenous PLCγ1. In these experiments, we utilized endogenous PLCγ1 as we found there is high basal level of PLCγ1 in

COS7 cells. As shown in Figure 1B, ephrin-A stimulation caused a significant activation of PLCγ1 as indicated by its phosphorylation on tyrosine 783. This effect was observed with both recombinant ephrin-A3 Fc and ephrin-A5 Fc fusion proteins, but not control Fc (Fc vs. ephrin-A3 Fc, $p < 0.05$; Fc vs. ephrin-A5 Fc, $p < 0.01$; ANOVA). We further determined the specificity of this effect using lysates from EphA4 transfected cells stimulated with Fc or ephrin-A5 Fc and found that ephrin treatment caused a significant increase in PLCγ1 activation (pY783, 260% of control Fc stimulation; $p = 0.016$; two-tail t-test) (Figure 1C). Phosphorylation on tyrosine 771, a residue whose phosphorylation is not correlated with PLCγ1 activity (Kim et al 1991), or serine 1248 which is potentially an inhibitory phosphorylation site for protein kinases C and A (Park et al 1992) were not significantly changed (pY771; $p = 0.78$ two-tail t-test; pS1248; $p = 0.091$ two-tail t-test) (Kim et al 1991; Kim et al 1990). Consistent with these biochemical studies, we detected an increase in pY783 labelling of EphA4 transfected COS7 cells stimulated with ephrin-A Fc using immunofluorescence microscopy (Figure 1D). Increased labelling was especially apparent as clusters on the cell body and processes of stimulated cells. These combined results show that EphA4 stimulation with ephrin ligands induces PLCγ1 activation by specifically enhancing its phosphorylation on tyrosine 783.

To determine if ephrin stimulation could activate PLCγ1 signaling in the mouse hippocampus, we stimulated hippocampal slices with ephrin-A Fc and monitored the phosphorylation of EphA4 and PLCγ1. Similar to the experiments using COS7 cells, we found that ephrin-A Fc treatment caused an increase in phosphorylation of PLCγ1 on tyrosine 783 (Figure 2A). To examine the time-course for this activation, we stimulated slices for varying time periods and found that PLCγ1 activation was significantly increased after 45 minutes of ephrin stimulation (Figures 2B and 2C). These results demonstrate that ephrin-A stimulation can activate endogenous EphA4 and PLCγ1 signaling in slices derived from the hippocampus. However, based on these results we cannot conclude if PLCγ1 is activated earlier (i.e. between 15 and 45 minutes) after the onset of ephrin stimulation. Furthermore, we cannot exclude the possibility that EphA4

activates PLCγ1 through an intermediary protein or that other proteins are activated in parallel (i.e. a counteracting phosphatase) that cause the delayed kinetics of PLCγ1 activation.

EphA4 binds the C-terminal SH2 domain of PLCγ1 through juxtamembrane tyrosines

PLCγ1 is a multi-domain signaling protein that contains, in addition to functional catalytic regions, two SH2 domains (N- and C-terminal) and an SH3 domain. The SH2 domains of PLCγ1, in particular, have been shown to play an important role in regulating its function through protein interactions with activated receptor tyrosine kinases (Rebecchi & Pentyala 2000). We were interested in testing if EphA4 may interact with PLCγ1 through binding its SH2 domains. Indeed, EphA4 has been reported to recruit SH2 domain containing proteins including Fyn, Src, and Vav2 through its highly conserved juxtamembrane tyrosine residues (Cowan et al 2005; Kalo & Pasquale 1999). To address if EphA4 binds PLCγ1 through an SH2 domain interaction, we performed GST pulldown experiments using the SH2 domains of PLCγ1 fused to GST and EphA4 transfected COS7 cell lysates. We found that the C-terminal SH2 domain of PLCγ1 bound strongly to ephrin-A stimulated EphA4 expressing COS7 cells (Figure 3A). We could not detect binding of the N-terminal SH2 domain to EphA4. The binding to the C-terminal SH2 domain, however, was severely diminished after mutating either of the conserved juxtamembrane tyrosines of EphA4 to glutamic acid (Y596E or Y602E). Glutamic acid mutations have been shown to eliminate SH2 domain interactions of Eph receptors without interfering with kinase activity (Cowan et al 2005; Zisch et al 2000). We did observe very weak binding of the EphA4 Y596E mutant to the C-terminal SH2 domain of PLCγ1 upon long film exposures (data not shown), but no binding to the Y602E mutant. Phosphorylation of these tyrosines may function cooperatively to recruit PLCγ1.

We further extended these findings by investigating the requirement of the

EphA4 juxtamembrane tyrosines for PLCγ1 activation upon ephrin stimulation. We found that both the Y596E and Y602E mutants were compromised in their ability to activate PLCγ1 above control Fc treatment levels in the presence of ephrin stimulation (Figure 3B). However, the Y596E mutant appeared to have higher basal ability to cause PLCγ1 phosphorylation in the absence of ephrin, suggesting that this mutation may mimick phosphorylation on EphA4 and lead to a partial activation of PLCγ1 in the absence of ligand. The Y602E mutant, in contrast, only weakly phosphorylated PLCγ1 in the presence of ephrin, indicating that phosphorylation of tyrosine 602 of EphA4 is important for activating PLCγ1. Altogether, these results suggest that EphA4 utilizes juxtamembrane tyrosines to interact with the C-terminal SH2 domain of PLCγ1.

We also further tested the interaction between EphA4 and PLCγ1 by co-immunoprecipitation experiments, *in vitro* kinase assays, and double-label immunofluorescence in hippocampal slices. We found that EphA4 co-immunoprecipitated with PLCγ1 from lysates derived from COS7 cells (data not shown) and adult mouse hippocampus (Figure 3C). The EphA4 kinase domain was also able to phosphorylate Y783 of PLCγ1 (Figure 3D) in *in vitro* kinase assays. Furthermore, we found that EphA4 and PLCγ1 co-localized on at least a subset of spines (Supplemental Figure 2). However, we could not rule out the possibility that we did not detect the full extent of these proteins since immunofluorescence is not a sensitive method to detect the subcellular location of proteins in tissues. Thus, these proteins may be more prevalent than what is observed in Supplemental Figure 2. Synaptosome fractionation, a more sensitive technique, was carried out to further characterize the postsynaptic localization of PLCγ1.

PLCγ1 is localized in several compartments of brain synaptosomes and co-fractionates with postsynaptic density proteins

Several reports have implicated PLCγ1 in synaptic transmission and plasticity (Gartner et al 2006; Micheva et al 2001; Reyes-Harde & Stanton 1998). It also has

been shown that PLCγ1 is detected in the adult brain and hippocampus (CA1-3 regions) through *in situ* hybridization and immunohistochemistry (Gerfen et al 1988; Ross et al 1989). One report suggested that PLC isoforms function postsynaptically to block long-term synaptic plasticity (Reyes-Harde & Stanton 1998). This was observed after infusion of the PLC inhibitor, U73122, into CA1 pyramidal cells which blocked the induction of hippocampal long-term depression. However, it remains unclear whether PLCγ1 is positioned to influence the postsynaptic terminal, including dendritic spines. To pursue this issue, we purified brain synaptosomes and further separated them into pre- and postsynaptic elements (Phillips et al 2001). We found that PLCγ1 is found in multiple synaptic compartments, showing co-fractionation with presynaptic active zones and extra-junctional regions. However, similar to PSD-95, PLCγ1 was readily apparent in postsynaptic density fractions, including the triton-insoluble "core" PSD fraction (PSD III; see supplemental methods) (Figure 4). These results indicate that PLCγ1 is localized to various regions of the synapse including postsynaptic terminals and could play a role in regulating postsynaptic properties including dendritic spine structure.

PLC signaling maintains dendritic spine morphology

Since PLCγ1 is found in postsynaptic fractions of synaptosomes and is known to be involved in synaptic function, we were interested in testing whether PLCγ1 activity may influence postsynaptic dendritic spine morphology. To test this possibility, we used Semliki Forest viruses to introduce wild type PLCγ1 or a lipase-inactive mutant of PLCγ1 (PLCγ1 LIM) into CA1 pyramidal cells of organotypic hippocampal slices (Figure 5A). The latter of which has been shown to function as a dominant-negative protein (Huang et al 1995; Rong et al 2003; Ronnstrand et al 1999). We analyzed the morphology of CA1 pyramidal cell spines following 20 hours of expression. No apparent changes in overall dendrite length, branching or signs of dendritic pathology were observed in any of the conditions. Overexpression of wild type PLCγ1 did not significantly affect the

structural properties of dendritic spines when compared to EGFPf controls. Interestingly, the PLCγ1 LIM induced profound changes in spine morphology. In particular, spines showed a significant increase in length and area while the number of spines per unit length was reduced (Figure 5). In some cases, the spines showed an abnormal phenotype, having multiple head portions with a very complex architecture. However, most spines in this condition retained a bulbous appearance with an enlarged head portion attached to the dendritic shaft through a narrow neck region. This was further corroborated by classifying spines into mushroom, stubby, elongated, or other-type morphologies. We found that expression of the PLCγ1 LIM caused a significant loss of stubby spines. Although expression of wild type PLCγ1 did slightly reduce the amount of stubby spines, this effect was not significant when compared to the control. These results suggest that PLCγ1 signaling is required for spine stability and maintaining dendritic spine architecture, especially those with a stubby, retracted appearance.

In a separate set of experiments, we also tested the requirement of PLCγ1 in maintaining dendritic spine morphology. To investigate this, we performed RNA interference (RNAi) by biolistically delivering a plasmid to CA1 pyramidal cells that simultaneously induces the expression of a short-hairpin RNA directed against PLCγ1 (Supplemental Figure 1) and drives the expression of EGFPf. The sequence used for RNAi has been previously characterized and shown to selectively knock-down PLCγ1 expression, while leaving the expression of the closely related family member, PLCγ2, intact (Patterson et al 2002). A plasmid that drives the expression a scrambled sequence of the PLCγ1 shRNA was used as a control. Consistent with the experiments above using the PLCγ1 LIM, knock-down of PLCγ1 expression significantly reduced the density of dendritic spines. However, we could not detect significant changes in overall spine morphology or classification (data not shown). A potential explanation for this may be that the RNAi experiments were performed following 72 hours of knock-down in CA1 cells (versus 20 hours for the PLCγ1 LIM experiments). It is possible that spines with perturbed morphology collapsed during the 72 hour period of PLCγ1 knockdown which, in turn, caused the reduction in spine density.

We attempted to rescue the spine phenotype using a mutated form of PLCγ1 (with the RNAi site mutated in 4 wobble positions) but this was not successful (data not shown). However, many technical issues could have complicated the rescue. One reason may be due to the timing of expression of the PLCγ1 shRNA and the rescue protein, which utilize different promoters (H1 RNA pol III and CMV, respectively) and different cellular mechanisms for their production. Based on our experiments with PLCγ1 RNAi in NIH3T3 cells (which found that 72 hours was needed for efficient PLCγ1 knock-down), we assessed spine morphology and density in CA1 neurons in hippocampal slices following 72 hours of expression. However it was unclear if the lack of rescue was due to insufficient levels of the rescue protein present during PLCγ1 knock-down.

PLC signaling is necessary for ephrin-induced spine shrinkage

We next wanted to determine if PLCγ1 signaling was required for transmitting signals downstream of EphA4 in dendritic spines. Previously, we showed that EphA4 is localized on dendritic spines and 45 minutes of ephrin treatment of hippocampal slices induced spine retraction in a kinase-dependent manner (Murai et al 2003a). We further showed that EphA4 is the main EphA class receptor mediating these effects. Furthermore, stimulation of EphB receptors only induced small changes in dendritic spines in area CA1 of the hippocampus. To address if PLC signaling was required for the acute effects of ephrin treatment on dendritic spine morphology, we incubated hippocampal slices with either ephrin-A or control Fc proteins in the presence of either the PLC inhibitor U73122 (see methods) or control analog U73343 (Figure 6). We found that incubation of slices with control Fc proteins along with the PLC inhibitor did not significantly affect the individual parameters of dendritic spines. The PLC inhibitor, however, caused a significant reduction in mushroom-type spines when compared to the control condition (Fc with control analog) (Figure 6E), while not affecting the percentage of stubby, elongated, or other-type spines. This result differs from what we observed previously after longer-term expression of the PLCγ1 LIM and may reflect differential effects on spines under acute (PLC inhibitor) or prolonged

(PLCγ1 LIM) blockade of PLC signaling. Similar to what was reported previously (Murai et al 2003a), acute ephrin-A treatment induced spine retraction (Kolmogorov-Smirnoff two sample test; $p < 0.05$) and significantly promoted the generation of stubby spines (Figure 6E). The generation of these spines was likely at the expense of mushroom-type spines as overall spine density was not significantly perturbed in any of the treatments. Remarkably, simultaneous treatment of slices with U73122 along with ephrin blocked the effects of ephrin on inducing the stubby dendritic spine phenotype (Figure 6D and 6E). The percentage of both mushroom and stubby type spines was similar between conditions composed of the U73122 with either Fc or ephrin-A. These results suggest that PLC signaling is necessary for the effects of ephrin-A-induced generation of stubby and retracted dendritic spines. It should be noted that U73122, although specific for PLC enzymes, can inhibit multiple PLC isoforms (Smith et al 1990). However, the only other PLC isoform that is known to signal downstream of RTKs other than PLCγ1 is PLCγ2, whose expression is restricted to the anterior lobe of the pituitary and the cerebellum (Tanaka & Kondo 1994). However, we cannot rule out the possibility that Eph receptors can signal through other PLC proteins (i.e. PLC forms that are not commonly associated with RTKs) and that this signaling would be blocked by U73122.

PLC signaling regulates the localization of the actin depolymerizing and severing factor cofilin

Recent studies have proposed that PLCγ1, by generating IP_3 and DAG second messengers from cleavage of PIP_2, plays an important role in regulating cell membrane levels of PIP_2. PIP_2 itself can have dramatic effects on cell behavior and cytoskeletal-plasma membrane adhesion (Raucher et al 2000). PIP_2 may act as a second messenger by binding and modifying the activity state of various proteins including ion channels and actin binding proteins such as cofilin, a protein recently implicated in the structural plasticity of spines (Zhou et al 2004). Cleavage of PIP_2 by PLCγ1 may thus serve to modulate PIP_2-protein interactions. It has been shown that PIP_2 tethers gelsolin to the cell surface and releases it upon

EGF stimulation and PLCγ signaling (Chou et al 2002). We were interested in investigating the possibility that EphA4 and PLCγ1 signaling regulates cofilin association with the cell membrane since cofilin is highly expressed in dendritic spines, binds PIP_2, and has been implicated in mediating the effects of dendritic spine shrinkage upon low-frequency, LTD-inducing stimuli (Racz & Weinberg 2006; Zhou et al 2004). In order to test this, we performed cellular fractionation experiments where we isolated membrane components of COS7 cells following U73122 or control analog treatment. We found that blocking PLC activity with U73122 significantly enhanced the level of cofilin that was associated with the cell membrane (Figure 7A). This is in contrast to the transferrin receptor, a non-raft localized receptor associated with the cell membrane, whose membrane association was not altered by U73122 treatment. These results are in accordance with other reports that indicate that a portion of cofilin is associated with the cell periphery (Heyworth et al 1997; Suzuki et al 1995). Interestingly, we also found that transfection of EphA4 alone could reduce the levels of cofilin found in the membrane fraction. We could also further decrease this amount with ephrin-A stimulation (Figure 7B). Similarly, ephrin stimulation of hippocampal slices derived from postnatal day 10 mouse brain, also significantly caused a reduction in the level of cofilin associated with the cell membrane (Figure 7C). However, because we are using hippocampal tissue, the effects that we observed may be complicated by cofilin located in other cell types besides neurons that are found in slices such as oligdendrocytes and astrocytes.

These collective results suggest that EphA4 signaling and PLC activation contribute to the release of a pool of cofilin associated with the cell membrane. Removal of the membrane tethering of cofilin may release it from inhibition and allow it to bind and depolymerize actin filaments (DesMarais et al 2005).

Discussion

The structural properties of dendritic spines are believed to be closely linked to the physiology of excitatory synapses (Segal 2005). Spine anatomy is also

disrupted in several diseases affecting the brain including Down, Fragile-X, and Williams syndromes, suggesting altered synapse morphology is related to cognitive impairments (Sawa & Snyder 2002). Recent studies have elucidated the molecular composition of spines and mechanisms that govern their morphology (Tada & Sheng 2006). However, few reports have revealed the signaling cascades that couple receptors to direct regulators of the actin-rich cytoskeleton in spines. Here we report a novel signaling pathway downstream of the EphA4 receptor tyrosine kinase linking PLCγ1 to the actin depolymerizing/severing protein, cofilin. We found that ephrin stimulation promotes the interaction between the juxtamembrane tyrosines of EphA4 and the C-terminal SH2 domain of PLCγ1. PLCγ1 signaling is critical for maintaining spine morphology and PLC activity is required for ephrin-induced spine retraction. Remarkably, the amount of cofilin associated with the cell membrane is regulated by PLC and EphA4 activity. This signaling may be important for the local remodeling of the actin cytoskeleton in spines at sites of ephrin-A/EphA4 contact.

Spines rely on actin filaments for their dynamics and these filaments are in a constant state of equilibrium, cycling between filamentous actin (F-actin) and globular actin (G-actin) forms. Time-lapse imaging has shown that actin is rapidly reorganized in spines over minutes (Fischer et al 1998). LTP-inducing stimuli increases F-actin in spines which occurs during spine enlargement (Okamoto et al 2004). Low frequency stimulation, in contrast, increases G-actin levels and causes spine shrinkage. Furthermore, pharmacological inhibition of actin polymerization blocks the induction and maintenance of LTP in hippocampal slices (Kim & Lisman 1999) . Thus, actin filament dynamics are related to bidirectional changes in the structural and physiological plasticity of excitatory synapses.

Recent studies indicate a critical role for Eph receptors in spine morphogenesis and maintenance (Murai & Pasquale 2004). EphB2 induces spine development in hippocampal neurons by phosphorylating the proteoglycan syndecan-2 (Ethell et al 2001) and assembling a complex that elicits RhoA signaling (Moeller et al 2006). Other studies have shown that EphB2 activates the exchange factors intersectin and kalirin to promote spine development through

Cdc42 and Rac, respectively (Irie & Yamaguchi 2002; Penzes et al 2003). There is some redundancy for EphB receptors since only neurons from double and triple knock-outs of EphB1, EphB2 and EphB3 exhibit changes in spine density and morphology (Henkemeyer et al 2003; Hoogenraad et al 2005). Interestingly, F-actin is accumulated in dendritic shafts rather than spines of EphB knock-out mice, suggesting that EphB receptors influence the distribution of actin filaments (Henkemeyer et al 2003). To date, the only EphA receptor shown to modulate spine morphology is EphA4 (Murai et al 2003a). EphA4 is enriched in the developing and adult mouse hippocampus and is localized on spines (Murai et al 2003a; Murai et al 2003b). Activation of EphA4 by ephrin-A results in spine retraction (Murai et al 2003a). This could be mediated by EphA4 signaling induced by contact with ephrins on neurons or glia. Interestingly, during the review of this paper, a study showed that EphA4 mediates spine development through the Rho-family GTPase exchange factor, ephexin-1, and the serine/threonine kinase Cdk5 (Fu et al 2007). *In vivo*, EphA4 knock-out mice have disorganized and abnormally shaped spines (Murai et al 2003a) and decreases in early phase LTP and in LTD (Grunwald et al 2004). However, mice with the cytoplasmic portion of EphA4 replaced by GFP appear to have normal LTP and LTD under standard induction paradigms. Thus, EphA4 may have kinase-dependent and independent functions that control the structural and physiological plasticity of excitatory synapses. These collective studies demonstrate that Eph receptors are important determinants of spine shape *in vitro* and *in vivo*.

Our findings suggest that EphA4 regulates spine morphology through a pathway different from what has been previously described for Eph receptors. Many of the events downstream of Eph receptors require activation of small GTPases that remodel the spine's actin cytoskeleton. Eph receptors also interact with the PDZ-domain proteins, GRIP and AF6 (Hock et al 1998; Torres et al 1998). These interactions, however, may be more pertinent to receptor trafficking (Hoogenraad et al 2005). Our results suggest that EphA4 likely utilizes tyrosine 602 in the juxtamembrane region to activate PLCγ1 through its C-terminal

SH2-domain. Co-immunoprecipitation experiments further indicate that EphA4 and PLCγ1 can interact directly or within the same molecular complex in the hippocampus. EphA4 is known to recruit and bind several proteins including Src, Fyn, and Vav2 through SH2 domain interactions (Cowan et al 2005; Ellis et al 1996; Zisch et al 1998). The significance of these interactions at synapses has not been reported. Interestingly, cortical neurons derived from Fyn null mice show reduced spine density (Kalo & Pasquale 1999; Morita et al 2006). Thus, Fyn and PLCγ1 may similarly bind to the juxtamembrane tyrosines of EphA4 to modify synaptic structure. However, the delayed kinetics of PLCγ1 activation upon ephrin treatment and the fact that EphA4 and PLCγ1 only partially co-localize in a subset of spines leaves open the possibility that an intermediary protein downstream of EphA4 induces the activation of PLCγ1. Additional experiments are necessary to fully develop the direct or indirect nature of the EphA4-PLCγ1 interaction.

Upon activation by RTKs, phosphorylated PLCγ1 plays diverse roles in cellular behavior (Rebecchi & Pentyala 2000). Recent data suggests that PLCγ1 controls the level of membrane-bound PIP_2, which by itself acts as a potent second messenger that modifies actin-plasma membrane interactions and cell adhesion (DesMarais et al 2005; Raucher et al 2000). PIP_2 also modulates the function of many proteins including potassium and TRP channels (Lopes et al 2005; Rohacs et al 2005) and actin-binding proteins (Sechi & Wehland 2000). Furthermore, PIP_2 actively competes with actin for binding cofilin and inhibits its actin depolymerizing ability *in vitro* (Yonezawa et al 1991a; Yonezawa et al 1990). Reciprocally, cofilin binding to PIP_2 blocks PLCγ1-mediated cleavage of PIP_2 (Yonezawa et al 1991b). PLCγ-PIP_2 interactions are known to be important for the dynamic regulation of the actin cytoskeleton and for cell motility upon EGF stimulation (Chou et al 2002). Ephrin/EphA4 signaling may provide a trigger for PLCγ1-dependent regulation of cofilin at the cell surface in dynamic compartments of neurons such as spines and growth cones. At the same time, generation of the second messengers IP_3 and DAG by PIP_2 hydrolysis may influence synaptic function (Lynch et al 1988; Nagase et al 2003; Taufiq et al 2005). Further experiments are needed to determine if EphA4-PLCγ1 interactions

modify spine morphology and synaptic function through these second messenger systems.

Cofilin may exist in different transient states that are important for spine morphology. Reports have suggested that cofilin association near the cell membrane is enhanced when it is in the dephosphorylated, activated state (Mulholland et al 1994; Nagaoka et al 1996; Suzuki et al 1995). Phosphorylation of cofilin/ADF proteins on serine-3 also blocks their ability to bind actin (Morgan et al 1993; Moriyama et al 1996). Thus, PIP_2 may tether cofilin to the cell surface and maintain it in a "primed" (dephophorylated but inactive) state awaiting RTK autophosphorylation. Upon PLCγ1 activation by EphA4, cofilin may be released to depolymerize and sever actin filaments in the spine (Matus 2000). Cofilin may need to be released from PIP_2 inhibition and from the outer membrane perimeter of the spine in order to play a role in the "core" of the spine to alter its structure (Racz & Weinberg 2006).

Following release, Lim and Tes kinases may decrease cofilin activity through phosphorylation on serine-3. Indeed, Lim kinase 1 (LK1) knockout mice have reductions in cofilin phosphorylation and spine size (Meng et al 2002). This is consistent with cofilin promoting actin filament disassembly and spine shrinkage (Zhou et al 2004). Physiological recordings and behavioural analysis of LK1 knock-out mice have shown that basal synaptic transmission is normal, however, the mice have elevated LTP and impairments on memory tasks (Meng et al 2002). Additionally, a microRNA that reduces the translation of LK1 is modulated by BDNF and blocks spine development (Schratt et al 2006). Cofilin is reactivated by slingshot proteins through dephosphorylation of serine-3 (Niwa et al 2002) and the mRNAs for these proteins are found in the developing and adult mouse brain (Ohta et al 2003). The role of SSH proteins in regulating spine morphology, however, remains unknown. Remarkably, a recent study suggests that cofilin phosphorylation/dephosphorylation events are not necessarily required for cofilin activity in dynamic leading edges of carcinoma cells in response to EGF treatment (Song et al 2006). In this context, translocation of cofilin is likely critical for its function in cellular remodeling. This supports the hypothesis that cofilin exists in

different states and is regulated at multiple levels to control its localization and activity.

In summary, our results provide new insight into how EphA receptors control spine morphology. The combinatorial control over multiple downstream targets of activated EphA and B receptors, including signaling through PLCγ1, ephexin-1, Rho-family GTPases and cofilin, is likely required for proper spine development and maintenance.

Figures

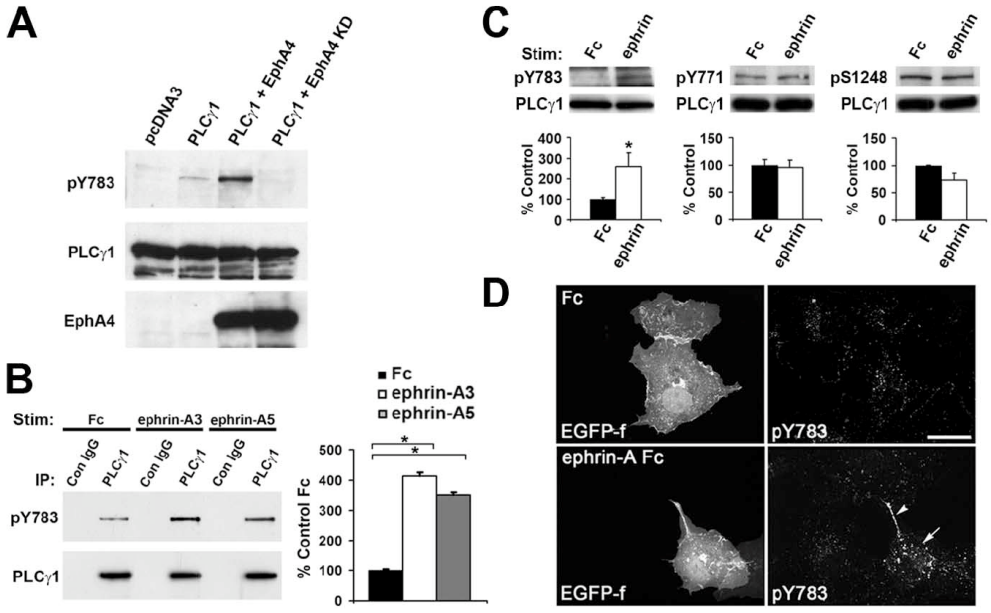
A
pcDNA3
PLCγ1
PLCγ1 + EphA4
PLCγ1 + EphA4 KD
pY783
PLCγ1
EphA4
B
Stim:
Fc
ephrin-A3
ephrin-A5
IP:
Con IgG
PLCγ1
pY783
PLCγ1
% Control Fc
C
Stim:
Fc
ephrin
pY783
PLCγ1
pY771
pS1248
% Control
D
Fc
EGFP-f
pY783
ephrin-A Fc

Figure 3-1. EphA4 activates PLCγ1. (A) Transfection of EphA4 increased the phosphorylation of overexpressed PLCγ1 on tyrosine 783, a site known to correlate with PLC activity. Expression of a kinase-dead form of EphA4, however, did not elevate PLCγ1 phosphorylation. Note that transfection of PLCγ1 alone led to a slight increase in phosphorylation over the control transfected condition (pcDNA3). Shown are blots of lysates derived from cells transfected with the indicated constructs. (B) Stimulation (Stim) of EphA4 transfected COS7 cells for 45 minutes with ephrin-A3 Fc or ephrin-A5 Fc induced phosphorylation of endogenous PLCγ1. PLCγ1 was immunoprecipitated after stimulation of cells with control Fc, ephrin-A3 Fc or ephrin-A5 Fc and probed for phosphorylation on tyrosine 783. The membrane was subsequently stripped and reprobed for PLCγ1. Control IgG's were used to confirm the specificity of the immunoprecipitation. Quantification of these changes showed that both ephrin-A3 Fc and ephrin-A5 Fc significantly increased PLCγ1 phosphorylation (*$p < 0.05$; ANOVA). (C) Immunoblots of lysates of cells stimulated with control Fc or ephrin-A Fc. Ephrin-A stimulation caused a significant increase in phosphorylation of Y783, but not Y771 or S1248 of PLCγ1 (*$p < 0.02$, t-test). (D) Immunofluorescence labeling showing increased labeling of EphA4 transfected COS7 cells with the anti-pY783 antibody. Note that the labeling was seen as clusters on the cell body (arrow) and processes (arrowhead) of EphA4, but not control transfected cells (EGFP-f). KD, kinase-dead, Scale bar, 30 μm. Error bars indicate SEM.

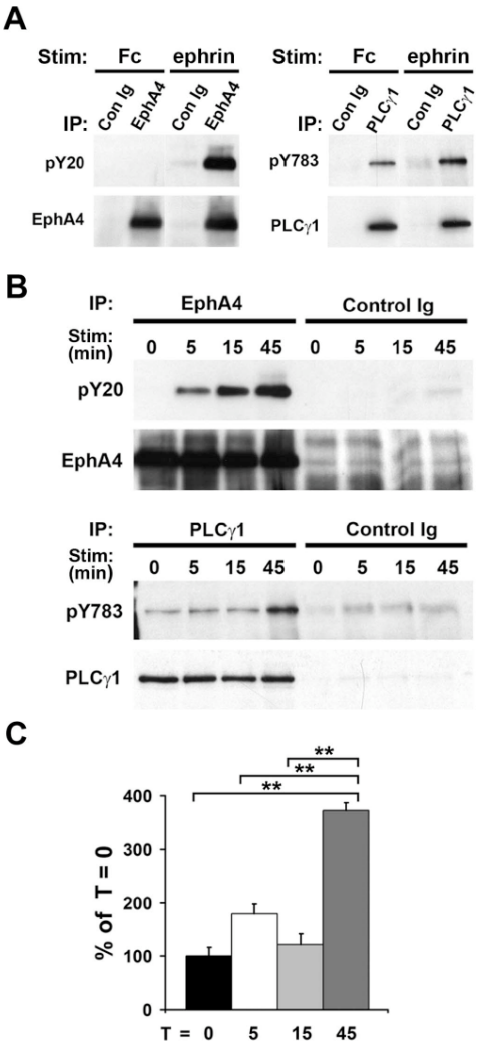
A
Stim:
Fc
ephrin
Con Ig
EphA4
IP:
pY20
EphA4
Stim:
Fc
ephrin
Con Ig
PLCγ1
IP:
pY783
PLCγ1
B
IP:
EphA4
Control Ig
Stim: (min)
0 5 15 45 0 5 15 45
pY20
EphA4
IP:
PLCγ1
Control Ig
Stim: (min)
0 5 15 45 0 5 15 45
pY783
PLCγ1
C
**
**
**
400
300
200
100
0
% of T = 0
T = 0 5 15 45

Figure 3-2. Ephrin stimulation induces the activation of PLCγ1 in hippocampal slices. (A) Stimulation (Stim) of hippocampal slices with ephrin-A Fc induced phosphorylation of endogenous EphA4 and PLCγ1. After 45 min of ephrin-A Fc or control Fc stimulation of slices, EphA4 or PLCγ1 were immunoprecipitated and blotted for phosphotyrosine (pY20) or pY783 of PLCγ1, respectively. Control IgGs were used to confirm the specificity of the immunoprecipitation (IP). Membranes were subsequently stripped and reprobed for either EphA4 or PLCγ1 to ensure that equal amounts of protein were initially immunoprecipitated. (B,C) Time-course analysis showing PLCγ1 phosphorylation following 45 min of stimulation. Quantification of these changes showed a significant increase in phosphorylation at 45 min (**$p < 0.01$; ANOVA). Error bars indicate SEM.

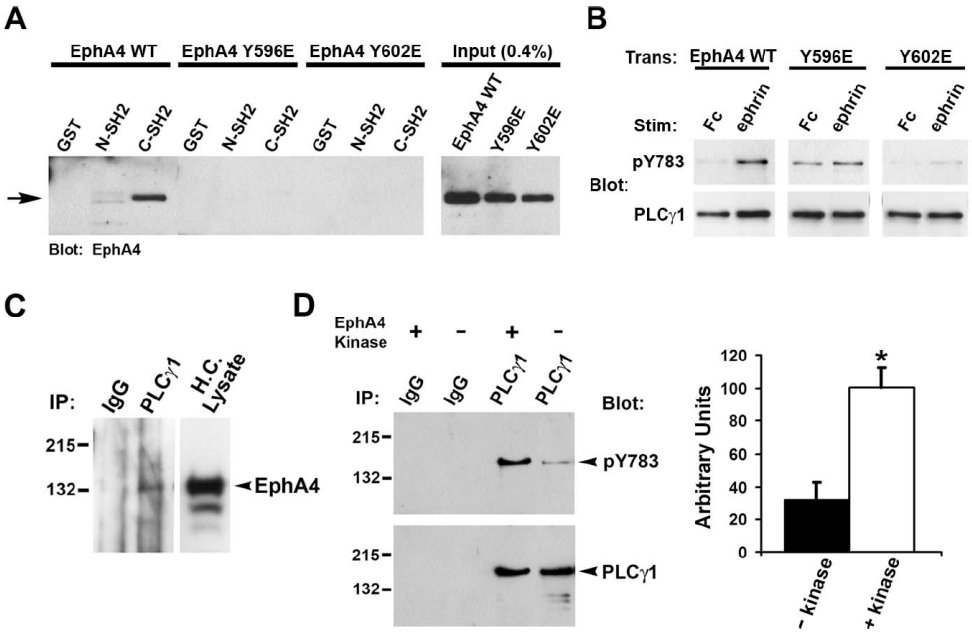
A
EphA4 WT
EphA4 Y596E
EphA4 Y602E
Input (0.4%)
GST
N-SH2
C-SH2
EphA4 WT
Y596E
Y602E
Blot: EphA4
B
Trans: EphA4 WT
Y596E
Y602E
Stim:
Fc
ephrin
Blot:
pY783
PLCγ1
C
IP:
IgG
PLCγ1
H.C.
Lysate
215
132
EphA4
D
EphA4 Kinase
+
-
IP:
IgG
PLCγ1
Blot:
pY783
PLCγ1
Arbitrary Units
120
100
80
60
40
20
0
*
- kinase
+ kinase

Figure 3-3. EphA4 interacts with PLCγ1. (A) GST pulldown assay using the N- (N-SH2) and C-terminal SH2 domains (C-SH2) of PLCγ1 and lysates from COS7 cells transfected with wild type EphA4, Y596E EphA4 mutant, or Y602E EphA4 mutant and stimulated with ephrin-A Fc. EphA4 strongly bound the C-terminal SH2 domain of PLCγ1. We observed very weak binding of the C-terminal SH2 domain to the Y596E mutant upon long film exposures. Lysates to the right (representing only 0.4% of total input) confirm the expression of the transfected receptors in each of the conditions used for the pulldown experiments. (B) Stimulation of transfected (trans) COS7 cells expressing wild-type, Y596E, or Y602E mutants of EphA4 with ephrin-A Fc showed that both Y596E and Y602E EphA4 mutants have compromised ability to activate PLCγ1 upon ephrin-A stimulation. PLCγ1 was immunoprecipitated after stimulation of cells with control Fc or ephrin-A Fc and probed for phosphorylation on tyrosine 783. The membrane was subsequently stripped and reprobed for PLCγ1. The Y596E mutant appeared to have higher basal ability to activate PLCγ1. The Y602E mutant showed only low levels of PLCγ1 activation upon ephrin-A stimulation. (C) EphA4 co-immunoprecipitated with PLCγ1 from postnatal day 21 mouse hippocampus. PLCγ1 or control IgG immunoprecipitates were blotted for EphA4. (D) PLCγ1 immunoprecipitates were subjected to *in vitro* kinase assays with or without a recombinant EphA4 kinase domain. The EphA4 kinase domain phosphorylated PLCγ1 on tyrosine 783. The blots were subsequently stripped and reprobed for PLCγ1 protein (*$p < 0.05$; t-test). Error bars indicate SEM.

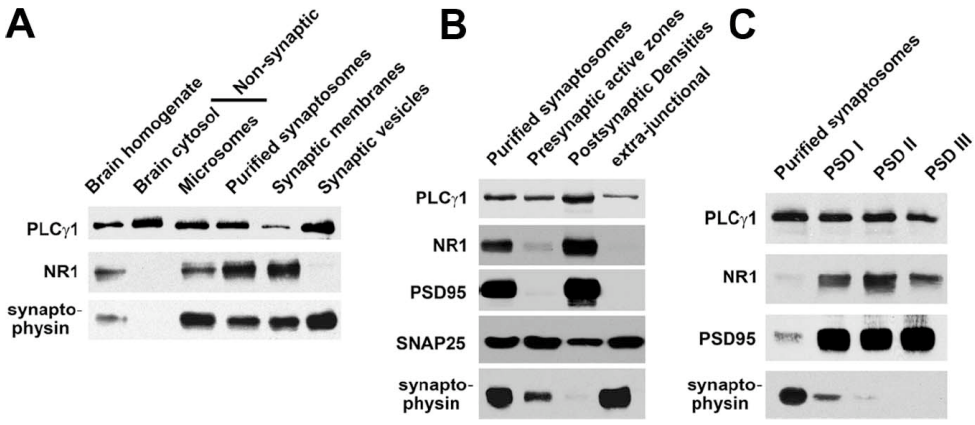
A
Brain homogenate
Brain cytosol
Non-synaptic
Microsomes
Purified synaptosomes
Synaptic membranes
Synaptic vesicles
PLCγ1
NR1
synapto-physin
B
Purified synaptosomes
Presynaptic active zones
Postsynaptic Densities
extra-junctional
PLCγ1
NR1
PSD95
SNAP25
synapto-physin
C
Purified synaptosomes
PSD I
PSD II
PSD III
PLCγ1
NR1
PSD95
synapto-physin

Figure 3-4. PLCγ1 is found in multiple compartments of synaptosomes, but is enriched in postsynaptic density fractions. (A) PLCγ1 was found in non-synaptic fractions (cytosolic and microsomal) and in synaptic membranes and vesicles in the adult mouse brain as shown by immunoblotting with the anti-PLCγ1 polyclonal antisera. Antibodies against NR1 and synaptophysin were used as synaptic membrane and synaptic vesicle markers, respectively. (B) PLCγ1 was present on both sides of the synapse. PLCγ1 was detected in presynaptic active zones and extra-junctional membrane fractions and was readily apparent in the PSD fraction. SNAP25 and PSD95 were used as presynaptic and post-synaptic density markers, respectively. (C) PLCγ1 is strongly associated with PSDs. PLCγ1 was insoluble to 1% Triton X-100 (PSD I and II) and 3% sarcosyl (PSD III) and remained associated with the "core" PSD (PSD III; see supplemental methods).

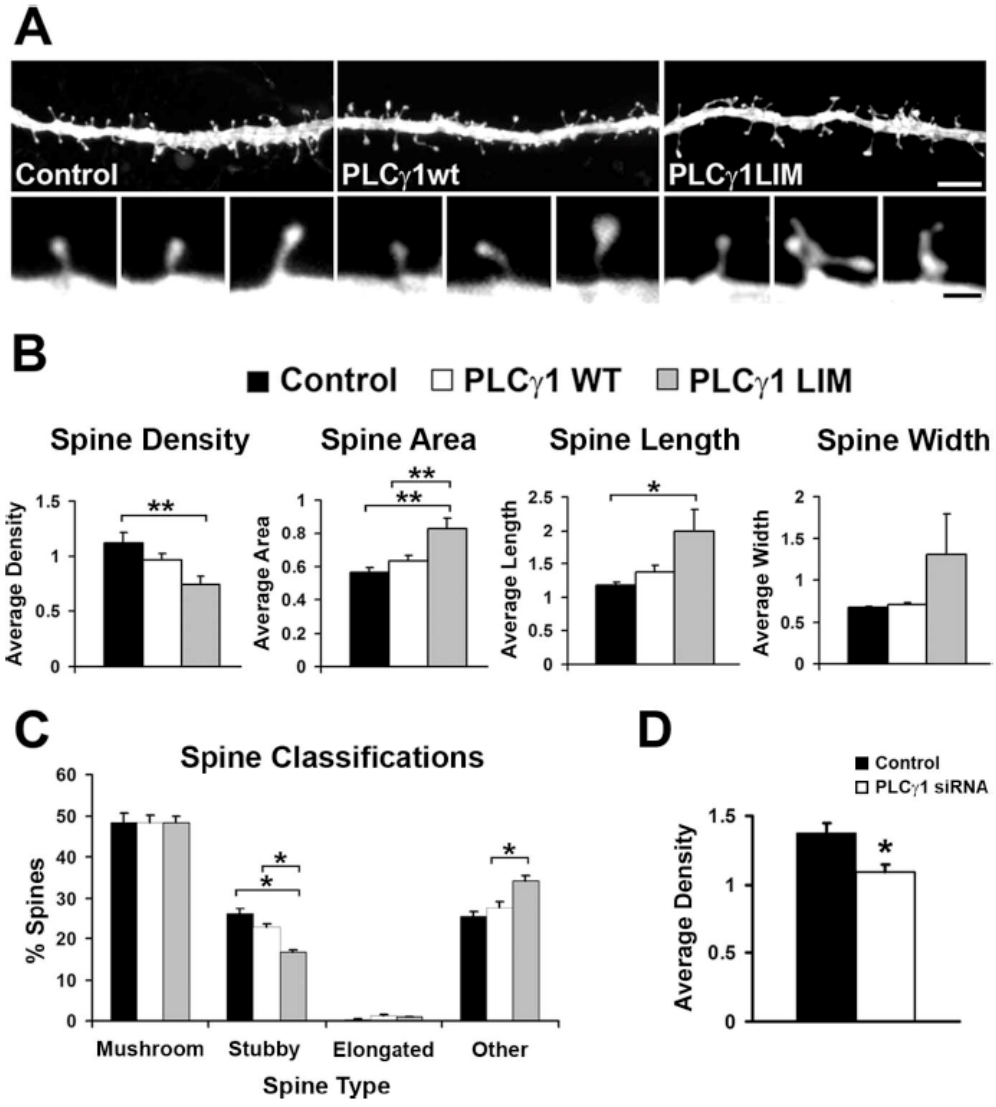
A
Control
PLCγ1wt
PLCγ1LIM
B
Control
PLCγ1 WT
PLCγ1 LIM
Spine Density
Spine Area
Spine Length
Spine Width
Average Density
Average Area
Average Length
Average Width
C
Spine Classifications
% Spines
Mushroom
Stubby
Elongated
Other
Spine Type
D
Control
PLCγ1 siRNA
Average Density

Figure 3-5. PLCγ1 activity is necessary for maintaining CA1 dendritic spine morphology. (A) Examples showing abnormal dendritic spine morphology after expression of the PLCγ1 LIM (lipase-inactive mutant) when compared to control CA1 cells expressing membrane-targeted EGFPf. (B) Quantification of spine parameters showed that spine density was significantly reduced following expression of the PLCγ1 LIM when compared to control. Significant increases in area and length of spines were also found. Spine width, although on average larger in the PLCγ1 LIM condition, was not significantly different among groups. No prominent changes were observed after overexpressing wild type PLCγ1 (*$p < 0.05$, ** $p < 0.01$, ANOVA with Student-Newman-Keuls *post-hoc* comparisons). (C) Expression of the PLCγ1 LIM also induced a significant decrease in the number of stubby-type spines (*$p < 0.05$, ** $p < 0.01$, ANOVA with Student-Newman-Keuls *post-hoc* comparisons). (D) RNAi in organotypic slices following biolistic delivery of a vector expressing a PLCγ1 shRNA showed that PLCγ1 is necessary for maintaining spine density (*$p < 0.05$. t-test). Scale Bars: A, 5 μm, high magnification images of individual spines, 1 μm. Error bars indicate SEM.

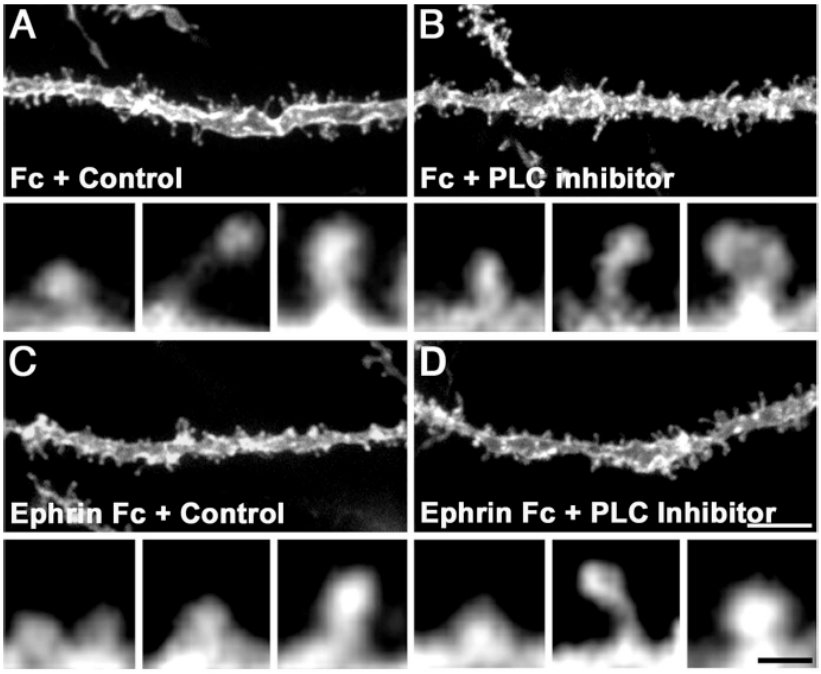
A
Fc + Control
B
Fc + PLC inhibitor
C
Ephrin Fc + Control
D
Ephrin Fc + PLC Inhibitor

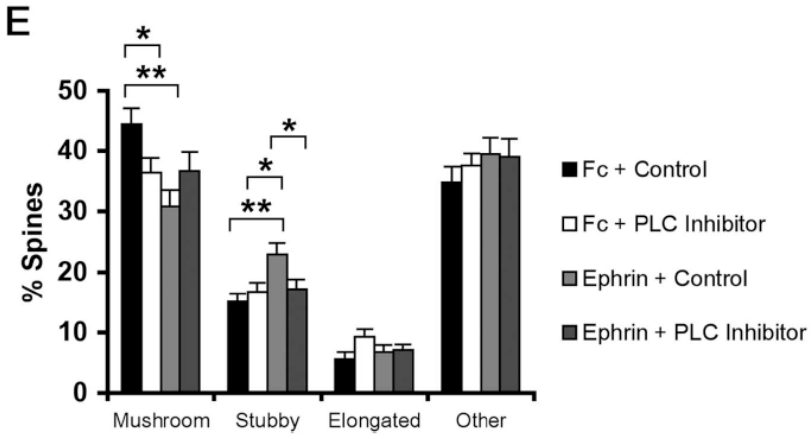
E
% Spines
50
40
30
20
10
0
Mushroom
Stubby
Elongated
Other
Fc + Control
Fc + PLC Inhibitor
Ephrin + Control
Ephrin + PLC Inhibitor

Figure 3-6. PLC activity is necessary for ephrin-A induced dendritic spine retraction. DiI-labeled CA1 dendritic spines in hippocampal slices stimulated with Fc and control analog (A), Fc and PLC inhibitor (B), ephrin Fc and control analog (C), or ephrin Fc and PLC inhibitor (D). Note the retracted appearance of dendritic spines in (C). Classification of spines showed that application of the PLC inhibitor blocked the ability of ephrin to induce a retracted, stubby spine phenotype. Treatment of slices with Fc or ephrin Fc with the PLC inhibitor significantly decreased the percentage of mushroom shaped spines, suggesting that blocking PLC activity alone can destabilize mushroom-type spines (*$p < 0.05$, **$p < 0.01$, ANOVA with Student-Newman-Keuls *post-hoc* comparisons). Scale Bars: 5 μm in (A) and 0.5 μm in high magnification. Error bars indicate SEM.

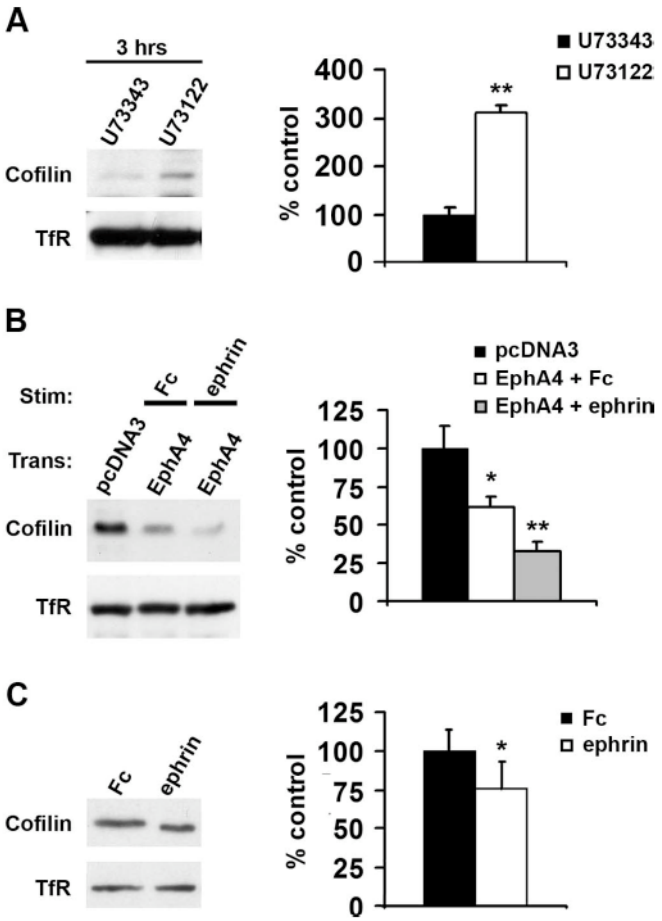
A
3 hrs
U73343
U73122
Cofilin
TfR
U73343
U73122
% control
400
300
200
100
0
**
B
Stim:
Fc
ephrin
Trans:
pcDNA3
EphA4
EphA4
Cofilin
TfR
pcDNA3
EphA4 + Fc
EphA4 + ephrin
% control
125
100
75
50
25
0
*
**
C
Fc
ephrin
Cofilin
TfR
Fc
ephrin
% control
125
100
75
50
25
0
*

Figure 3-7. PLC activity and ephrin stimulation alter the membrane association of the actin depolymerizing/severing protein cofilin. (A) Application of the PLC inhibitor (3 hrs) increased the levels of cofilin associated with the cell membrane of COS7 cells. The transferrin receptor (TfR) was used to ensure equal loading among lanes. (B) EphA4 expression in COS7 cells reduces the membrane-association of cofilin. This association was further reduced by ephrin stimulation (*$p < 0.05$; ANOVA with Student-Newman-Keuls *post-hoc* comparisons; **$p < 0.01$; t-test or ANOVA with Student-Newman-Keuls *post-hoc* comparisons). (C) Ephrin treatment of postnatal day 10 hippocampal slices also reduced the level of cofilin associated with the cell membrane (*$p < 0.05$; t-test). Error bars indicate SEM.

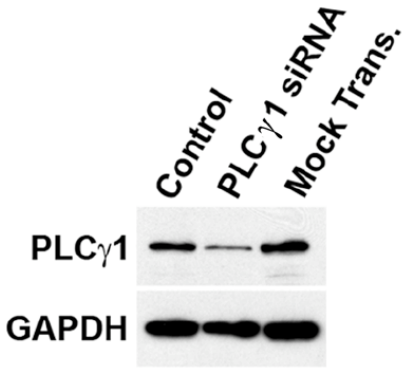
Control
PLCγ1 siRNA
Mock Trans.
PLCγ1
GAPDH

Supplemental Figure 3-1. Knock-down of PLCγ1 expression using RNAi. A pSUPER plasmid inducing the expression of a short-hairpin RNA directed against PLCγ1 and driving EGFPf was used for RNAi in NIH3T3 cells. The sequence used for RNAi has been previously characterized and shown to selectively knock-down PLCγ1 expression, while leaving the expression of the closely related family member, PLCγ2, intact (Patterson et al 2002). A plasmid that drives the expression a scrambled sequence of the PLCγ1 shRNA and EGFPf was used as a control. To verify the efficacy of the PLCγ1 RNAi, 10μg of control or PLCγ1 shRNA plasmid was transfected into NIH3T3 cells. 72 hours following transfection, the cells were lysed and the level of PLCγ1 protein detected by western blot. Blotting for GAPDH verified approximate equal loading between lanes. In the mock transfection lane, cells were subjected to the same experimental conditions except the DNA was omitted.

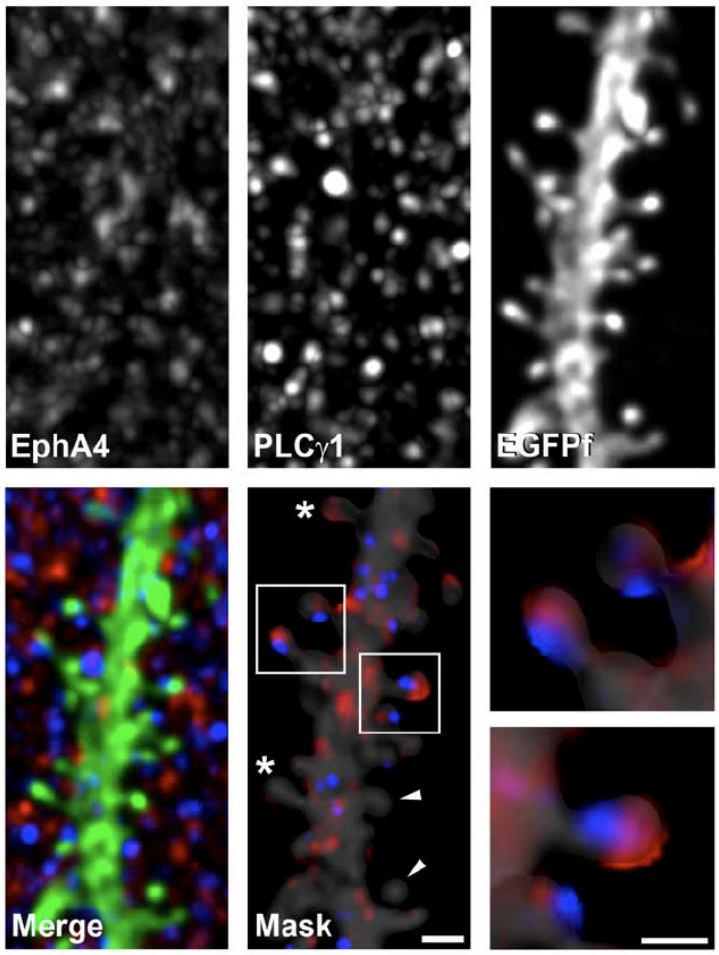
EphA4
PLCγ1
EGFPf
Merge
Mask
*
*

Supplemental Figure 3-2. EphA4 and PLCγ1 partially colocalize in CA1 pyramidal cell dendritic spines. Max projection of an EGFPf-infected organotypic hippocampal CA1 pyramidal neuron apical dendrite (green) immunolabeled for EphA4 (red) and PLCγ1 (green). (TOP) Shown are individual channels in grayscale for EphA4, PLCγ1 and EGFPf, respectively. (BOTTOM) Merged image showing a composite of the three channels above. Masked image refers to the same field shown to the left following a three-dimensional "masking" procedure to preserve only the EphA4 and PLCγ1 punctae found within the volume of the dendrite. High magnification images show spines that reveal co-expression of both EphA4 and PLCγ1. Asterisks label example spines that have EphA4 only (or low levels of PLCγ1) and arrowheads show spines that do not have (or have low levels of) EphA4 or PLCγ1. Scale bars, 1 μm.

Supplemental Material and Methods

Synaptosome Preparations

Brain fractions were prepared according to the method described in (Huttner et al 1983). Briefly, 3-4 adult mice were anesthesized with Halothane, decapitated and the forebrains dissected out on ice. All the procedures necessary to prepare the brain fractions were done at 0-4°C and aliquots of all brain fractions were saved for western blot purposes. The forebrains were homogenized with 9 up-and-down strokes at 900 rpm in 10 volumes (w/vol.) of an ice-cold sucrose/HEPES buffer (0.32M Sucrose, 10 mM HEPES and protease inhibitors (100 µg/ml Benzamidine, 0.5 µg/ml aprotonin, 0.5 µg/ml leupeptin and 20 µg/ml PMSF), pH 7.4). The nuclear material (P1) was removed by centrifugation at 1,000xg for 10 min and the supernatant (S1) was centrifuged at 17,500xg for 30 min. The resulting supernatant (S2) was used to prepare S3 (cytosol) and P3 (microsomes) fractions (see below). The pellet P2 (crude synaptosomal fraction) was resuspended with sucrose/HEPES buffer and layered on top of a discountinous sucrose gradient (2.6, 1.2 and 0.8 M). The gradient was ultracentrifuged as described in (Corera et al 1996). 6ml of a fraction, collected at the 0.8/1.2M interface, was washed by addition of 2 volumes of sucrose/HEPES buffer followed by a centrifugation at 20,000 x g for 20 min. The final pellet P2' (purified synaptosomal fraction) was resuspended in approximately 2 ml of sucrose/HEPES buffer.

One to 1.5 ml of P2' was osmotically lysed in 10 volumes of HEPES buffer [10 mM HEPES and the above mentioned protease inhibitors, pH 7.4], homogenized with 3 up-and-down strokes at 2,000 rpm and centrifuged at 33,000 x g for 20 min. The pellet LP1 (total membrane fraction) is resuspended in sucrose/HEPES buffer whereas the supernatant (LS1) as well as the S2 fraction were ultracentrifuged at 260,000 x g for 2 h to obtain respectively LP2 (crude synaptic vesicle fraction) and P3 pellets. Protein concentrations were determined with the BCA protein assay kit (Pierce), using BSA as a standard.

Presynaptic, postsynaptic and "extra-junctional" proteins were separated according to the method previously described in (Phillips et al 2001) with some modifications. Briefly, 1 volume of purified synaptosomes (P2') was diluted 1:10 with ice-cold 0.1 mM $CaCl_2$ solution, and an equal volume of 2 X solubilization buffer (2% Triton X-100, 40 mM Tris, pH 6.0) was added to the suspension. At pH 6, the synaptic junctional complexes can be isolated in high yield and purity. Membranes were incubated for 30 min on ice with gentle agitation and the insoluble synaptic junctions were pelleted (40,000 x g, 30 min). The supernatant ("extra-junctional" fraction) was decanted and proteins precipitated with 6 volumes acetone at -20°C, and recovered by centrifugation at 18,000 x g for 30 min. The pellet was washed twice in pH 6.0 solubilization buffer, resuspended in pH 8.0 solubilization buffer (1% Triton X-100, 20 mM Tris, pH 8.0; 10 volumes of the initial P2' suspension) and incubated for 30 min on ice with gentle agitation, and centrifuged at 40,000 x g for 30 min. This pH elevation (6 – 8) solubilizes the extracellular matrix, releasing the presynaptic active zone (supernatant) from the postsynaptic densities, which remain in the insoluble fraction. The latter fraction was subjected to a subsequent extraction in the pH 8.0 solubilization buffer and centrifuged as above for a maximum recovery of the presynaptic active zone proteins. The two supernatants were combined, precipitated with acetone and spun down for 30 min at 18,000 x g. The subsynaptic fractions were solubilized in 5% SDS, and the protein contents quantified as above.

PSD fractions were obtained as described in (Cho et al 1992). Briefly, P2' fraction was resuspended with 50 mM Tris buffer (pH 7.4) containing 0.5% Triton X-100 and incubated on ice for 20 min. Solubilized P2' was centrifuged (32,000 x g, 20 min) and the resulting pellet (PSD I fraction) was resuspended in 50 mM Tris buffer. PSD II and III fractions were obtained by solubilizing 1 volume of the PSD I fraction with 8 volumes of either 50 mM Tris buffer (pH 7.4) containing 0.5% Triton X-100 or 3% sarcosyl in 50 mM Tris buffer containing 1mM EDTA, respectively, followed by centrifugation at 200,000 x g for 1h. The resulting PSD II and III fractions were solubilized in 5% SDS and the proteins quantified as above. Equal amount of proteins of each fraction were separated on SDS-PAGE

and blotted onto nitrocellulose membrane. The membranes were incubated with antibodies and revealed with enhanced chemiluminescence (Pierce).

References for Supplemental Material and Methods

Cho KO, Hunt CA, Kennedy MB (1992) The rat brain postsynaptic density fraction contains a homolog of the Drosophila discs-large tumor suppressor protein. Neuron 9:929-942.

Corera AT, Costentin J, Bonnet JJ (1996) Effect of low concentrations of K+ and Cl- on the Na(+)-dependent neuronal uptake of [3H] dopamine. Naunyn-Schmiedebergs Archives of Pharmacology 353:610-615.

Huttner WB, Schiebler W, Greengard P, De Camilli P (1983) Synapsin I (protein I), a nerve terminal-specific phosphoprotein. III. Its association with synaptic vesicles studied in a highly purified synaptic vesicle preparation. Journal of Cell Biology 96:1374-1388.

Phillips GR, Huang JK, Wang Y, Tanaka H, Shapiro L, Zhang W, Shan WS, Arndt K, Frank M, Gordon RE, Gawinowicz MA, Zhao Y, Colman DR (2001) The presynaptic particle web: ultrastructure, composition, dissolution, and reconstitution.[see comment]. Neuron 32:63-77.

In the previous chapter, I demonstrated that PLCγ1 regulates cofilin through controlling its membrane association. After it is released from the cell membrane, cofilin enters another level of regulation through phosphorylation/dephosphorylation by kinases and phosphatases. In chapter 4, I focuse on cofilin phosphatase Slingshot and its roles in regulating dendritic spine morphology downstream of EphA receptors.

Chapter 4 EphA Signaling Through Slingshot Regulates Dendritic Spine Plasticity

The text in this chapter is a reprint from a manuscript prepared for peer review.

EphA Signaling Through Slingshot Regulates Dendritic Spine Plasticity

(EphA signaling and slingshot promote spine plasticity)

Lei Zhou, Emma V. Jones, and Keith K. Murai*

Centre for Research in Neuroscience, Department of Neurology and Neurosurgery, The Research Institute of the McGill University Health Centre, Montreal General Hospital, 1650 Cedar Avenue, Montreal, QC, H3G 1A4 Canada.

Contribution of Authors

I performed the majority of the experiments including constructing SSH plasmids, performing all the ephrin treatment studies, cell rounding assays, SSH1 knock-down experiments, immunostaining studies, and spine morphology analysis as shown in figures in the manuscript. Emma V. Jones helped to purify the SSH antibody, performed part of the ephrin stimulation experiment as shown in figure 1C, and helped with part of the SSH1 expression pattern study as shown in figure 3A.

Abstract

The morphological plasticity of dendritic spines is believed to play an important role in storing information at excitatory synapses in the brain. Imaging studies have revealed that stimuli that drive neural circuit activation also lead to modifications in dendritic spines. At the molecular level, spine remodeling is highly dependent on actin filament reorganization. However, the upstream receptors and signaling pathways that provoke actin-based spine changes remain to be fully described. Previously we demonstrated that EphA receptor signaling promotes the structural plasticity of spines. We now show that EphA receptors signal through the slingshot 1 (SSH1) phosphatase to activate the actin filament depolymerizing/severing factor cofilin in heterologous cells and neurons. In the hippocampus, SSH1 expression is developmentally regulated and SSH1 phosphatase activity is required to preserve normal spine morphology of CA1 pyramidal neurons in organotypic slices and dissociated neurons. Interestingly, both SSH1 and the upstream phosphatase calcineurin are required for EphA-induced morphological changes in heterologous cells and remodeling of spines in hippocampal neurons. These findings indicate that EphA receptors facilitate the structural plasticity of synapses by activating cofilin and rearranging actin filaments in spines.

Introduction

The reorganization of dendritic spines is implicated in learning and memory processes in the brain and many findings support the concept that spines are shaped by synaptic activity and experience (Kasai et al 2010). Single synapse analysis has shown that spines exhibit activity-dependent changes in size, although other studies didn't see the same effect (Bagal et al 2005; Okamoto et al 2004). Furthermore, spine number and turnover can be regulated *in vivo* by behavioral training (Roberts et al 2010; Xu et al 2009; Yang et al 2009). Thus, spine remodeling is likely an important feature of neurons that is needed for the

storage of information at synapses.

Spines vary in morphology and size, but typically have an enlarged head that is connected to the dendrite shaft by a constricted neck. This architecture helps compartmentalize ion channels, scaffolding proteins and other signaling components at postsynaptic sites. At the interface between the structural and molecular properties of spines is an array of actin filaments (Matus 2000). Actin filaments play numerous roles in regulating synapses including anchoring proteins to the synapse and controlling spine morphology. Several pools of actin are enriched in spines and in a constant state of dynamic equilibrium between filamentous and globular forms (Honkura et al 2008; Star et al 2002). This equilibrium is re-adjusted by synaptic activity (Okamoto et al 2004) and the recruitment of molecules that fine-tune the actin cytoskeleton (Ethell & Pasquale 2005). Interestingly, increases and decreases in actin polymerization and spine size occur with LTP and LTD-inducing stimuli, respectively (Okamoto et al 2004). Furthermore, stabilizing actin filaments or inhibiting actin polymerization blocks spine dynamics and prevents the induction and maintenance of LTP in hippocampal slices (Kim & Lisman 1999). Thus, reorganization of the actin network is important for spine remodeling and associated changes in synaptic strength.

One class of proteins that triggers changes in spines are receptors of the Eph family (Klein 2009; Lai & Ip 2009). EphAs and EphBs comprise a family of receptor tyrosine kinases that are activated by ligands known as ephrins (Murai & Pasquale 2003). Ephs activate factors that regulate actin cytotoskeletal reorganization (Ethell & Pasquale 2005). EphBs promote spine development and stability following their maturation through members of Rho-family of small GTPases (Henkemeyer et al 2003b; Kayser et al 2008; Shi et al 2009) while EphAs induce spine remodeling through several mechanisms (Murai et al 2003a; Zhou et al 2007). However, the direct mechanisms that enable Ephs to stabilize or remodel the actin cytoskeleton in spines are not well understood. Here we dissect the signaling pathways downstream of EphAs that regulate the structural plasticity of spines. We identify that EphAs activate the actin depolymerising/severing

factor cofilin to regulate cell morphology and spines. Importantly, EphA-induced cofilin activation and spine remodeling requires the function of the cofilin phosphatase SSH1 and its upstream phosphatase calcineurin. This study identifies a novel pathway utilized by EphAs to reorganize the actin network in spines.

Methods

DNA constructs. Full-length V5-tagged, human Slingshot 1 and a phosphatase-inactive mutant (C393S) were cloned into pcDNA3 (Hsieh et al 2006). For Semliki Forest virus (SFV) constructs, V5-tagged SSH1 or the C393S mutant cDNAs were subcloned into the vector pScaPD containing a viral subgenomic promotor followed by farnesylated enhanced green fluorescent protein (EGFP-f) (Lundstrom et al 2003; Zhou et al 2007). Control plasmid contains only EGFP-f.

Antibodies, recombinant proteins and inhibitors. A custom rabbit polyclonal antibody was raised against a synthesized peptide containing a sequence of 16 amino acids of SSH1 (KSAPEHLKSPSRVNKS) that covers a conserved region in both human and mouse SSH1, but not retained in SSH2 or SSH3. Antibodies for the following proteins were also used: Cofilin (Cell Signaling Technology, Beverly, MA); phospho-Cofilin (Cell Signaling Technology); GAPDH (Abcam, Cambridge, MA); Actin filament (Phalloidin-Alexa 568, Invitrogen, Carlsbad, CA). PSD-95 (BD Biosciences, Franklin Lakes, NJ); V5 (Sigma, St. Louis, MO), and control mouse IgGs (Jackson Immunochemicals, West Grove, PA). The following recombinant proteins were used: human IgG Fc (Jackson Immunochemicals); and ephrin-A3 Fc (R & D Systems, Minneapolis, MN). Calcineurin inhibitor FK506 (Sigma).

RNAi. The siRNA duplexes composed of 21bp sense and antisense oligonucleotides were purchased from Qiagen. Control siRNA are Allstars Negative Control siRNA. The sequence of siRNA for mouse SSH1 used was GGC UUG UUUGCG UAC CAU ATT. The fluorescence tagged siRNA for both control and mSSH1 were the same oligo sequence except with a 3'-Alexa 488

modification. HT22 cells were transfected with 30pM siRNA using HiPerFect (Qiagen, Valencia, CA) for 72 hours. For primary neuron cultures, cells were transfected with 30pM siRNA for 72 hours using Lipofectamine (Invitrogen) before subjected to immunostaining.

Western Blot Analysis. For HT22 cell experiments, cells were seeded day before, the second day, cell reached ~80% confluency. Cells were serum-starved for 1 hour before being stimulated with dimeric control Fc or ephrin-A3 Fc (10 μg/ml) for 5 minutes. Cells were then lysed in RIPA buffer (1% Triton X-100; 1% Na deoxycholate; 0.1% SDS; 20 mM Tris; 150 mM NaCl; 1 mM EDTA) containing protease inhibitors and orthovanadate. Lysates were then subjected to western blot. The degree of phosphorylation was determined using antibodies against phospho-cofilin antibody. Membranes were then stripped and reprobed for total level of cofilin using cofilin antibody. For densitometry, the amount of phosphorylation was quantified using ImageJ and was normalized against the total cofilin levels. Data was collected over three independent experiments.

For biochemistry involving hippocampal neurons, 14 DIV dissociated hippocampal neurons were treated with dimeric control Fc or ephrin-A3 Fc (10 μg /ml) for 5 minutes, and then subjected to western blot analysis described as above.

Cell rounding assay. For cell rounding assays, HT22 cells were plated onto chambered slides (Nunc, Rochester, NY) and transfected as previously described. Cells were fixed with 4% paraformaldehyde/0.1M phosphate buffer for 30 minutes, rinsed with TBS and incubated for 1 hour in blocking solution (5% goat serum/0.1%Triton X-100 in TBS (Tris-buffered saline)). Cells were then incubated with phalloidin-568 in blocking solution for 1hour followed by brief washes with TBS/0.1%TX-100. cells were mounted for microscopy. 10 images were taken from randomly chosen areas for each condition. Then cell numbers of each morphological category for each condition were counted blinded.

Dissociated neuronal cultures. Primary hippocampal neurons were cultured from P0 mice on coverslips above an astrocyte feeder layer using a modified method previously published (Kaech & Banker 2006). Briefly, the hippocampal

astrocytes for feeder layer was prepared from P2 mice, maintained in astrocyte media (Minimal Essential Medium containing Earles salts and L-glutamine supplemented with 10% Horse serum, 0.6% glucose and 1% penicillin/streptomycin (Invitrogen) 5 days before neuronal dissection. Hippocampal neurons were dissociated by papain treatment (0.1% papain, 0.02% BSA in Neurobasal-A medium) followed by titrations. Neurons were then plated on coverslips and transferred to dishes containing the astrocyte feeder layers after 3 hours.

Hippocampal Slice Preparation. Organotypic hippocampal slices were prepared as described (Murai et al 2003a). Briefly, 300μm slices from postnatal 5 day (P6-7) mouse pups were made using a McIllwain tissue chopper (Stoelting, Kiel, WI) and transferred onto semi-porous tissue culture inserts (0.4 μm pore size; Millipore) containing media (50% Minimum Essential Medium / 25% Horse Serum/25% Hanks Balanced Salt Solution / 6.5mg/ml D-glucose / 0.5% penicillin / streptomyosin, pH~7.2). Media was replaced every two days and slices were cultured for 1 week before viral gene delivery. 16-20 hours post-infection, slices were either fixed and mounted for confocal imaging or fixed and subjected to immunofluorescence using anti-V5 antibodies.

Semliki Forest Virus Plasmid Construction and Virus Preparation. For expressing SSH1 constructs and fluorescent proteins in hippocampal slices, Semliki Forest virus (SFV) constructs were created (Ehrengruber et al 1999). V5-tagged wild type SSH1 and phosphatase inactive SSH1(C393S) cDNAs were subcloned into a pScaPD vector containing a viral subgenomic promotor followed by farnesylated enhanced green fluorescent protein (EGFP-f). Control plasmid contains only EGFP-f (Zhou et al 2007). Viral particles were created by co-transfecting SFV vectors with a viral packaging vector into baby hamster kidney cells (DiCiommo & Bremner 1998).

SSH1 and membrane-targeted farnesylated EGFP (EGFPf; Clontech) genes were each cloned 3' to a viral subgenomic promoter in modified SFV vectors (Lundstrom et al 2003). SFV particles were prepared by co-transfecting SFV vectors with a viral helper vector into baby hamster kidney cells (DiCiommo &

Bremner 1998). 72 hours following transfection, the cell media was removed and purified on a sucrose gradient (20%, 55% W/V) by ultracentrifugation. Viral particles were collected and diluted with PBS and concentrated using a filter column (Millipore, Billerica, MA) and low-speed centrifugation. Viral particles were reconstituted in ice-cold PBS, activated with chymotrypsin (10mg/ml), and treated with aprotinin (10mg/ml). SFV particles were injected into hippocampal slices with a Picospritzer (Parker Hannifin, Cleveland, OH) or directly apply to culture media (for dissociated hippocampal neuronal cultures).

Confocal imaging and image analysis. Confocal imaging and analysis of dendritic spine morphology in hippocampal slices was performed as described previously (Zhou et al 2007). Briefly, images of dendrites were taken for each condition (control, wild-type slingshot phosphatase (SSHwt), or slingshot phosphatase-inactive mutant (SSH(CS)) from 3 independent experiments. Each image contained a Z-stack maximum projection of a primary apical dendrite from a CA1 pyramidal cell taken approximately 100µm from the cell body (Control = 16 dendritic segments with 568 spines total; SSHwt = 26 dendritic segments with 886 spines total; SSH(CS) = 22 dendritic segments with 603 spines total). All images were normalized for EGFPf signal intensity and thresholded in Photoshop. Geometric measurements of spine parameters (head length, head width, neck length, neck width, spine area, spine density) were acquired using the Reconstruct computer program.

SSH localization analysis. For the analysis of SSH protein location in neurons, SSHwt was introduced into hippocampal slice using SFV containing V5 tagged SSHwt as well as EGFP-f for 16 hours. Cells were then subjected to immunostaining for V5 epitope. Fluorescence intensity of V5 and EGFP-f at spine tip, spine neck and neighbouring dendritic shaft were measured by placing a measuring circle at these locations. Integrated fluorescence intensity of both channels from the measuring circles were obtained using Metamorph (Molecular Devices, Downingtown, PA). The signal for the SSH proteins (V5 fluorescence intensity) was normalized to the intensity of EGFP-f at the same location to correct for differences in signal due to volume of the structures or differences in

expression levels among cells.

Immunostaining of dissociated neurons. To visualize the dendritic spines as well as F-actin and PSD structures in primary hippocampal neurons, 13 day old neurons were infected with Semliki Forest Virus containing EGFP-f only or SSH(CS) and EGFP-f. The second day, neurons were pretreated with FK506 for 10min, or directly treated with Fc or ephrin-A3 Fc for 10 min. Neurons were then washed with ice-cold PBS and fixed with 4% paraformaldehyde/0.1 M phosphate buffer/2% Sucrose for 10 minutes. Cells were then briefly washed with PBS/Glycine, then permeabilised with PBS containing 0.2% Triton X-100 for 15min. After blocked in 5%BSA/0.1% Triton X-100/PBS for 1 hour, neurons were washed and incubated with primary antibody PSD-95 (mouse monoclonal, 1:100) for 90 min. Neurons on coverslips were washed three times with PBS before incubation with either goat anti-mouse Alexa 647 mixed with phallodin-568 (1:50) for 1 hour, then washed and imaged using confocal microscopy. Single plane images were taken in three channels at the same time for F-actin, PSD-95, and GFP. Images were cropped to the region of interest using Photoshop. All measurements described below were obtained using ImageJ (NIH). The sizes of F-actin or PSD-95 clusters were measured by the areas of the clusters. F-actin cluster intensity was measured by the mean gray value within the area of clusters. F-actin cluster circularity was measured using shape indicator in ImageJ. The distance of PSD-95 clusters to dendrite was measured as from the center of clusters to the center of dendritic shaft.

Results

EphA Signaling Promotes Dephosphorylation of Cofilin

We previously showed that EphA receptors regulate dendritic spine remodeling in the hippocampus and can initiate a series of signaling events that facilitate spine retraction in organotypic hippocampal slice cultures (Murai et al 2003a). We further showed that EphA activation with ephrin-A ligands alters the association of cofilin with the cell membrane (Zhou et al 2007). However, an

important question that remained was whether EphA activation resulted in the activation of cofilin, a potent regulator of actin filaments that is enriched in spines (Bernstein & Bamburg 2010). Cofilin is an actin-binding protein that depolymerises and severs filamentous (F-actin), increasing globular (G-actin) monomer levels and producing additional barbed ends on actin filaments. The activity of cofilin is tightly regulated by phosphorylation on serine-3 at the N-terminus of the protein (Van Troys et al 2008). Phosphorylation of serine-3 by LIMK and TESK proteins serve to inactivate cofilin whereas dephosphorylation of serine-3 by SSH and chronophin (CIN) phosphatases activate cofilin (Gohla et al 2005). The degree of serine-3 phosphorylation of cofilin can be probed using antibodies raised against the phosphorylated residue. We followed up on the possibility that activation of EphAs with ephrin-A ligands regulates the phosphorylation state of cofilin. We found that stimulation of HT22 cells, an immortalized mouse hippocampal cell line (Li et al 1997), with recombinant ephrin-A3 fused to the Fc domain of human IgG (ephrin-A3 Fc) caused a significant reduction in cofilin phosphorylation after 45 minutes when compared to control Fc (Figure 1A). Since cofilin has been shown to undergo rapid phosphorylation/dephosphorylation in response to various stimuli (Van Troys et al 2008), we tested the time-course of the dephosphorylation event. Cofilin was dephosphorylated over the course of minutes (2 and 5 minutes shown; Figure 1B), suggesting rapid dephosphorylation and activation of cofilin in response to EphA stimulation. To determine if this signaling event occurs in neurons, we stimulated hippocampal neurons grown for 14 days *in vitro* (D.I.V.). At this stage of culture, many of the synapses on the neurons are mature and dendritic spines are easily observed. Similar to the results with HT-22 cells, stimulation of hippocampal neurons with ephrin-A3-Fc led to a rapid decrease in cofilin phosphorylation (5 minute stimulation; Figure 1C). These results show that stimulation of EphA receptors with ephrin-A causes a rapid decrease in cofilin phosphorylation in both heterologous cells and neurons in culture.

The Cofilin Phosphatase Slingshot 1 (SSH1) is Required for EphA-mediated

Cofilin Dephosphorylation and Cell Morphology Changes

Cofilin activity is directly related to the phosphorylation state of serine-3 in the N-terminus of the molecule, with the dephosphorylated molecule having depolymerising/severing activity (Bernstein & Bamburg 2010). To date, only members of the SSH and CIN family of phosphatases have been found to dephosphorylate and activate cofilin (Gohla et al 2005; Huang et al 2008; Kurita et al 2008; Niwa et al 2002). Previously it was shown that SSH family members (SSH1, SSH2 and SSH3) are expressed in the adult CNS including the hippocampus (Ohta et al 2003). Thus, we were interested in investigating if SSH phosphatases may contribute to cofilin dephosphorylation in response to ephrin-A treatment. To test the requirement of SSH proteins on EphA-mediated cofilin dephosphorylation, we utilized a phosphatase inactive form of SSH1 (now referred to as SSH(CS) that harbors a mutation (cysteine 393 replaced by serine in the phosphatase domain) (Niwa et al 2002). This phosphatase-inactive mutant has been used to interfere with endogenous SSH protein activity in cells in several cellular contexts (Hsieh et al 2006; Kurita et al 2008; Niwa et al 2002). Consistent with other reports, transfection of the SSH(CS) into heterologous cells results in an increase in cofilin phosphorylation (Supplemental Figure 2). We next tested the importance of SSH1 function in EphA-mediated cofilin dephosphorylation by treating SSH(CS)-transfected HT22 cells with control Fc or ephrin-A3-Fc. Expression of SSH(CS) effectively blocked the ability of ephrin-A3-Fc to cause cofilin dephosphorylation (Figure 2A). Importantly, the blockade of cofilin dephosphorylation upon ephrin-A stimulation was also observed in dissociated hippocampal neurons expressing SSH(CS) (Figure 2A). To test if the SSH(CS) protein caused a similar effect as direct loss of SSH protein, we reduced endogenous SSH1 in HT22 cells using short-interfering RNAs (siRNAs) specific for mouse SSH1. Double-stranded control siRNAs or SSH siRNAs (with and without Alexa-488 tags) were transfected into HT22 cells and endogenous SSH1 proteins level were examined 72 hours later by Western blot. SSH1 protein levels in cells transfected with SSH1 siRNAs were reduced compared to cells transfected with the control siRNAs (Supplemental Figure 1). Loss of SSH1

protein was observed with mouse N1E115 and HT22 cells and primary hippocampal neurons transfected with SSH1 siRNAs (Supplemental Figure 1). Consistent with the effect of the SSH(CS) protein, SSH siRNAs interfered with the ability of ephrin-A3-Fc to reduce cofilin phosphorylation levels (Figure 2B). These results suggest that SSH1 mediates the dephosphorylation of cofilin upon EphA activation.

Eph signaling is known to induce rapid actin remodeling and cell rounding in heterologous cells (Dail et al 2006; Irie et al 2008; Lawrenson et al 2002). Consistent with this, HT22 showed robust actin reorganization and cell rounding when treated with ephrin-A3-Fc for 20 minutes. This was revealed by labelling for actin in cells with Alexa-568 conjugated phalloidin (Figure 2C). Ephrin-A3-Fc treatment increased the percentage of cells showing a rounded/shrunken morphology from 19.6% (control levels) to 80.4% following ephrin-A3 Fc treatment (Figure 2C). We were next interested in determining if the loss of SSH1 would prevent ephrin-A-induced actin reorganization and cell rounding. To do this, HT-22 cells were transfected with either control or SSH siRNAs and then stimulated with ephrin-A3-Fc for 20 minutes. We found that ephrin-A-Fc treatment caused about 81.3% cell rounding in control siRNA transfected cells, however, this was reduced to 33.1% following transfection with SSH siRNA. These results, along with those presented earlier, indicate that SSH1 is required for ephrin-A-induced cofilin dephosphorylation, actin remodeling and cell morphology changes.

SSH1 is Expressed in the Developing and Adult Hippocampus and is Necessary for Normal Dendritic Spine Morphology

SSH phosphatases were first identified in *Drosophila* mutants, which show a bifurcated bristle phenotype (Niwa et al 2002). In mammals, three genes are known to encode SSH proteins (SSH1, -2 and –3), with SSH1 and 2 having alternative splice forms (Niwa et al 2002; Ohta et al 2003). A study using *In situ* hybridization reported that all three SSH genes are expressed in the adult

hippocampus, cerebellum, and olfactory bulb (Ohta et al 2003).

As a first step toward understanding the properties of SSH proteins in the hippocampus, we investigated the temporal expression of SSH1 in the early postnatal and adult hippocampus. Western blot analysis showed that SSH1 protein is detectable at early postnatal time points (P1-P12), prior to being found at a reduced level in the adult hippocampus (Figure 3A). To resolve the subcellular localization of the protein, we turned to dissociated neuronal cultures where individual neurites and synapses can be resolved more easily. Immunostaining dissociated hippocampal neurons at 14 D.I.V. for SSH1 showed that the protein was distributed as punctae along the neurites of hippocampal neurons. SSH1 was found in the shafts of dendrites and spines and showed partial co-localization with PSD-95, a marker of the postsynaptic density (Figure 3B).

To further examine if SSH1 can be targeted to specific compartments of neurons, we expressed a V5-tagged version of SSH1 in organotypic hippocampal slices utilizing a Semliki Forest virus (SFV) expression system. The SSH proteins were expressed simultaneously with membrane-targeted EGFP (EGFP-f) in order to delineate the dendrites of CA1 cells including their spines. 16 hours post-infection with SFVs, slices were fixed and immunostained using an antibody against the V5-epitope. Similar to the endogenous SSH1 expression, we found that SSH1-V5 protein was highly expressed in dendrites of CA1 cells and often found in the spine head region (Figure 3C). We measured the localization of this protein by quantifying its intensity at the tip of the dendritic spine head, neck of the spine, and in the nearby dendritic shaft region. We found that SSH1 protein was concentrated in the spine tip (Figure 3D) versus the neck and dendrite. These findings, along with the previous immunostaining results, suggest that SSH proteins are found in the dendrites of neurons and can be localized in dendritic spines.

Since SSH1 was detected during early postnatal development of the hippocampus, a time when dendritic spines are developing, we tested whether SSH proteins influence dendritic spine morphology. As before, Semliki Forest viruses were used to introduce wild type SSH1 (SSHwt) or SSH(CS) into CA1

pyramidal cells of organotypic hippocampal slices and EGFP-f was used to delineate dendritic spine morphology. 16 hours post-infection, spine density and morphology in CA1 pyramidal neurons were quantified (Figure 4). Overexpression of SSHwt did not significantly affect the structural properties of dendritic spines as compared to control neurons only expressing EGFP-f. However, the SSH(CS) protein caused significant spine changes, including an increase in spine head length and a reduction in spine head width (Figure 4F). Taking several parameters of the spines in the various conditions into account (including spine length, width, and ratios of these parameters), expression of the SSH(CS) protein in CA1 cells significantly increased the number of elongated spines and caused a reduction in mushroom-looking spines (Figure 4H). These results suggest that the activity of SSH proteins help preserve dendritic spine structure.

Calcineurin is Required for Ephrin-A-Induced Cofilin Dephosphorylation and Changes in Cell Morphology

Previous studies have shown that calcineurin dephosphorylates SSH1 (Wang et al 2005b) and is responsible for activating SSH1 in developing and mature neurons (Wang et al 2005b; Wen et al 2007; Yuen & Yan 2009). This has important consequences for actin remodeling in non-neuronal cells (Wang et al 2005b), steering growth cones of developing axons (Wen et al 2007) and AMPA receptor trafficking at synapses (Yuen & Yan 2009). Thus, calcineurin is an important upstream regulator of SSH1 in several contexts. We were interested in determining if calcineurin was required for EphA-dependent cofilin dephosphorylation and actin reorganization. To test this, we treated HT22 cells and dissociated hippocampal neurons with the calcineurin inhibitor FK506 for 10 minutes prior to control Fc or ephrin-A3 Fc application. We found that FK506 blocked ephrin-induced cofilin dephosphorylation in HT22 cells and neurons (Figure 5A). To determine if calcineurin was needed for EphA-mediated cell rounding, we treated HT22 with FK506 prior to ephrin-A3 Fc treatment and labelled F-actin using Alexa-568 phalloidin. We found that actin remodeling and

cell rounding was significantly blocked by application of FK506. These results suggest that calcineurin is required for both EphA triggered cofilin dephosphorylation and cell rounding (Figure 5B).

EphA Receptors Regulate Dendritic Spine Morphology through SSH1 and Calcineurin

We previously reported that EphA4 activation with ephrin-A ligand induces dendritic spine remodeling (Murai et al 2003a). Furthermore, dendritic spine morphology is perturbed in EphA4 knock-out mice and following expression of a kinase-dead EphA4 (Murai et al 2003a). Among the ligands that activate EphA4 is ephrin-A3 which is found on glial cell processes in the hippocampus. Recent findings have found that ephrin-A3 regulates glutamate transporter levels in astrocytes and this is likely related to defects in LTP in ephrin-A3 knock-out mice (Carmona et al 2009; Filosa et al 2009). We were interested in determining if SSH1 and calcineurin are required for the EphA-induced spine changes in neurons. To avoid complications related to the regulation of glutamate transporter levels and neuron-glial interactions through ephrin-A3 and EphA receptor interactions, we turned to experiments with dissociated hippocampal neurons. This allowed us to investigate the effects of ephrin-A treatment on dendritic spine morphology of neurons in the absence of significant physical contact of neurons with glial cells (see methods section for culture system used). At 13 D.I.V, neurons were infected with Semliki Forest Viruses to drive expression of EGFP-f to reveal spine morphology. The next day, neurons were treated with either control Fc or ephrin-A3 Fc for 10 minutes prior to fixation and imaging. Spine density and morphology were compared in each of the conditions. Within minutes of treating neurons with ephrin-A3 Fc, spines showed a significant increase in length and a decrease in head width (Figure 6A). Using the parameters of the measured spines, we found that EphA activation reduced the percentage of mushroom shaped spines and increased the percentage of elongated/filopodial-like spines (Figure 6E). Importantly, all of these modifications to spine morphology and classification upon EphA receptor activation were blocked by the presence of the calcineurin

inhibitor FK506 or expression of SSH(CS). One complication that needs to be mentioned, however, is the fact that the SSH(CS) condition produced baseline alterations in spine length, width, and classification (Figure 6H and 6I). Thus, we cannot rule out the possibility that a prior spine phenotype may preclude the ability of spines to respond to EphA signals. Interestingly, the baseline changes in spines were remarkably similar to those found in SSH(CS)-expressing CA1 neurons of organotypic cultures (Figure 4).

EphA Signaling Causes F-Actin Reorganization and PSD Repositioning in Spines

SSH1 binds F-actin through its C-terminal protein interaction domain (named the S domain; (Ohta et al 2003). The binding to F-actin enhances SSH1 activity to dephosphorylate cofilin, promoting actin remodeling (Kurita et al 2008). To further study how EphA-induced spine remodeling is related to the reorganization of the F-actin network and postsynaptic structure in spines, we investigated the distribution of F-actin and PSD-95 in dissociated hippocampal neurons following ephrin-A treatment and manipulations that block SSH1 and calcineurin function. As shown in Figure 6A, 10 minutes of ephrin-A application caused spines to elongate, leading to the loss of a defined head region on spines. Staining for F-actin with Alexa-568 phalloidin revealed that F-actin was redistributed within spines (Figure 7A). Although overall changes in F-actin cluster size or intensity were not detected (Figure 7B and 7C), the shape of the F-actin clusters was significantly altered. This was determined by calculating the degree of circularity of F-actin clusters using ImageJ. Normally, F-actin labeling is detected as round/circular structures enriched in the spine head (Matus 2000). However, ephrin-A treatment caused a significant elongation of F-actin clusters with a reduced circularity index (Figure 7D). Application of the FK506 or expression of SSH(CS) blocked the reorganization of F-actin by ephrin-A treatment. Interestingly, expression of the SSH(CS) protein in neurons alone caused an abnormal localization of F-actin in the spine neck and a reduction in the tip of spine heads (Figure 7A). These results indicate that ephrin-A treatment

reorganizes the F-actin cytoskeleton in spines and this activity requires the function of SSH1 and calcineurin.

We next examined the effects of ephrin-A treatment on postsynaptic organization by labeling for PSD-95 in spines. PSD-95 labeling is largely localized to the head of dendritic spines in dissociated neurons (Figure 7A). However, treating neurons with ephrin-A caused a significant decrease in the density of PSD-95 punctae (Figure 7E). Of the remaining PSD-95 sites, punctae size was not significantly altered (Figure 7F). We also found that the remaining PSD-95 clusters were significantly closer to the dendritic shaft following ephrin-A treatment, indicating a repositioning of postsynaptic molecules upon EphA activation (Figure 7G). This was measured by measuring the distance of PSD-95 punctae to the dendritic shaft and comparing it to total spine length. Interestingly, ephrin-A treatment caused many PSD-95 punctae to be positioned away from the head of spines and in some cases near the base of spines. Importantly, the alterations in PSD positioning were blocked with FK506 application or expression of SSH(CS) protein, suggesting that calcineurin and SSH1 signaling are essential for this process. These collective results indicate that EphA activation causes a reorganization of postsynaptic sites that result in spine remodeling.

Discussion

Eph receptors have an established role in the morphogenesis and maintenance of dendritic spines (Ethell & Pasquale 2005). However, exactly how these receptors perform these functions remains to be fully demonstrated. Our results reveal a novel pathway downstream of the EphA class of receptors that regulates spine plasticity. We show that EphA activation causes the dephosphorylation of cofilin, an important actin filament severing/depolymerising factor implicated in regulating dendritic spine development and morphology. The ability of EphAs to activate cofilin requires the activity of the phosphatases slingshot and calcineurin. Furthermore, both phosphatases are needed for EphA-mediated reorganization of actin filaments, PSD-95 positioning, and dendritic spine remodeling. This study

contributes new insight into the intricate signaling mechanisms downstream of EphAs that regulate the molecular and structural plasticity of excitatory synapses in the central nervous system.

Early work by Matus and colleagues showed the importance of actin filament dynamics in spine remodeling (for review see (Matus 2000)). Actin filaments serve as the primary structural scaffold of dendritic spines and provide a core for the assembly of many protein complexes at synapses. Recent studies have further revealed how actin remodeling and spine rearrangements are related to changes in synaptic efficacy and plasticity (Ethell & Pasquale 2005). Key to these changes is the recruitment of signaling proteins that refine the actin cytoskeletal network. Indeed, molecules that nucleate, sever, depolymerise, and cap actin filaments including profilin, gelsolin, Arp2/3, cortactin, and cofilin have been found to regulate spine development and maintenance (Star et al 2002). Thus, a complex network of actin filament regulatory proteins is available to control the structural plasticity of spines. However, the ability of upstream receptors and signaling proteins to recruit these proteins and coordinate the stabilization and destabilization of F-actin in spines remains to be fully understood.

Our results indicate that EphAs signal to cofilin to elicit changes in spine morphology. Cofilin plays a central role in turning over actin filaments in many cell types and is implicated in regulating the development and morphological plasticity of spines (Fedulov et al 2007; Hotulainen et al 2009; Shi et al 2009; Zhou et al 2007). Indeed, direct manipulation of cofilin function perturbs spinogenesis and the maintenance of spines (Hotulainen et al 2009; Shi et al 2009). In mature neurons, expressing a constitutively active form of cofilin (S3A; serine-3 mutated to alanine) in hippocampal neurons results in longer, immature-looking spines. In contrast, overexpression of an inactive form of cofilin (S3D; serine-3 mutated to aspartic acid to mimic phosphorylation) results in a decrease in spine length. Thus phospho-cycling on serine-3 of cofilin is likely a key point of convergence of many signaling pathways that serve to remodel the actin cytoskeleton in spines through actin filament severing and depolymerization. Interestingly, Shi et al. also revealed a critical role of EphB receptors in stabilizing

dendritic spines through Fak activation and cofilin phosphorylation/inactivation in mature neurons. EphB receptors are key receptors that promote spine morphogenesis during development (Ethell et al 2001a; Henkemeyer et al 2003b; Penzes et al 2003) and serve to maintain spine morphology in mature neurons (Kayser et al 2008; Shi et al 2009). Thus, in spines of mature neurons, cofilin activity may be bi-directionally controlled by counterbalancing EphA and EphB signaling pathways. This form of Eph receptor modulation of cofilin phosphorylation may serve to fine-tune actin remodeling events and dendritic spine morphology. Further experiments are needed to determine the interaction between EphA and B classes in regulating the structural plasticity of synapses.

Cofilin is known to be regulated by kinases of the LIMK and TesK family (Bernstein & Bamburg 2010). These proteins directly phosphorylate cofilin on serine-3, leading to its inactivation. This has relevance for brain plasticity as LIMK1 knockout mice have spine abnormalities and learning/memory deficits (Meng et al 2002a). Spines in LIMK1 knock-out mice have reduced spine head size and have a thickening of the spine neck region. The importance of LIMK1 on regulating spines has been further demonstrated in a study that identified a micro-RNA that targets LIMK1 mRNA and helps control spine development (Schratt et al 2006). Both LIMKs and TesKs are activated by Pak and Rho kinases, and integrate signaling events downstream of multiple receptor systems. While cofilin inactivation by LIMK1 is essential for spine development, the role of TesKs remains unclear.

Cofilin inactivation by LIMKs and TesKs is counterbalanced by the phosphatases SSH and CIN (Van Troys et al 2008). Our results indicate that SSH1 is required for EphAs to induce cofilin dephosphorylation and activation. Furthermore, we provide evidence that SSH1 activity is required for regulating dendritic spine morphology. Intriguingly, organotypic and dissociated hippocampal neurons expressing a phosphatase-inactive form of SSH1 exhibit spines with an irregular morphology, being thinner and elongated. This is consistent with the finding that F-actin is accumulated in the neck region of spines. One important role for SSH1 may be to control F-actin levels in the spine neck, a

region of the spine that has recently been shown to be critical for activity-dependent spine plasticity (Honkura et al 2008). The regulatory mechanisms of SSH1 in spines deserve further attention as SSH proteins are subject to various regulatory processes including phosphorylation. It has been reported that phosphorylation by PAK4 decreases SSH phosphatase activity (Soosairajah et al 2005b). Phosphorylation of SSH family proteins also increases their inhibition by 14-3-3 family proteins (Nagata-Ohashi et al 2004b). Dephosphorylation of SSH1 by calcineurin, however, serves to activate SSH1 and this interaction facilitates growth cone remodeling during development (Wen et al 2007) and AMPA receptor turnover in GABAergic interneurons (Yuen & Yan 2009). We also found that EphA signaling though SSH1 requires calcineurin. Calcineurin is also downstream of many signaling events at synapses including NMDA receptor activation, and is critical for forms of synaptic plasticity including LTD (Mulkey et al 1994). Future experiments will investigate how EphA activation upregulates calcineurin function to promote spine remodeling and the crosstalk of EphA signaling with other pathways.

EphA activation is known to trigger a variety of signaling events that induce spine remodeling. For example, EphA signaling promotes spine changes through promoting Cdk5 phosphorylation of the Rho GTPase exchange factor ephexin (Fu et al 2007), activating PLCγ1 (Zhou et al 2007), and reducing β1-integrin-mediated adhesion through p130CAS (Bourgin et al., 2007). Interestingly, these studies showed that activation of EphA signaling leads to spine retraction (Bourgin et al 2007; Murai et al 2003a) and loss (Murai et al 2003a) following prolonged EphA activation with ephrin-A ligands in organotypic slice cultures. We now show that EphA activation elicits spines changes over a rapid time scale (minutes) in dissociated hippocampal neurons. Our current model is that initial EphA activation promotes rapid actin cytoskeletal reorganization and spine remodeling in dissociated neurons. However, chronic activation causes spine retraction and collapse (Murai et al 2003a). Indeed, we found that two components of the postsynaptic terminal are reorganized under short time frames in spines upon EphA activation. F-actin clusters become irregular in shape and

PSD-95 punctae become less abundant and are found closer to the dendritic shaft. One possibility is that the actin skeleton which supports postsynaptic structures in spines undergoes restructuring which destabilizes PSD-95 clusters. Perhaps the fate of a remodeling spine depends on the degree of stability of postsynaptic sites. Future experiments will explore this possibility.

Figures

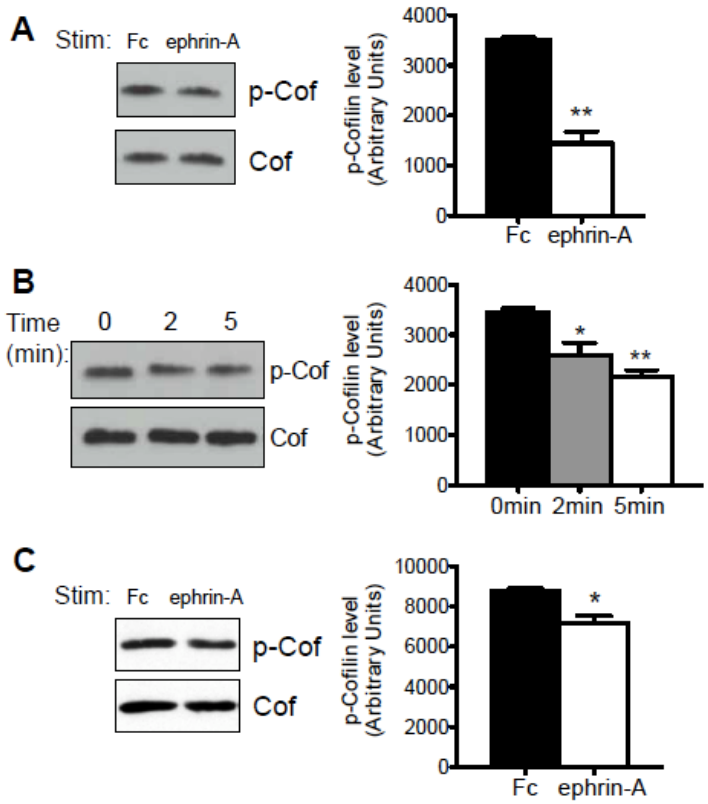
A
Stim: Fc ephrin-A
p-Cof
Cof
p-Cofilin level (Arbitrary Units)
4000
3000
2000
1000
0
**
Fc ephrin-A
B
Time (min): 0 2 5
p-Cof
Cof
p-Cofilin level (Arbitrary Units)
4000
3000
2000
1000
0
*
**
0min 2min 5min
C
Stim: Fc ephrin-A
p-Cof
Cof
p-Cofilin level (Arbitrary Units)
10000
8000
6000
4000
2000
0
*
Fc ephrin-A

Figure 4-1. EphA stimulation leads to cofilin dephosphorylation and activation in HT22 cells and dissociated hippocampal neurons. A, Stimulation of HT22 cells with ephrin-A3 Fc for 45 min decreased the level of phosphorylated cofilin compared to cells treated with control Fc (**p<0.01, unpaired t-test). B, Cofilin dephosphorylation was observed 2 and 5 min after initiating ephrin-A3-Fc stimulation of HT22 cells (*p<0.05, **p<0.01, one-way ANOVA with Bonferroni test). C, Ephrin-A3 Fc treatment of dissociated hippocampal neurons (14 D.I.V) for 5 min caused a significant reduction in the level of phospho-cofilin as compared to neurons treated with control Fc (*p<0.05, unpaired t-test). Phospho-cofilin levels were corrected according to total cofilin levels in all graphs and error bars indicate SEM.

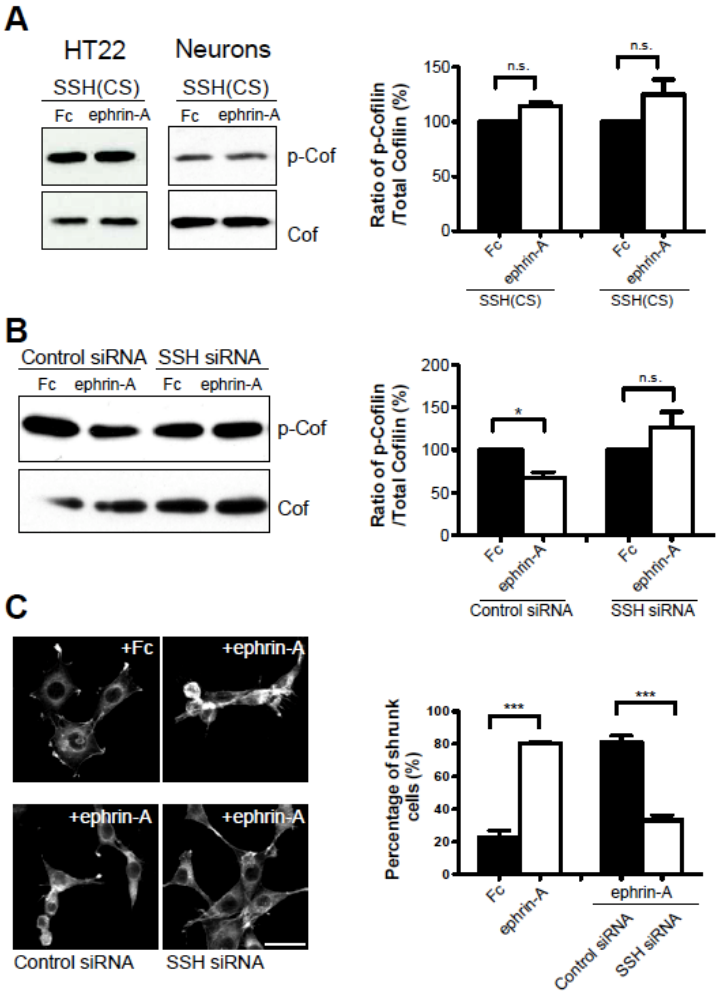
A
HT22
Neurons
SSH(CS)
SSH(CS)
Fc
ephrin-A
Fc
ephrin-A
p-Cof
Cof
Ratio of p-Cofilin /Total Cofilin (%)
n.s.
n.s.
150
100
50
0
Fc
ephrin-A
Fc
ephrin-A
SSH(CS)
SSH(CS)
B
Control siRNA
SSH siRNA
Fc
ephrin-A
Fc
ephrin-A
p-Cof
Cof
Ratio of p-Cofilin /Total Cofilin (%)
200
150
100
50
0
*
n.s.
Fc
ephrin-A
Fc
ephrin-A
Control siRNA
SSH siRNA
C
+Fc
+ephrin-A
+ephrin-A
+ephrin-A
Control siRNA
SSH siRNA
Percentage of shrunk cells (%)
100
80
60
40
20
0
***
***
Fc
ephrin-A
ephrin-A
Control siRNA
SSH siRNA

Figure 4-2. SSH phosphatases are required for EphA-mediated cofilin dephosphorylation. A, Expression of SSH(CS) blocked ephrin-A3 Fc induced cofilin dephosphorylation in HT22 cells and hippocampal neurons (14 D.I.V.) (5 minute stimulation; **p<0.01, t-test). The ratio of phospho-cofilin to total cofilin levels was normalized to Fc control or Fc + SSH(CS) control, respectively. B, Knockdown of SSH1 expression with SSH1 siRNAs blocked the ability of ephrin-A3 Fc to reduce phospho-cofilin levels in HT22 cells (*p<0.5, one-way ANOVA with Kruskal-Wallis test). C, HT22 cells were treated with Fc or ephrinA-Fc and cell morphology and F-actin structures were visualized with Alexa 568-conjugated phalloidin. Graph (top right), ephrin-A3 Fc treatment caused a significant increase in the number of shrunken cells when compared to Fc treatment (***p<0.001, t-test). Graph (bottom), HT22 cells transfected with control siRNAs or SSH1 siRNAs for 72 hours were treated with Fc or ephrin-A3 Fc. SSH1 siRNAs significantly reduced the percentage of shrunk cells upon ephrin-A3 Fc treatment (***p<0.001, t-test). Scale bar = 10 μm and error bars indicate SEM.

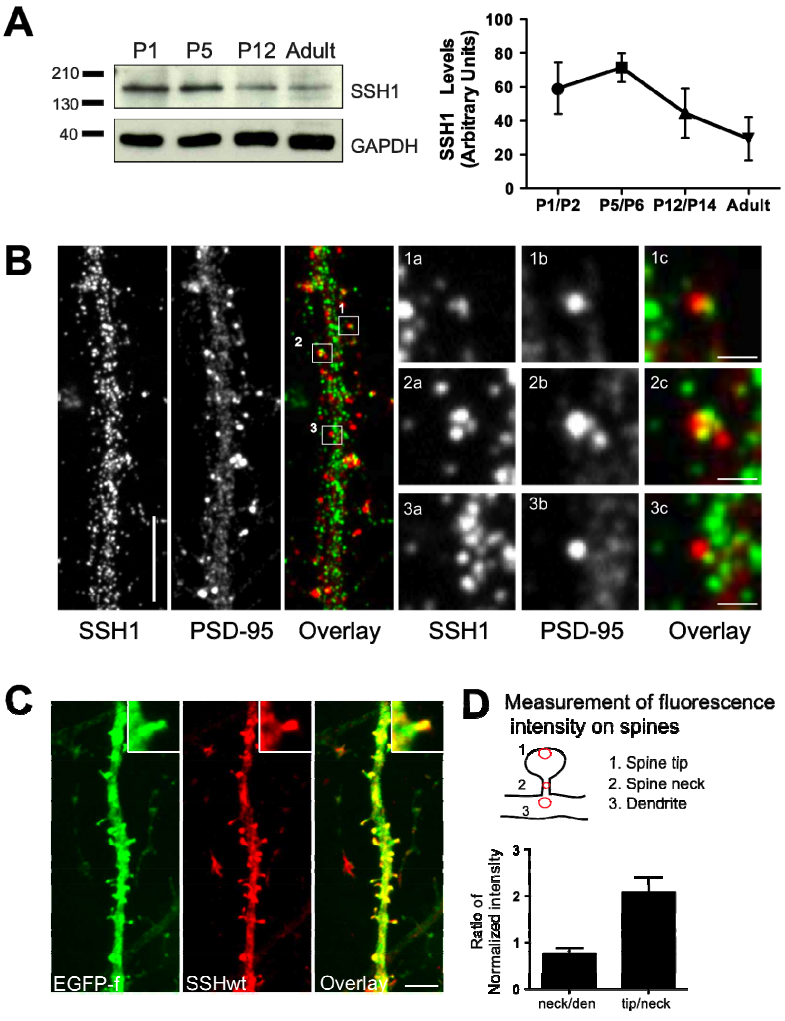
A
P1
P5
P12
Adult
210
130
40
SSH1
GAPDH
SSH1 Levels (Arbitrary Units)
100
80
60
40
20
0
P1/P2
P5/P6
P12/P14
Adult
B
1a
1b
1c
2a
2b
2c
3a
3b
3c
SSH1
PSD-95
Overlay
SSH1
PSD-95
Overlay
C
EGFP-f
SSHwt
Overlay
D
Measurement of fluorescence intensity on spines
1. Spine tip
2. Spine neck
3. Dendrite
Ratio of Normalized intensity
3
2
1
0
neck/den
tip/neck

Figure 4-3. SSH1 is expressed in the developing and adult mouse hippocampus and is localized at dendritic spines. A, Western blot analysis showing that SSH1 protein levels peak during the first postnatal week and decline toward adulthood in the mouse hippocampus. B, Immunostaining of dissociated hippocampal neurons (14 D.I.V.) reveal SSH1 punctae localized in neuronal processes (green), including dendrites and spine heads. 1a-3c, SSH1 showed partial co-localization with PSD-95 (red). C, Expression of V5-tagged SSH1 (SSHwt) in CA1 neurons in organotypic hippocampal slices. SSH1 was concentrated in the head region of the spines. D, Schematic showing the regions used to quantify the fluorescence intensity of SSH1 in spines. Three regions were measured: spine tip, neck, and dendritic shaft. SSH1 showed higher levels of fluorescence intensity in spine head tip compared to spine neck. Scale bars are 5 μm in B, C and 1 μm in the inset (1a-3c) and error bars indicate SEM.

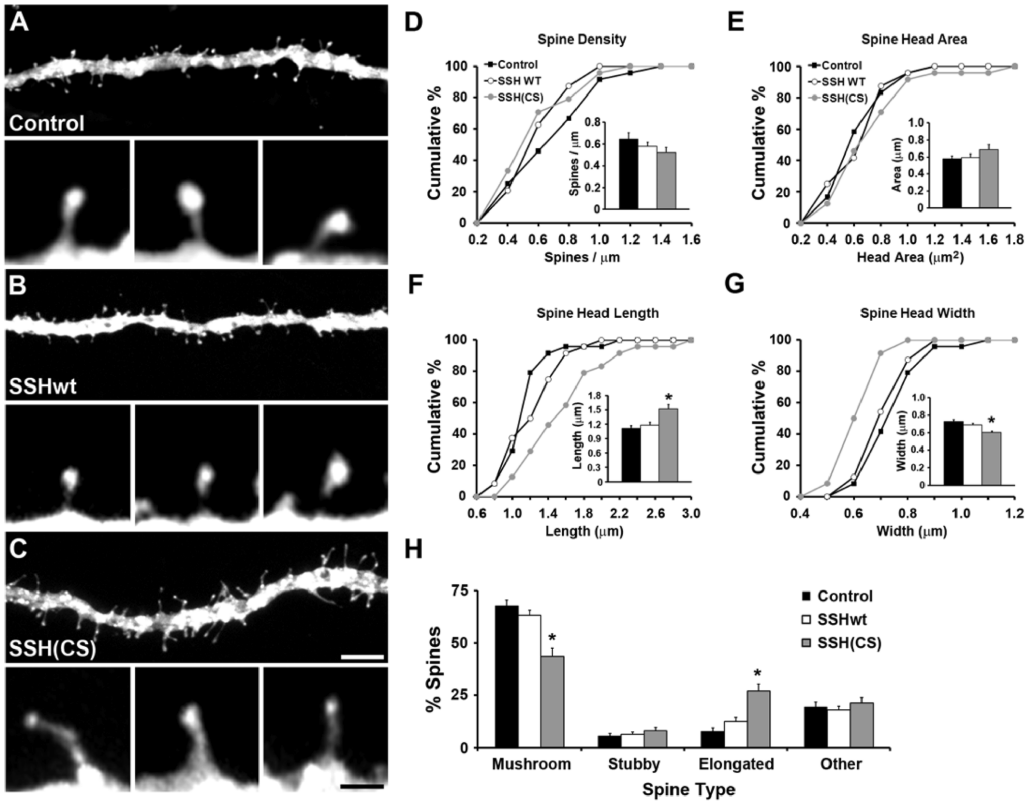
A
Control
B
SSHwt
C
SSH(CS)
D
Spine Density
Control
SSH WT
SSH(CS)
Cumulative %
Spines / μm
E
Spine Head Area
Head Area (μm²)
F
Spine Head Length
Length (μm)
G
Spine Head Width
Width (μm)
H
% Spines
Mushroom
Stubby
Elongated
Other
Spine Type

Figure 4-4. SSH is necessary for maintaining CA1 dendritic spine morphology in organotypic hippocampal slice. A-C, Examples showing abnormal dendritic spine morphology after expression of SSH(CS) when compared to control and SSHwt-expressing CA1 cells. Membrane-targeted enhanced green fluorescent protein (EGFP-f) was expressed alone (control) or co-expressed with SSHwt or SSH(CS) to visualize dendrites and spines. D-G, Quantification of spine parameters shows that spine properties are not affected with SSHwt expression. However, spine head length is significantly increased and spine head width is significantly decreased after expression of SSH(CS). H, Expression of SSH(CS) decreased the number of mushroom-shaped spines, and increased the number of elongated spines (*$p<0.05$, **$p<0.01$, ANOVA with Student-Newman-Keuls *post-hoc* comparison). Scale bars show 5 μm in A-C (1 μm in the inset) and error bars indicate SEM.

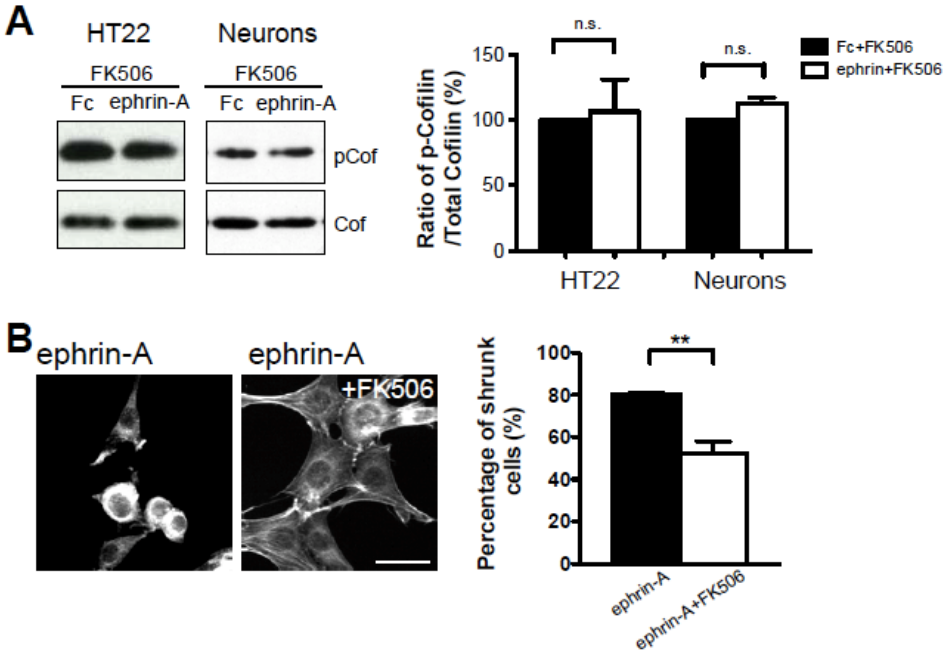
A
HT22
Neurons
FK506
Fc ephrin-A
FK506
Fc ephrin-A
pCof
Cof
n.s.
n.s.
Fc+FK506
ephrin+FK506
Ratio of p-Cofilin /Total Cofilin (%)
150
100
50
0
HT22
Neurons
B
ephrin-A
ephrin-A
+FK506
**
Percentage of shrunk cells (%)
100
80
60
40
20
0
ephrin-A
ephrin-A+FK506

Figure 4-5. Calcineurin is required for ephrin-induced cofilin dephosphorylation. A, HT22 cells or hippocampal neurons were pre-treated with the calcineurin inhibitor FK506 (10mM) for 10 min and then treated with Fc or ephrin-A3 Fc for 5 min. FK506 blocked the ability of ephrin-A3 Fc to reduce cofilin phosphorylation (n.s., t-test). B, HT22 cells were treated ephrin-A3 Fc in the absence or presence of FK506. Cell morphology and F-actin localization were visualized with Alexa 568-conjugated phalloidin. FK506 significantly reduced the ability of ephrin-A3 Fc to induce cell shrinkage (**$p<0.01$, t-test). Scale bar =10 μm and error bars indicate SEM.

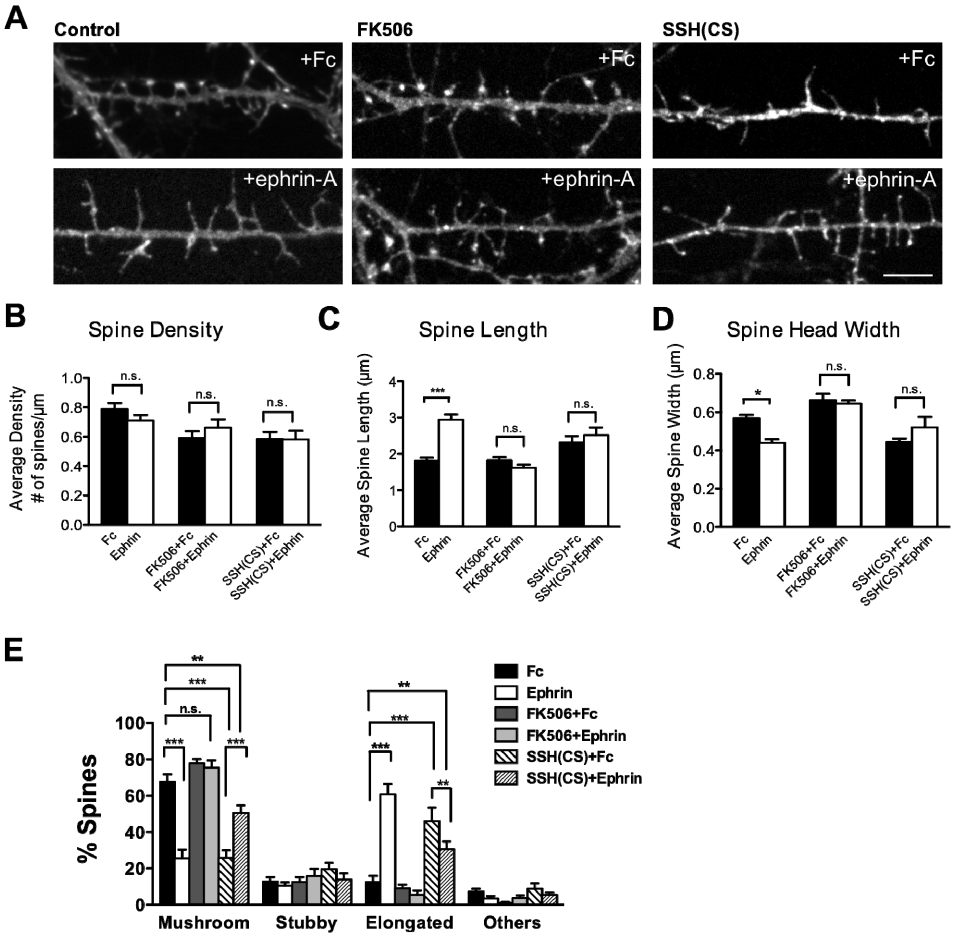
A
Control
FK506
SSH(CS)
+Fc
+ephrin-A
B
Spine Density
Average Density
# of spines/µm
n.s.
C
Spine Length
Average Spine Length (µm)
***
D
Spine Head Width
Average Spine Width (µm)
*
Fc
Ephrin
FK506+Fc
FK506+Ephrin
SSH(CS)+Fc
SSH(CS)+Ephrin
E
% Spines
Mushroom
Stubby
Elongated
Others

Figure 4-6. EphA receptors regulate dendritic spine morphology through SSH1 and calcineurin. A, Examples showing dendritic spine morphology after 10 min Fc or ephrin-A-Fc treatment. Neurons were infected with SFV expressing EGFP-f to outline spine morphology or EGFP-f and SSH(CS) to disrupt endogenous SSH1 function. B, Spine density is not significantly affected in any group. C, Ephrin-A3 Fc treatment caused a significant increase in spine length and a reduction in spine head width (***$p<0.001$, **$p<0.01$, one-way ANOVA with Bonferroni *post-hoc* analysis). The presence of FK506 or expression of SSH(CS) abolished ephrin-A3 Fc-induced spine changes. E, Ephrin-A3 Fc treatment also reduced the proportion of mushroom-shaped spines and increased the proportion of elongated spines. This effect was lost in the presence of FK506 or SSH(CS) (***$p<0.001$, **$p<0.01$, 2-way ANOVA with Bonferroni *post-hoc* comparison). Scale bar = 5 μm and error bars indicate SEM.

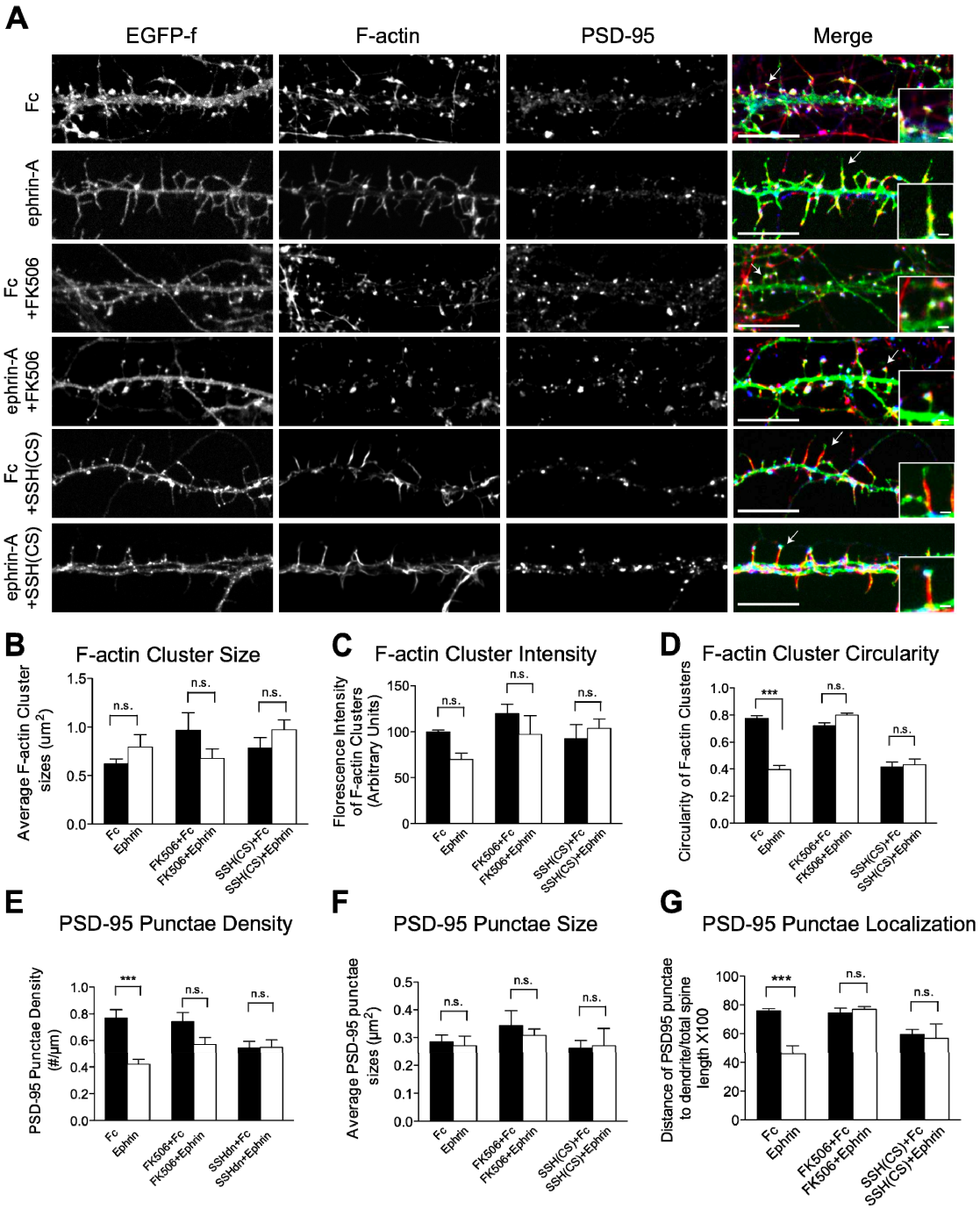
A
EGFP-f
F-actin
PSD-95
Merge
Fc
ephrin-A
Fc +FK506
ephrin-A +FK506
Fc +SSH(CS)
ephrin-A +SSH(CS)
B
F-actin Cluster Size
Average F-actin Cluster sizes (um2)
C
F-actin Cluster Intensity
Florescence Intensity of F-actin Clusters (Arbitrary Units)
D
F-actin Cluster Circularity
Circularity of F-actin Clusters
E
PSD-95 Punctae Density
PSD-95 Punctae Density (#/µm)
F
PSD-95 Punctae Size
Average PSD-95 punctae sizes (µm2)
G
PSD-95 Punctae Localization
Distance of PSD95 punctae to dendrite/total spine length X100
n.s.
***
Fc
Ephrin
FK506+Fc
FK506+Ephrin
SSH(CS)+Fc
SSH(CS)+Ephrin
SSHdn+Fc
SSHdn+Ephrin

Figure 4-7. EphA and SSH activity reorganizes F-actin in dendritic spines. A, Examples of dendrite segments from 14 D.I.V. primary hippocampal neurons treated with either Fc or ephrin-A3 Fc while in the presence of FK506 or SSH(CS) expression. Neurons were stained with Alexa 568-conjugated phalloidin (red), and PSD-95 antibody (blue) to visualize F-actin and postsynaptic structures in spines. All neurons were expressing EGFP-f to outline dendrite and spine morphology. B-D, Quantitative analysis of F-actin cluster size, intensity and circularity. F-actin cluster size and intensity were similar in all conditions (Kruskal-Wallis test). However, ephrin-A3 Fc treatment significantly changed F-actin cluster circularity (*$p<0.05$, Kruskal-Wallis test with Dunn's post comparisons). Expression of SSH(CS) alone, also significantly changed F-actin cluster circularity (*$p<0.05$, Kruskal-Wallis test with Dunn's post comparisons). E-G, Analysis of PSD-95 punctae density, size, and localization. Expression of SSH(CS) significantly reduced PSD-95 punctae density and altered its distribution (***$p<0.001$, Kruskal-Wallis test with Dunn's post comparisons). Scale bars = 10 μm. Error bars reflect SEM.

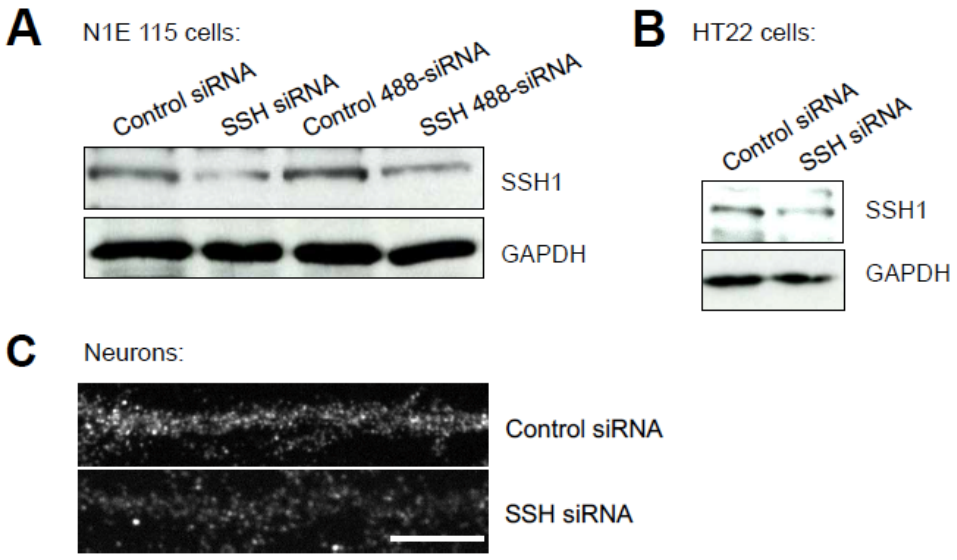
A
N1E 115 cells:
Control siRNA
SSH siRNA
Control 488-siRNA
SSH 488-siRNA
SSH1
GAPDH
B
HT22 cells:
Control siRNA
SSH siRNA
SSH1
GAPDH
C
Neurons:
Control siRNA
SSH siRNA

Supplemental Figure 4-1. SSH1 knockdown in NIE115, HT22 cells, and primary hippocampal neurons. A-B, Transfection of siRNAs for SSH1 (with and without Alexa 488 conjugation) reduced the amount of SSH1 protein in mouse NIE115 (A) or HT22 cells (B) after 72 hours. C, Endogenous SSH1 protein levels are decreased in hippocampal neurons (14 D.I.V) following transfection of SSH1 siRNAs (72 hours post transfection). Scale bar = 10 μm in C.

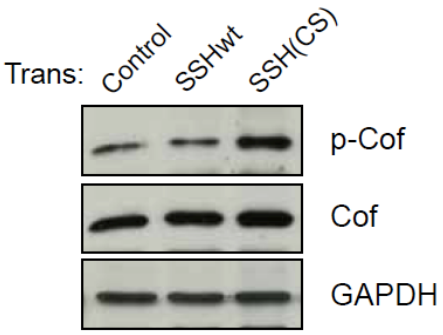
Trans:
Control
SSHwt
SSH(CS)
p-Cof
Cof
GAPDH

Supplemental Figure 4-2. SSH(CS) increase phospho-cofilin levels in COS7 cells. Western blot shows that expression of SSHwt did not change cofilin phosphorylation levels, whereas overexpression of SSH(CS) increased the phosphorylation level of cofilin.

Chapter 5 General Discussion

Ephrins and Eph receptors have established roles in axon guidance of the developing nervous system (Flanagan & Vanderhaeghen 1998; Kullander & Klein 2002; Orioli & Klein 1997; Palmer & Klein 2003). In several regions of the immature nervous system, ephrins and Eph receptors are expressed in different patterns that help with discrete axon target events (Lemke & Reber 2005; McLaughlin & O'Leary 2005; von Philipsborn et al 2006). In many cases, activation of signaling events downstream of these proteins causes growth cone retraction and repulsion (Goodman 1996; Sahin et al 2005; Wilkinson 2001). However, the binding between ephrins and Eph receptor can also promote cellular adhesion (Cooke et al 2005; Hansen et al 2004). Thus, fine control over the amount of ephrin and Eph receptor interactions and the degree of downstream signaling likely regulates how these proteins influence the connectivity of developing neurons (Halloran & Wolman 2006; Hansen et al 2004; Sela-Donenfeld & Wilkinson 2005).

Remarkably, some Eph receptors remain highly expressed in the adult brain (Flanagan & Vanderhaeghen 1998; Kullander & Klein 2002; Yamaguchi & Pasquale 2004). For example, EphA4 receptor is highly enriched in CA1 pyramidal neurons in the adult hippocampus and localized on dendritic spines (Murai et al 2003a; Murai et al 2003b). One ligand of EphA4, ephrin-A3, is expressed on astrocytic processes that surround dendritic spines. Astrocytes may play an important role in remodeling dendritic spines (Haber et al 2006; Nishida & Okabe 2007). Indeed, studies show that activation of EphA4 by ephrin-A3 results in spine retraction, whereas inhibiting the interaction between EphA4 and ephrin ligands by EphA4-Fc fusion protein, or transfecting neurons with kinase-inactive EphA4, leads to disorganization of spines (Murai et al 2003a). EphA4 knock-out mice also show disorganized and abnormally shaped spines.

Consistent with the importance of ephrin-A3-EphA4 interactions for spine morphology is the finding that EphA4 phosphorylation levels are reduced and dendritic spines of hippocampal pyramidal neurons are disrupted in ephrinA3

knock-out mice (Carmona et al 2009). Surprisingly, loss of either ephrin-A3 or EphA4 also leads to an increase the glial glutamate transporter levels. This causes an increased level glutamate removal during high-frequency stimulation of neurons and causes a partial impairment of LTP (Filosa et al 2009). In contrast, *in vivo* over-expression of ephrin-A3 in astrocytes decreases glutamate transporter levels and promotes glutamate excitotoxicity of neurons (Filosa et al 2009). Close contact between spines and astrocytes, may thus allow binding of EphA4 and ephrin-A3 and result in bi-directional signaling events. EphA4 activation is important for restricting dendritic spine size. At the same time, ephrin-A3 "reverse" signaling regulates the stability of glial glutamate transporters to regulate extracellular glutamate levels and pre- and/or postsynaptic properties. Thus, communication between neurons and glial cells through EphA4-ephrin-A3 interactions controls both synaptic morphology in neurons and glutamate transporter levels in astrocytes.

Studies indicate that EphA receptors preferentially bind to ephrinAs, whereas EphB receptors bind to ephrinBs (Pasquale 1997). However, EphA4 is an exception to this rule in that it binds several ephrin-A ligands, as well as ephrin-B2 and ephrin-B3 ligands (Gale et al 1996; Kullander et al 2001; Pasquale 2004; Wilkinson 2000). EphA4 may interact with ephrin-A or B's expressed presynaptically, postsynaptically, or on glial membranes and hence may be activated by different ephrins in the brain (Fu et al 2007; Grunwald et al 2004; Murai et al 2003a). This is consistent with the fact that loss of ephrin-A3 *in vivo* does not completely abolish receptor phosphorylation levels (Carmona et al 2009).

My studies revealed novel signaling events downstream of EphA4 that regulate dendritic spine morphology. I showed that PLCγ1 signaling was critical for maintaining spine morphology and PLC activity was required for ephrin-induced spine retraction. More specifically, I found that the C-terminal SH2 domain of PLCγ1 bound to phosophorylated tyrosine 602 in the juxtamembrane region of EphA4. Interestingly, the amount of cofilin associated with the cell membrane was regulated by PLCγ1 activity, likely through PIP_2

cleavage upon EphA4 activation. PIP_2 is known to anchor cofilin to the cell surface and maintain it in a dephophorylated but inactive state. Upon EphA4-mediated PLCγ1 activation, PIP_2 cleavage may locally release cofilin from the cell membrane in spines. This event could spatially confine actin filament reorganization events at the spine pheriphery. However, how the cofilin returns to the PIP_2-tethered state on the membrane in spines is not clear but would likely require the function of other kinases and phosphatases that regulate phosphoinositides (Liu & Bankaitis 2010; Saarikangas et al 2010).

Other recent studies have focused their attention on how EphA4 regulates downstream kinases including serine/thronine kinase Cdk5, and the tyrosine kinases Fyn and Pyk2 (Bourgin et al 2007; Fu et al 2007). In a separate, but related study, I found that EphA receptor activation also caused the dephosphorylation and activation of cofilin. This was mediated through the phosphatases slingshot (SSH) and calcineurin. Both phosphatases were required for EphA-mediated reorganization of actin filaments and dendritic spine remodeling. These results provide novel insight into discrete signaling cascades between EphA receptors and the F-actin network in dendritic spines. However, it remains to be tested how kinase, phosphatase, and lipase pathways intersect and ultimately regulate the final outcome of receptor activation. It is possible that signaling pathways downstream of EphA receptors that regulate cofilin membrane-association and phosphorylation/dephosphorylation interact cooperatively (Figure 5-1). Cofilin tethered on the cell membrane could serve as a storage pool. Upon activation of EphA receptors, release of cofilin from the cell membrane rapidly provides more cofilin protein to the active pool to depolymerize F-actin.

Since PLCγ1 hydrolyzes phosphatidylinositol 4,5-bisphosphate (PIP_2) to generate inositol 1,4,5-triphosphate (IP_3) and 1,2-diacylglycerol (DAG), second messenger signaling also needs to be considered. IP_3 is an important second messenger that binds to IP_3 receptors and causes release of calcium ions from endoplasmic reticulum (Berridge 1995). This may be especially relevant for calcineurin regulation, which is a calcium dependent phosphatase (Klee et al

1979). It is possible that downstream calcium signaling is critical for the pathways that I studied. Exactly how EphA receptor activation may elicit a calcium transient in neurons remains unknown. My preliminary data show that members of transient receptor potential (TRP) C family of channels are potentially involved (Clapham et al 2001). TRPC channels are non-selective cation channels, comprised of TRPC1-TRPC7. All 7 TRPC channels are expressed in mouse brain (Clapham et al 2001). Intriguingly, EphA-induced cofilin dephosphorylation can be blocked by a function blocking antibody of TRPC1 but not TRPC3 or TRPC5 (data not shown). It is possible that activation of EphA receptors leads to a calcium influx through TRPC1, which then activates calcineurin. Calcineurin then dephosphorylates SSH which activates cofilin to remodel dendritic spines. Future experiments are needed to investigate if EphA receptors activate TRPC1 and how this relates to spine morphology.

My studies also revealed that EphA and EphB receptor signaling may counter-balance each other to regulate dendritic spine structure. Activation of EphA receptors leads to a dephosphorylation and activation of cofilin, which could be directly responsible for actin depolymerization and spine shrinkage. Another study shows that EphB2 activation leads to increase in cofilin phosphorylation through activation of LK1 pathway (Shi et al 2009). The ability of Eph receptors to differentially control cofilin phosphorylation could reflect distinct functions of A-type and B-type Eph receptors on the common target. Cooperative control of cofilin through EphA and EphB receptors could differentially regulate the extent and timing of cofilin activation and actin organization in dendritic spines. Future studies are needed to investigate how EphA and EphB receptors function to coordinate synaptic plasticity through this pathway.

Recent progress in molecular and imaging techniques have provided a rapid increase in our understanding of the structural plasticity of spines. It is becoming increasingly clear that structure/function relationships exist at synapses and that specific molecules are needed to fine-tune the morphology of synapse. However, the picture is still far from complete. Determining the full network of molecules

present in spines and providing more detailed characterization of signaling events taking place will allow a greater understanding of structure/function relationships of synapses and likely allow important insight into brain diseases.

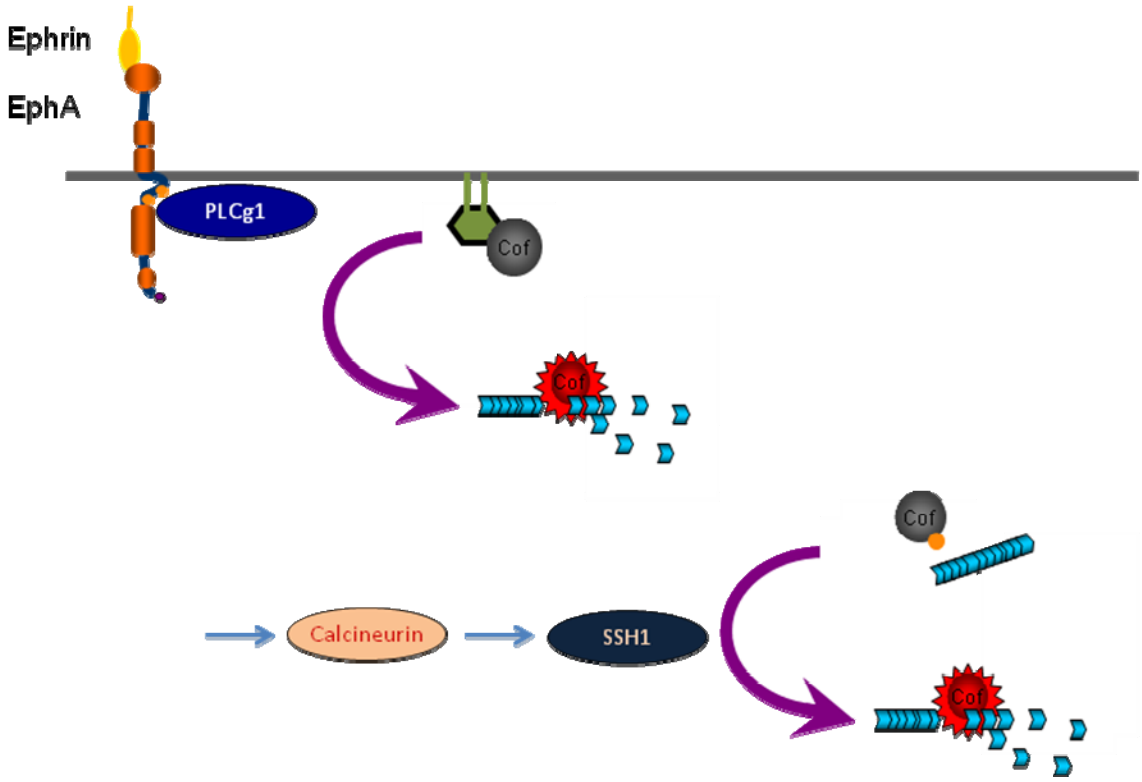
Ephrin
EphA
PLCg1
Cof
Cof
Cof
Calcineurin
SSH1
Cof

Figure 5-1. A schematic model for EphA receptors regulation of cofilin. EphA receptors regulate cofilin at two different levels. Upon EphA receptor activation, PLCγ1 modulates cofilin membrane association through PIP2 hydrolysis. After cofilin is released from the cell membrane, it enters another level of regulation through phosphorylation/dephosphorylation. SSH and calcineurin phosphatases are required for the ephrin-induce cofilin dephosphorylation downstream of EphA receptors.

Reference

Abeliovich A, Paylor R, Chen C, Kim JJ, Wehner JM, Tonegawa S. 1993. PKC gamma mutant mice exhibit mild deficits in spatial and contextual learning. *Cell* 75:1263-71

Agnew BJ, Minamide LS, Bamburg JR. 1995. Reactivation of phosphorylated actin depolymerizing factor and identification of the regulatory site. *Journal of Biological Chemistry* 270:17582-7

Aiba A, Kano M, Chen C, Stanton ME, Fox GD, et al. 1994. Deficient cerebellar long-term depression and impaired motor learning in mGluR1 mutant mice. *Cell* 79:377-88

Aizawa H, Wakatsuki S, Ishii A, Moriyama K, Sasaki Y, et al. 2001. Phosphorylation of cofilin by LIM-kinase is necessary for semaphorin 3A-induced growth cone collapse. *Nature Neuroscience* 4:367-73

Alvarez VA, Sabatini BL. 2007. Anatomical and physiological plasticity of dendritic spines. *Annu Rev Neurosci* 30:79-97

Arber S, Barbayannis FA, Hanser H, Schneider C, Stanyon CA, et al. 1998. Regulation of actin dynamics through phosphorylation of cofilin by LIM-kinase. *Nature* 393:805-9

Bagal AA, Kao JP, Tang CM, Thompson SM. 2005. Long-term potentiation of exogenous glutamate responses at single dendritic spines. *Proc Natl Acad Sci U S A* 102:14434-9

Bailey CH, Kandel ER. 1993. Structural changes accompanying memory storage. *Annu Rev Physiol* 55:397-426

Bailly M, Jones GE. 2003. Polarised migration: cofilin holds the front. *Curr Biol* 13:R128-30

Bamburg JR. 1999. Proteins of the ADF/cofilin family: essential regulators of actin dynamics. *Annu Rev Cell Dev Biol* 15:185-230

Bartlett WP, Banker GA. 1984. An electron microscopic study of the development of axons and dendrites by hippocampal neurons in culture. II. Synaptic relationships. *J Neurosci* 4:1954-65

Bastrikova N, Gardner GA, Reece JM, Jeromin A, Dudek SM. 2008. Synapse elimination accompanies functional plasticity in hippocampal neurons.

Proc Natl Acad Sci U S A 105:3123-7

Beique JC, Lin DT, Kang MG, Aizawa H, Takamiya K, Huganir RL. 2006. Synapse-specific regulation of AMPA receptor function by PSD-95. *Proc Natl Acad Sci U S A* 103:19535-40

Bernstein BW, Bamburg JR. 2010. ADF/cofilin: a functional node in cell biology. *Trends Cell Biol* 20:187-95

Berridge MJ. 1995. Inositol trisphosphate and calcium signaling. *Ann N Y Acad Sci* 766:31-43

Berridge MJ. 2002. The endoplasmic reticulum: a multifunctional signaling organelle. *Cell Calcium* 32:235-49

Biederer T, Stagi M. 2008. Signaling by synaptogenic molecules. *Curr Opin Neurobiol* 18:261-9

Binns KL, Taylor PP, Sicheri F, Pawson T, Holland SJ. 2000. Phosphorylation of tyrosine residues in the kinase domain and juxtamembrane region regulates the biological and catalytic activities of Eph receptors. *Molecular & Cellular Biology* 20:4791-805

Blanpied TA, Ehlers MD. 2004. Microanatomy of dendritic spines: emerging principles of synaptic pathology in psychiatric and neurological disease. *Biol Psychiatry* 55:1121-7

Bliss TV, Collingridge GL. 1993. A synaptic model of memory: long-term potentiation in the hippocampus. *Nature* 361:31-9

Bliss TV, Lomo T. 1973. Long-lasting potentiation of synaptic transmission in the dentate area of the anaesthetized rabbit following stimulation of the perforant path. *J Physiol* 232:331-56

Bloodgood BL, Sabatini BL. 2005. Neuronal activity regulates diffusion across the neck of dendritic spines. *Science* 310:866-9

Bourgin C, Murai KK, Richter M, Pasquale EB. 2007. The EphA4 receptor regulates dendritic spine remodeling by affecting beta1-integrin signaling pathways. *J Cell Biol* 178:1295-307

Bourne J, Harris KM. 2007. Do thin spines learn to be mushroom spines that remember? *Curr Opin Neurobiol* 17:381-6

Bramham CR. 2008. Local protein synthesis, actin dynamics, and LTP consolidation. *Curr Opin Neurobiol* 18:524-31

Buonomano DV, Merzenich MM. 1998. Cortical plasticity: from synapses to

maps. *Annu Rev Neurosci* 21:149-86

Byrne JH. 2008. Learning and Memory: A Comprehensive Reference, Volume 4.

Carmona MA, Murai KK, Wang L, Roberts AJ, Pasquale EB. 2009. Glial ephrin-A3 regulates hippocampal dendritic spine morphology and glutamate transport. *Proc Natl Acad Sci U S A*

Chen C, Tonegawa S. 1997. Molecular genetic analysis of synaptic plasticity, activity-dependent neural development, learning, and memory in the mammalian brain. *Annu Rev Neurosci* 20:157-84

Chen LY, Rex CS, Casale MS, Gall CM, Lynch G. 2007. Changes in synaptic morphology accompany actin signaling during LTP. *J Neurosci* 27:5363-72

Chicurel ME, Harris KM. 1992. Three-dimensional analysis of the structure and composition of CA3 branched dendritic spines and their synaptic relationships with mossy fiber boutons in the rat hippocampus. *J Comp Neurol* 325:169-82

Cho KO, Hunt CA, Kennedy MB. 1992. The rat brain postsynaptic density fraction contains a homolog of the Drosophila discs-large tumor suppressor protein. *Neuron* 9:929-42

Chou J, Stolz DB, Burke NA, Watkins SC, Wells A. 2002. Distribution of gelsolin and phosphoinositol 4,5-bisphosphate in lamellipodia during EGF-induced motility. *International Journal of Biochemistry & Cell Biology* 34:776-90

Cingolani LA, Goda Y. 2008. Actin in action: the interplay between the actin cytoskeleton and synaptic efficacy. *Nat Rev Neurosci* 9:344-56

Clapham DE, Runnels LW, Strubing C. 2001. The TRP ion channel family. *Nat Rev Neurosci* 2:387-96

Comery TA, Stamoudis CX, Irwin SA, Greenough WT. 1996. Increased density of multiple-head dendritic spines on medium-sized spiny neurons of the striatum in rats reared in a complex environment. *Neurobiol Learn Mem* 66:93-6

Cooke JE, Kemp HA, Moens CB. 2005. EphA4 is required for cell adhesion and rhombomere-boundary formation in the zebrafish. *Curr Biol* 15:536-42

Corera AT, Costentin J, Bonnet JJ. 1996. Effect of low concentrations of K+ and Cl- on the Na(+)-dependent neuronal uptake of [3H] dopamine. *Naunyn-Schmiedebergs Archives of Pharmacology* 353:610-5

Cote JF, Motoyama AB, Bush JA, Vuori K. 2005. A novel and evolutionarily

conserved PtdIns(3,4,5)P3-binding domain is necessary for DOCK180 signalling.[see comment]. *Nature Cell Biology* 7:797-807

Cowan CW, Shao YR, Sahin M, Shamah SM, Lin MZ, et al. 2005. Vav family GEFs link activated Ephs to endocytosis and axon guidance.[see comment]. *Neuron* 46:205-17

Dailey ME, Smith SJ. 1996. The dynamics of dendritic structure in developing hippocampal slices. *Journal of Neuroscience* 16:2983-94

Dalva MB, Takasu MA, Lin MZ, Shamah SM, Hu L, et al. 2000. EphB receptors interact with NMDA receptors and regulate excitatory synapse formation. *Cell* 103:945-56

Davis S, Butcher SP, Morris RG. 1992. The NMDA receptor antagonist D-2-amino-5-phosphonopentanoate (D-AP5) impairs spatial learning and LTP in vivo at intracerebral concentrations comparable to those that block LTP in vitro. *J Neurosci* 12:21-34

Dawe HR, Minamide LS, Bamburg JR, Cramer LP. 2003. ADF/cofilin controls cell polarity during fibroblast migration. *Curr Biol* 13:252-7

DesMarais V, Ghosh M, Eddy R, Condeelis J. 2005. Cofilin takes the lead. *Journal of Cell Science* 118:19-26

DiCiommo DP, Bremner R. 1998. Rapid, high level protein production using DNA-based Semliki Forest virus vectors. *J Biol Chem* 273:18060-6

Dunaevsky A, Tashiro A, Majewska A, Mason C, Yuste R. 1999. Developmental regulation of spine motility in the mammalian central nervous system. *Proceedings of the National Academy of Sciences of the United States of America* 96:13438-43

Ehrengruber MU, Lundstrom K, Schweitzer C, Heuss C, Schlesinger S, Gahwiler BH. 1999. Recombinant Semliki Forest virus and Sindbis virus efficiently infect neurons in hippocampal slice cultures. *Proc Natl Acad Sci U S A* 96:7041-6

Eiseler T, Doppler H, Yan IK, Kitatani K, Mizuno K, Storz P. 2009. Protein kinase D1 regulates cofilin-mediated F-actin reorganization and cell motility through slingshot. *Nat Cell Biol* 11:545-56

Ellis C, Kasmi F, Ganju P, Walls E, Panayotou G, Reith AD. 1996. A juxtamembrane autophosphorylation site in the Eph family receptor tyrosine kinase, Sek, mediates high affinity interaction with p59fyn. *Oncogene* 12:1727-36

Ethell IM, Irie F, Kalo MS, Couchman JR, Pasquale EB, Yamaguchi Y. 2001.

EphB/syndecan-2 signaling in dendritic spine morphogenesis. *Neuron* 31:1001-13

Ethell IM, Pasquale EB. 2005. Molecular mechanisms of dendritic spine development and remodeling. *Progress in Neurobiology* 75:161-205

Fedulov V, Rex CS, Simmons DA, Palmer L, Gall CM, Lynch G. 2007. Evidence that long-term potentiation occurs within individual hippocampal synapses during learning. *J Neurosci* 27:8031-9

Fiala JC, Feinberg M, Popov V, Harris KM. 1998. Synaptogenesis via dendritic filopodia in developing hippocampal area CA1. *J Neurosci* 18:8900-11

Fiala JC, Spacek J, Harris KM. 2002. Dendritic spine pathology: cause or consequence of neurological disorders? *Brain Res Brain Res Rev* 39:29-54

Fifkova E, Delay RJ. 1982. Cytoplasmic actin in neuronal processes as a possible mediator of synaptic plasticity. *J Cell Biol* 95:345-50

Filosa A, Paixao S, Honsek SD, Carmona MA, Becker L, et al. 2009. Neuron-glia communication via EphA4/ephrin-A3 modulates LTP through glial glutamate transport. *Nat Neurosci* 12:1285-92

Fischer M, Kaech S, Knutti D, Matus A. 1998. Rapid actin-based plasticity in dendritic spines. *Neuron* 20:847-54

Flanagan JG, Vanderhaeghen P. 1998. The ephrins and Eph receptors in neural development. *Annual Review of Neuroscience* 21:309-45

Frangiskakis JM, Ewart AK, Morris CA, Mervis CB, Bertrand J, et al. 1996. LIM-kinase1 hemizygosity implicated in impaired visuospatial constructive cognition. *Cell* 86:59-69

Frankland PW, Josselyn SA, Anagnostaras SG, Kogan JH, Takahashi E, Silva AJ. 2004. Consolidation of CS and US representations in associative fear conditioning. *Hippocampus* 14:557-69

Fu AK, Ip NY. 2007. Cyclin-dependent kinase 5 links extracellular cues to actin cytoskeleton during dendritic spine development. *Cell Adh Migr* 1:110-2

Fu WY, Chen Y, Sahin M, Zhao XS, Shi L, et al. 2007. Cdk5 regulates EphA4-mediated dendritic spine retraction through an ephexin1-dependent mechanism. *Nat Neurosci* 10:67-76

Fukazawa Y, Saitoh Y, Ozawa F, Ohta Y, Mizuno K, Inokuchi K. 2003. Hippocampal LTP is accompanied by enhanced F-actin content within the dendritic spine that is essential for late LTP maintenance in vivo.[see comment]. *Neuron* 38:447-60

Gale NW, Holland SJ, Valenzuela DM, Flenniken A, Pan L, et al. 1996. Eph receptors and ligands comprise two major specificity subclasses and are reciprocally compartmentalized during embryogenesis. *Neuron* 17:9-19

Gartner A, Polnau DG, Staiger V, Sciarretta C, Minichiello L, et al. 2006. Hippocampal long-term potentiation is supported by presynaptic and postsynaptic tyrosine receptor kinase B-mediated phospholipase Cgamma signaling. *J Neurosci* 26:3496-504

Gerfen CR, Choi WC, Suh PG, Rhee SG. 1988. Phospholipase C I and II brain isozymes: immunohistochemical localization in neuronal systems in rat brain. *Proceedings of the National Academy of Sciences of the United States of America* 85:3208-12

Gohla A, Bokoch GM. 2002. 14-3-3 regulates actin dynamics by stabilizing phosphorylated cofilin. *Current Biology* 12:1704-10

Goodman CS. 1996. Mechanisms and molecules that control growth cone guidance. *Annu Rev Neurosci* 19:341-77

Grant SG, Silva AJ. 1994. Targeting learning. *Trends Neurosci* 17:71-5

Grunwald IC, Korte M, Adelmann G, Plueck A, Kullander K, et al. 2004. Hippocampal plasticity requires postsynaptic ephrinBs. *Nature Neuroscience* 7:33-40

Grutzendler J, Kasthuri N, Gan WB. 2002. Long-term dendritic spine stability in the adult cortex. *Nature* 420:812-6

Haber M, Zhou L, Murai KK. 2006. Cooperative astrocyte and dendritic spine dynamics at hippocampal excitatory synapses. *J Neurosci* 26:8881-91

Halloran MC, Wolman MA. 2006. Repulsion or adhesion: receptors make the call. *Curr Opin Cell Biol* 18:533-40

Hansen MJ, Dallal GE, Flanagan JG. 2004. Retinal axon response to ephrin-as shows a graded, concentration-dependent transition from growth promotion to inhibition. *Neuron* 42:717-30

Harris KM, Jensen FE, Tsao B. 1992. Three-dimensional structure of dendritic spines and synapses in rat hippocampus (CA1) at postnatal day 15 and adult ages: implications for the maturation of synaptic physiology and long-term potentiation. *J Neurosci* 12:2685-705

Harris KM, Stevens JK. 1989. Dendritic spines of CA 1 pyramidal cells in the rat hippocampus: serial electron microscopy with reference to their biophysical characteristics. *J Neurosci* 9:2982-97

Hayashi Y, Majewska AK. 2005. Dendritic spine geometry: functional implication and regulation. *Neuron* 46:529-32

Henkemeyer M, Itkis OS, Ngo M, Hickmott PW, Ethell IM. 2003. Multiple EphB receptor tyrosine kinases shape dendritic spines in the hippocampus. *Journal of Cell Biology* 163:1313-26

Hering H, Sheng M. 2001. Dendritic spines: structure, dynamics and regulation. *Nat Rev Neurosci* 2:880-8

Hering H, Sheng M. 2003. Activity-dependent redistribution and essential role of cortactin in dendritic spine morphogenesis. *J Neurosci* 23:11759-69

Heyworth PG, Robinson JM, Ding J, Ellis BA, Badwey JA. 1997. Cofilin undergoes rapid dephosphorylation in stimulated neutrophils and translocates to ruffled membranes enriched in products of the NADPH oxidase complex. Evidence for a novel cycle of phosphorylation and dephosphorylation. *Histochemistry & Cell Biology* 108:221-33

Hirokawa N. 1989. The arrangement of actin filaments in the postsynaptic cytoplasm of the cerebellar cortex revealed by quick-freeze deep-etch electron microscopy. *Neuroscience Research* 6:269-75

Hock B, Bohme B, Karn T, Yamamoto T, Kaibuchi K, et al. 1998. PDZ-domain-mediated interaction of the Eph-related receptor tyrosine kinase EphB3 and the ras-binding protein AF6 depends on the kinase activity of the receptor. *Proceedings of the National Academy of Sciences of the United States of America* 95:9779-84

Holtmaat A, Wilbrecht L, Knott GW, Welker E, Svoboda K. 2006. Experience-dependent and cell-type-specific spine growth in the neocortex. *Nature* 441:979-83

Honkura N, Matsuzaki M, Noguchi J, Ellis-Davies GC, Kasai H. 2008. The subspine organization of actin fibers regulates the structure and plasticity of dendritic spines. *Neuron* 57:719-29

Hoogenraad CC, Milstein AD, Ethell IM, Henkemeyer M, Sheng M. 2005. GRIP1 controls dendrite morphogenesis by regulating EphB receptor trafficking. *Nature Neuroscience* 8:906-15

Horne EA, Dell'Acqua ML. 2007. Phospholipase C is required for changes in postsynaptic structure and function associated with NMDA receptor-dependent long-term depression. *J Neurosci* 27:3523-34

Hotulainen P, Llano O, Smirnov S, Tanhuanpaa K, Faix J, et al. 2009. Defining mechanisms of actin polymerization and depolymerization during dendritic spine morphogenesis. *J Cell Biol* 185:323-39

Hsieh SH, Ferraro GB, Fournier AE. 2006. Myelin-associated inhibitors regulate cofilin phosphorylation and neuronal inhibition through LIM kinase and Slingshot phosphatase. *J Neurosci* 26:1006-15

Huang PS, Davis L, Huber H, Goodhart PJ, Wegrzyn RE, et al. 1995. An SH3 domain is required for the mitogenic activity of microinjected phospholipase C-gamma 1. *FEBS Letters* 358:287-92

Huang TY, DerMardirossian C, Bokoch GM. 2006. Cofilin phosphatases and regulation of actin dynamics. *Current Opinion in Cell Biology* 18:26-31

Huttner WB, Schiebler W, Greengard P, De Camilli P. 1983. Synapsin I (protein I), a nerve terminal-specific phosphoprotein. III. Its association with synaptic vesicles studied in a highly purified synaptic vesicle preparation. *Journal of Cell Biology* 96:1374-88

Ikebe C, Ohashi K, Fujimori T, Bernard O, Noda T, et al. 1997. Mouse LIM-kinase 2 gene: cDNA cloning, genomic organization, and tissue-specific expression of two alternatively initiated transcripts. *Genomics* 46:504-8

Irie F, Yamaguchi Y. 2002. EphB receptors regulate dendritic spine development via intersectin, Cdc42 and N-WASP. *Nature Neuroscience* 5:1117-8

Irwin SA, Galvez R, Greenough WT. 2000. Dendritic spine structural anomalies in fragile-X mental retardation syndrome. *Cerebral Cortex* 10:1038-44

Kaech S, Banker G. 2006. Culturing hippocampal neurons. *Nat Protoc* 1:2406-15

Kaech S, Fischer M, Doll T, Matus A. 1997. Isoform specificity in the relationship of actin to dendritic spines. *Journal of Neuroscience* 17:9565-72

Kalo MS, Pasquale EB. 1999. Signal transfer by Eph receptors. *Cell & Tissue Research* 298:1-9

Kang H, Sun LD, Atkins CM, Soderling TR, Wilson MA, Tonegawa S. 2001. An important role of neural activity-dependent CaMKIV signaling in the consolidation of long-term memory. *Cell* 106:771-83

Kasai H, Matsuzaki M, Noguchi J, Yasumatsu N, Nakahara H. 2003. Structure-stability-function relationships of dendritic spines. *Trends in Neurosciences* 26:360-8

Kaufmann WE, Moser HW. 2000. Dendritic anomalies in disorders associated with mental retardation. *Cerebral Cortex* 10:981-91

Kennedy MJ, Ehlers MD. 2006. Organelles and trafficking machinery for postsynaptic plasticity. *Annu Rev Neurosci* 29:325-62

Kim CH, Lisman JE. 1999. A role of actin filament in synaptic transmission and long-term potentiation. *Journal of Neuroscience* 19:4314-24

Kim E, Sheng M. 2004. PDZ domain proteins of synapses. *Nature Reviews Neuroscience* 5:771-81

Kim HK, Kim JW, Zilberstein A, Margolis B, Kim JG, et al. 1991. PDGF stimulation of inositol phospholipid hydrolysis requires PLC-gamma 1 phosphorylation on tyrosine residues 783 and 1254. *Cell* 65:435-41

Kim JW, Sim SS, Kim UH, Nishibe S, Wahl MI, et al. 1990. Tyrosine residues in bovine phospholipase C-gamma phosphorylated by the epidermal growth factor receptor in vitro. *Journal of Biological Chemistry* 265:3940-3

Klee CB, Crouch TH, Krinks MH. 1979. Calcineurin: a calcium- and calmodulin-binding protein of the nervous system. *Proc Natl Acad Sci U S A* 76:6270-3

Klein R. 2004. Eph/ephrin signaling in morphogenesis, neural development and plasticity. *Current Opinion in Cell Biology* 16:580-9

Knott GW, Holtmaat A, Wilbrecht L, Welker E, Svoboda K. 2006. Spine growth precedes synapse formation in the adult neocortex in vivo. *Nat Neurosci* 9:1117-24

Korkotian E, Segal M. 2001. Regulation of dendritic spine motility in cultured hippocampal neurons. *Journal of Neuroscience* 21:6115-24

Korobova F, Svitkina T. 2010. Molecular architecture of synaptic actin cytoskeleton in hippocampal neurons reveals a mechanism of dendritic spine morphogenesis. *Mol Biol Cell* 21:165-76

Kousaka K, Kiyonari H, Oshima N, Nagafuchi A, Shima Y, et al. 2008. Slingshot-3 dephosphorylates ADF/cofilin but is dispensable for mouse development. *Genesis* 46:246-55

Kullander K, Klein R. 2002. Mechanisms and functions of Eph and ephrin signalling. *Nat Rev Mol Cell Biol* 3:475-86

Kullander K, Mather NK, Diella F, Dottori M, Boyd AW, Klein R. 2001. Kinase-dependent and kinase-independent functions of EphA4 receptors in major axon tract formation in vivo. *Neuron* 29:73-84

Kurita S, Watanabe Y, Gunji E, Ohashi K, Mizuno K. 2008. Molecular dissection of the mechanisms of substrate recognition and F-actin-mediated activation of cofilin-phosphatase Slingshot-1. *J Biol Chem* 283:32542-52

Lemke G, Reber M. 2005. Retinotectal mapping: new insights from molecular

genetics. *Annu Rev Cell Dev Biol* 21:551-80

Li S, Tian X, Hartley DM, Feig LA. 2006. Distinct roles for Ras-guanine nucleotide-releasing factor 1 (Ras-GRF1) and Ras-GRF2 in the induction of long-term potentiation and long-term depression. *J Neurosci* 26:1721-9

Lin B, Kramar EA, Bi X, Brucher FA, Gall CM, Lynch G. 2005. Theta stimulation polymerizes actin in dendritic spines of hippocampus. *J Neurosci* 25:2062-9

Lippman J, Dunaevsky A. 2005. Dendritic spine morphogenesis and plasticity. *J Neurobiol* 64:47-57

Lisman JE, Harris KM. 1993. Quantal analysis and synaptic anatomy--integrating two views of hippocampal plasticity. *Trends Neurosci* 16:141-7

Liu Y, Bankaitis VA. 2010. Phosphoinositide phosphatases in cell biology and disease. *Prog Lipid Res* 49:201-17

Lopes CM, Rohacs T, Czirjak G, Balla T, Enyedi P, Logothetis DE. 2005. PIP2 hydrolysis underlies agonist-induced inhibition and regulates voltage gating of two-pore domain K+ channels. *Journal of Physiology* 564:117-29

Lundstrom K, Abenavoli A, Malgaroli A, Ehrengruber MU. 2003. Novel Semliki Forest virus vectors with reduced cytotoxicity and temperature sensitivity for long-term enhancement of transgene expression. *Mol Ther* 7:202-9

Lynch MA, Clements MP, Errington ML, Bliss TVP. 1988. Increased hydrolysis of phosphatidylinositol-4,5-bisphosphate in long-term potentiation. *Neuroscience Letters* 84:291-96

Malenka RC, Nicoll RA. 1999. Long-term potentiation--a decade of progress? *Science* 285:1870-4

Maletic-Savatic M, Malinow R, Svoboda K. 1999. Rapid dendritic morphogenesis in CA1 hippocampal dendrites induced by synaptic activity. *Science* 283:1923-7

Malleret G, Haditsch U, Genoux D, Jones MW, Bliss TV, et al. 2001. Inducible and reversible enhancement of learning, memory, and long-term potentiation by genetic inhibition of calcineurin. *Cell* 104:675-86

Marrs GS, Green SH, Dailey ME. 2001. Rapid formation and remodeling of postsynaptic densities in developing dendrites. *Nat Neurosci* 4:1006-13

Matsuzaki M, Ellis-Davies GC, Nemoto T, Miyashita Y, Iino M, Kasai H. 2001. Dendritic spine geometry is critical for AMPA receptor expression in

hippocampal CA1 pyramidal neurons. *Nat Neurosci* 4:1086-92

Matsuzaki M, Honkura N, Ellis-Davies GC, Kasai H. 2004. Structural basis of long-term potentiation in single dendritic spines. *Nature* 429:761-6

Mattila PK, Lappalainen P. 2008. Filopodia: molecular architecture and cellular functions. *Nat Rev Mol Cell Biol* 9:446-54

Matus A. 2000. Actin-based plasticity in dendritic spines. *Science* 290:754-8

Matus A, Brinkhaus H, Wagner U. 2000. Actin dynamics in dendritic spines: a form of regulated plasticity at excitatory synapses. *Hippocampus* 10:555-60

McLaughlin T, O'Leary DD. 2005. Molecular gradients and development of retinotopic maps. *Annu Rev Neurosci* 28:327-55

Meng Y, Takahashi H, Meng J, Zhang Y, Lu G, et al. 2004. Regulation of ADF/cofilin phosphorylation and synaptic function by LIM-kinase. *Neuropharmacology* 47:746-54

Meng Y, Zhang Y, Tregoubov V, Janus C, Cruz L, et al. 2002. Abnormal spine morphology and enhanced LTP in LIMK-1 knockout mice.[see comment]. *Neuron* 35:121-33

Micheva KD, Holz RW, Smith SJ. 2001. Regulation of presynaptic phosphatidylinositol 4,5-biphosphate by neuronal activity. *J Cell Biol* 154:355-68

Miller M, Peters A. 1981. Maturation of rat visual cortex. II. A combined Golgi-electron microscope study of pyramidal neurons. *J Comp Neurol* 203:555-73

Mizuno K, Okano I, Ohashi K, Nunoue K, Kuma K, et al. 1994. Identification of a human cDNA encoding a novel protein kinase with two repeats of the LIM/double zinc finger motif. *Oncogene* 9:1605-12

Moeller ML, Shi Y, Reichardt LF, Ethell IM. 2006. EphB receptors regulate dendritic spine morphogenesis through the recruitment/phosphorylation of focal adhesion kinase and RhoA activation. *Journal of Biological Chemistry* 281:1587-98

Monfils MH, Teskey GC. 2004. Induction of long-term depression is associated with decreased dendritic length and spine density in layers III and V of sensorimotor neocortex. *Synapse* 53:114-21

Morgan TE, Lockerbie RO, Minamide LS, Browning MD, Bamburg JR. 1993. Isolation and characterization of a regulated form of actin depolymerizing

factor. *Journal of Cell Biology* 122:623-33

Mori T, Okano I, Mizuno K, Tohyama M, Wanaka A. 1997. Comparison of tissue distribution of two novel serine/threonine kinase genes containing the LIM motif (LIMK-1 and LIMK-2) in the developing rat. *Brain Research. Molecular Brain Research* 45:247-54

Morita A, Yamashita N, Sasaki Y, Uchida Y, Nakajima O, et al. 2006. Regulation of dendritic branching and spine maturation by semaphorin3A-Fyn signaling. *Journal of Neuroscience* 26:2971-80

Moriyama K, Iida K, Yahara I. 1996. Phosphorylation of Ser-3 of cofilin regulates its essential function on actin. *Genes to Cells* 1:73-86

Mulholland J, Preuss D, Moon A, Wong A, Drubin D, Botstein D. 1994. Ultrastructure of the yeast actin cytoskeleton and its association with the plasma membrane. *Journal of Cell Biology* 125:381-91

Mulkey RM, Endo S, Shenolikar S, Malenka RC. 1994. Involvement of a calcineurin/inhibitor-1 phosphatase cascade in hippocampal long-term depression. *Nature* 369:486-8

Murai KK, Nguyen LN, Irie F, Yamaguchi Y, Pasquale EB. 2003a. Control of hippocampal dendritic spine morphology through ephrin-A3/EphA4 signaling. *Nature Neuroscience* 6:153-60

Murai KK, Nguyen LN, Koolpe M, McLennan R, Krull CE, Pasquale EB. 2003b. Targeting the EphA4 receptor in the nervous system with biologically active peptides. *Molecular & Cellular Neurosciences* 24:1000-11

Murai KK, Pasquale EB. 2003. 'Eph'ective signaling: forward, reverse and crosstalk. *Journal of Cell Science* 116:2823-32

Murai KK, Pasquale EB. 2004. Eph receptors, ephrins, and synaptic function. *Neuroscientist* 10:304-14

Nagaoka R, Abe H, Obinata T. 1996. Site-directed mutagenesis of the phosphorylation site of cofilin: its role in cofilin-actin interaction and cytoplasmic localization. *Cell Motility & the Cytoskeleton* 35:200-9

Nagaoka R, Kusano K, Abe H, Obinata T. 1995. Effects of cofilin on actin filamentous structures in cultured muscle cells. Intracellular regulation of cofilin action. *J Cell Sci* 108 (Pt 2):581-93

Nagase T, Ito K-I, Kato K, Kaneko K, Kohda K, et al. 2003. Long-term potentiation and long-term depression in hippocampal CA1 neurons of mice lacking the IP3 type 1 receptor. *Neuroscience* 117:821-30

Nagata-Ohashi K, Ohta Y, Goto K, Chiba S, Mori R, et al. 2004. A pathway of neuregulin-induced activation of cofilin-phosphatase Slingshot and cofilin in lamellipodia. *Journal of Cell Biology* 165:465-71

Nagerl UV, Eberhorn N, Cambridge SB, Bonhoeffer T. 2004. Bidirectional activity-dependent morphological plasticity in hippocampal neurons. *Neuron* 44:759-67

Nakagawa T, Engler JA, Sheng M. 2004. The dynamic turnover and functional roles of alpha-actinin in dendritic spines. *Neuropharmacology* 47:734-45

Nimchinsky EA, Sabatini BL, Svoboda K. 2002. Structure and function of dendritic spines. *Annu Rev Physiol* 64:313-53

Nishida H, Okabe S. 2007. Direct astrocytic contacts regulate local maturation of dendritic spines. *J Neurosci* 27:331-40

Niwa R, Nagata-Ohashi K, Takeichi M, Mizuno K, Uemura T. 2002. Control of actin reorganization by Slingshot, a family of phosphatases that dephosphorylate ADF/cofilin. *Cell* 108:233-46

Noguchi J, Matsuzaki M, Ellis-Davies GC, Kasai H. 2005. Spine-neck geometry determines NMDA receptor-dependent Ca2+ signaling in dendrites. *Neuron* 46:609-22

Nunoue K, Ohashi K, Okano I, Mizuno K. 1995. LIMK-1 and LIMK-2, two members of a LIM motif-containing protein kinase family. *Oncogene* 11:701-10

Ohta Y, Kousaka K, Nagata-Ohashi K, Ohashi K, Muramoto A, et al. 2003. Differential activities, subcellular distribution and tissue expression patterns of three members of Slingshot family phosphatases that dephosphorylate cofilin. *Genes to Cells* 8:811-24

Okabe S, Miwa A, Okado H. 2001. Spine formation and correlated assembly of presynaptic and postsynaptic molecules. *J Neurosci* 21:6105-14

Okamoto K, Nagai T, Miyawaki A, Hayashi Y. 2004. Rapid and persistent modulation of actin dynamics regulates postsynaptic reorganization underlying bidirectional plasticity. *Nat Neurosci* 7:1104-12

Okano I, Hiraoka J, Otera H, Nunoue K, Ohashi K, et al. 1995. Identification and characterization of a novel family of serine/threonine kinases containing two N-terminal LIM motifs. *Journal of Biological Chemistry* 270:31321-30

Orioli D, Klein R. 1997. The Eph receptor family: axonal guidance by contact repulsion. *Trends in Genetics* 13:354-9

Palmer A, Klein R. 2003. Multiple roles of ephrins in morphogenesis, neuronal networking, and brain function. *Genes Dev* 17:1429-50

Park DJ, Min HK, Rhee SG. 1992. Inhibition of CD3-linked phospholipase C by phorbol ester and by cAMP is associated with decreased phosphotyrosine and increased phosphoserine contents of PLC-gamma 1. *Journal of Biological Chemistry* 267:1496-501

Parnass Z, Tashiro A, Yuste R. 2000. Analysis of spine morphological plasticity in developing hippocampal pyramidal neurons. *Hippocampus* 10:561-8

Pasquale EB. 1997. The Eph family of receptors. *Curr Opin Cell Biol* 9:608-15

Pasquale EB. 2004. Eph-ephrin promiscuity is now crystal clear. *Nat Neurosci* 7:417-8

Patterson RL, van Rossum DB, Ford DL, Hurt KJ, Bae SS, et al. 2002. Phospholipase C-gamma is required for agonist-induced Ca2+ entry. *Cell* 111:529-41

Patterson RL, van Rossum DB, Nikolaidis N, Gill DL, Snyder SH. 2005. Phospholipase C-gamma: diverse roles in receptor-mediated calcium signaling. *Trends Biochem Sci* 30:688-97

Penzes P, Beeser A, Chernoff J, Schiller MR, Eipper BA, et al. 2003. Rapid induction of dendritic spine morphogenesis by trans-synaptic ephrinB-EphB receptor activation of the Rho-GEF kalirin. *Neuron* 37:263-74

Peters A, Palay S, Webster H. 1991. *The fine structure of the nervous system*: Oxford

Pfeiffer BE, Huber KM. 2009. The state of synapses in fragile X syndrome. *Neuroscientist* 15:549-67

Phillips GR, Huang JK, Wang Y, Tanaka H, Shapiro L, et al. 2001. The presynaptic particle web: ultrastructure, composition, dissolution, and reconstitution.[see comment]. *Neuron* 32:63-77

Poulin B, Sekiya F, Rhee SG. 2005. Intramolecular interaction between phosphorylated tyrosine-783 and the C-terminal Src homology 2 domain activates phospholipase C-gamma 1. *Proceedings of the National Academy of Sciences of the United States of America* 102:4276-81

Racz B, Weinberg RJ. 2006. Spatial organization of cofilin in dendritic spines. *Neuroscience* 138:447-56

Racz B, Weinberg RJ. 2008. Organization of the Arp2/3 complex in hippocampal

spines. *J Neurosci* 28:5654-9

Ramon y Cajal S. 1893. The structure of Ammon's horn. *Ann Soc Esp Hist Nat*

Rao A, Craig AM. 2000. Signaling between the actin cytoskeleton and the postsynaptic density of dendritic spines. *Hippocampus* 10:527-41

Raucher D, Stauffer T, Chen W, Shen K, Guo S, et al. 2000. Phosphatidylinositol 4,5-bisphosphate functions as a second messenger that regulates cytoskeleton-plasma membrane adhesion. *Cell* 100:221-8

Rebecchi MJ, Pentyala SN. 2000. Structure, function, and control of phosphoinositide-specific phospholipase C. *Physiol Rev* 80:1291-335

Reyes-Harde M, Stanton PK. 1998. Postsynaptic phospholipase C activity is required for the induction of homosynaptic long-term depression in rat hippocampus. *Neurosci Lett* 252:155-8

Robinson TE, Kolb B. 1999. Alterations in the morphology of dendrites and dendritic spines in the nucleus accumbens and prefrontal cortex following repeated treatment with amphetamine or cocaine. *Eur J Neurosci* 11:1598-604

Rohacs T, Lopes CM, Michailidis I, Logothetis DE. 2005. PI(4,5)P2 regulates the activation and desensitization of TRPM8 channels through the TRP domain. *Nature Neuroscience* 8:626-34

Rong R, Ahn JY, Chen P, Suh PG, Ye K. 2003. Phospholipase activity of phospholipase C-gamma1 is required for nerve growth factor-regulated MAP kinase signaling cascade in PC12 cells. *Journal of Biological Chemistry* 278:52497-503

Ronnstrand L, Siegbahn A, Rorsman C, Johnell M, Hansen K, Heldin CH. 1999. Overactivation of phospholipase C-gamma1 renders platelet-derived growth factor beta-receptor-expressing cells independent of the phosphatidylinositol 3-kinase pathway for chemotaxis. *Journal of Biological Chemistry* 274:22089-94

Ross CA, MacCumber MW, Glatt CE, Snyder SH. 1989. Brain phospholipase C isozymes: differential mRNA localizations by in situ hybridization. *Proceedings of the National Academy of Sciences of the United States of America* 86:2923-7

Saarikangas J, Zhao H, Lappalainen P. 2010. Regulation of the actin cytoskeleton-plasma membrane interplay by phosphoinositides. *Physiol Rev* 90:259-89

Sahin M, Greer PL, Lin MZ, Poucher H, Eberhart J, et al. 2005. Eph-dependent

tyrosine phosphorylation of ephexin1 modulates growth cone collapse. *Neuron* 46:191-204

Sawa A, Snyder SH. 2002. Schizophrenia: diverse approaches to a complex disease. *Science* 296:692-5

Schikorski T, Stevens CF. 1997. Quantitative ultrastructural analysis of hippocampal excitatory synapses. *J Neurosci* 17:5858-67

Schratt GM, Tuebing F, Nigh EA, Kane CG, Sabatini ME, et al. 2006. A brain-specific microRNA regulates dendritic spine development. *Nature* 439:283-9

Scicolone G, Ortalli AL, Carri NG. 2009. Key roles of Ephs and ephrins in retinotectal topographic map formation. *Brain Res Bull* 79:227-47

Sdrulla AD, Linden DJ. 2007. Double dissociation between long-term depression and dendritic spine morphology in cerebellar Purkinje cells. *Nat Neurosci* 10:546-8

Sechi AS, Wehland J. 2000. The actin cytoskeleton and plasma membrane connection: PtdIns(4,5)P(2) influences cytoskeletal protein activity at the plasma membrane. *Journal of Cell Science* 113 Pt 21:3685-95

Segal M. 2005. Dendritic spines and long-term plasticity. *Nat Rev Neurosci* 6:277-84

Sekino Y, Kojima N, Shirao T. 2007. Role of actin cytoskeleton in dendritic spine morphogenesis. *Neurochem Int* 51:92-104

Sela-Donenfeld D, Wilkinson DG. 2005. Eph receptors: two ways to sharpen boundaries. *Curr Biol* 15:R210-2

Sheng M, Hoogenraad CC. 2007. The postsynaptic architecture of excitatory synapses: a more quantitative view. *Annu Rev Biochem* 76:823-47

Shi Y, Pontrello CG, DeFea KA, Reichardt LF, Ethell IM. 2009. Focal adhesion kinase acts downstream of EphB receptors to maintain mature dendritic spines by regulating cofilin activity. *J Neurosci* 29:8129-42

Sidani M, Wessels D, Mouneimne G, Ghosh M, Goswami S, et al. 2007. Cofilin determines the migration behavior and turning frequency of metastatic cancer cells. *J Cell Biol* 179:777-91

Silva AJ, Paylor R, Wehner JM, Tonegawa S. 1992a. Impaired spatial learning in alpha-calcium-calmodulin kinase II mutant mice. *Science* 257:206-11

Silva AJ, Stevens CF, Tonegawa S, Wang Y. 1992b. Deficient hippocampal

long-term potentiation in alpha-calcium-calmodulin kinase II mutant mice. *Science* 257:201-6

Smith R, Sam L, Justen J, Bundy G, Bala G, Bleasdale J. 1990. Receptor-coupled signal transduction in human polymorphonuclear neutrophils: effects of a novel inhibitor of phospholipase C-dependent processes on cell responsiveness. *J Pharmacol Exp Ther* 253:688-97

Soans C, Holash JA, Pasquale EB. 1994. Characterization of the expression of the Cek8 receptor-type tyrosine kinase during development and in tumor cell lines. *Oncogene* 9:3353-61

Song X, Chen X, Yamaguchi H, Mouneimne G, Condeelis JS, Eddy RJ. 2006. Initiation of cofilin activity in response to EGF is uncoupled from cofilin phosphorylation and dephosphorylation in carcinoma cells. *Journal of Cell Science* in press

Soosairajah J, Maiti S, Wiggan O, Sarmiere P, Moussi N, et al. 2005. Interplay between components of a novel LIM kinase-slingshot phosphatase complex regulates cofilin. *EMBO Journal* 24:473-86

Sorra KE, Harris KM. 2000. Overview on the structure, composition, function, development, and plasticity of hippocampal dendritic spines. *Hippocampus* 10:501-11

Sotelo C, Alvarado-Mallart RM, Gardette R, Crepel F. 1990. Fate of grafted embryonic Purkinje cells in the cerebellum of the adult "Purkinje cell degeneration" mutant mouse. I. Development of reciprocal graft-host interactions. *J Comp Neurol* 295:165-87

Spacek J, Harris KM. 1997. Three-dimensional organization of smooth endoplasmic reticulum in hippocampal CA1 dendrites and dendritic spines of the immature and mature rat. *J Neurosci* 17:190-203

Star EN, Kwiatkowski DJ, Murthy VN. 2002. Rapid turnover of actin in dendritic spines and its regulation by activity. *Nat Neurosci* 5:239-46

Steward O, Levy WB. 1982. Preferential localization of polyribosomes under the base of dendritic spines in granule cells of the dentate gyrus. *J Neurosci* 2:284-91

Sumi T, Matsumoto K, Nakamura T. 2001. Specific activation of LIM kinase 2 via phosphorylation of threonine 505 by ROCK, a Rho-dependent protein kinase. *Journal of Biological Chemistry* 276:670-6

Sumi T, Matsumoto K, Takai Y, Nakamura T. 1999. Cofilin phosphorylation and actin cytoskeletal dynamics regulated by rho- and Cdc42-activated LIM-kinase 2. *Journal of Cell Biology* 147:1519-32

Suzuki K, Yamaguchi T, Tanaka T, Kawanishi T, Nishimaki-Mogami T, et al. 1995. Activation induces dephosphorylation of cofilin and its translocation to plasma membranes in neutrophil-like differentiated HL-60 cells. *Journal of Biological Chemistry* 270:19551-6

Tada T, Sheng M. 2006. Molecular mechanisms of dendritic spine morphogenesis. *Curr Opin Neurobiol* 16:95-101

Takacs J, Gombos G, Gorcs T, Becker T, de Barry J, Hamori J. 1997. Distribution of metabotropic glutamate receptor type 1a in Purkinje cell dendritic spines is independent of the presence of presynaptic parallel fibers. *J Neurosci Res* 50:433-42

Takasu MA, Dalva MB, Zigmond RE, Greenberg ME. 2002. Modulation of NMDA receptor-dependent calcium influx and gene expression through EphB receptors. *Science* 295:491-5

Takumi Y, Matsubara A, Rinvik E, Ottersen OP. 1999. The arrangement of glutamate receptors in excitatory synapses. *Ann N Y Acad Sci* 868:474-82

Tanaka O, Kondo H. 1994. Localization of mRNAs for three novel members ([beta]3, [beta]4 and [gamma]2) of phospholipase C family in mature rat brain. *Neuroscience Letters* 182:17-20

Taufiq AM, Fujii S, Yamazaki Y, Sasaki H, Kaneko K, et al. 2005. Involvement of IP3 receptors in LTP and LTD induction in guinea pig hippocampal CA1 neurons. *Learn. Mem.* 12:594-600

Tolias KF, Bikoff JB, Kane CG, Tolias CS, Hu L, Greenberg ME. 2007. The Rac1 guanine nucleotide exchange factor Tiam1 mediates EphB receptor-dependent dendritic spine development. *Proc Natl Acad Sci U S A* 104:7265-70

Torres R, Firestein BL, Dong H, Staudinger J, Olson EN, et al. 1998. PDZ proteins bind, cluster, and synaptically colocalize with Eph receptors and their ephrin ligands. *Neuron* 21:1453-63

Toshima J, Toshima JY, Amano T, Yang N, Narumiya S, Mizuno K. 2001. Cofilin phosphorylation by protein kinase testicular protein kinase 1 and its role in integrin-mediated actin reorganization and focal adhesion formation. *Molecular Biology of the Cell* 12:1131-45

Trachtenberg JT, Chen BE, Knott GW, Feng G, Sanes JR, et al. 2002. Long-term in vivo imaging of experience-dependent synaptic plasticity in adult cortex. *Nature* 420:788-94

van Spronsen M, Hoogenraad CC. 2010. Synapse pathology in psychiatric and neurologic disease. *Curr Neurol Neurosci Rep* 10:207-14

Van Troys M, Huyck L, Leyman S, Dhaese S, Vandekerkhove J, Ampe C. 2008. Ins and outs of ADF/cofilin activity and regulation. *Eur J Cell Biol* 87:649-67

von Philipsborn AC, Lang S, Loeschinger J, Bernard A, David C, et al. 2006. Growth cone navigation in substrate-bound ephrin gradients. *Development* 133:2487-95

Wang Y, Shibasaki F, Mizuno K. 2005. Calcium signal-induced cofilin dephosphorylation is mediated by Slingshot via calcineurin. *Journal of Biological Chemistry* 280:12683-9

Whitlock JR, Heynen AJ, Shuler MG, Bear MF. 2006. Learning induces long-term potentiation in the hippocampus. *Science* 313:1093-7

Wilkinson DG. 2000. Eph receptors and ephrins: regulators of guidance and assembly. *Int Rev Cytol* 196:177-244

Wilkinson DG. 2001. Multiple roles of EPH receptors and ephrins in neural development. *Nat Rev Neurosci* 2:155-64

Wybenga-Groot LE, Baskin B, Ong SH, Tong J, Pawson T, Sicheri F. 2001. Structural basis for autoinhibition of the Ephb2 receptor tyrosine kinase by the unphosphorylated juxtamembrane region. *Cell* 106:745-57

Yamaguchi Y, Pasquale EB. 2004. Eph receptors in the adult brain. *Curr Opin Neurobiol* 14:288-96

Yang G, Pan F, Gan WB. 2009. Stably maintained dendritic spines are associated with lifelong memories. *Nature* 462:920-4

Yang N, Higuchi O, Ohashi K, Nagata K, Wada A, et al. 1998. Cofilin phosphorylation by LIM-kinase 1 and its role in Rac-mediated actin reorganization.[see comment]. *Nature* 393:809-12

Yonezawa N, Homma Y, Yahara I, Sakai H, Nishida E. 1991a. A short sequence responsible for both phosphoinositide binding and actin binding activities of cofilin. *Journal of Biological Chemistry* 266:17218-21

Yonezawa N, Nishida E, Iida K, Kumagai H, Yahara I, Sakai H. 1991b. Inhibition of actin polymerization by a synthetic dodecapeptide patterned on the sequence around the actin-binding site of cofilin. *Journal of Biological Chemistry* 266:10485-9

Yonezawa N, Nishida E, Iida K, Yahara I, Sakai H. 1990. Inhibition of the interactions of cofilin, destrin, and deoxyribonuclease I with actin by phosphoinositides. *Journal of Biological Chemistry* 265:8382-6

Yuen EY, Yan Z. 2009. Dopamine D4 receptors regulate AMPA receptor trafficking and glutamatergic transmission in GABAergic interneurons of prefrontal cortex. *J Neurosci* 29:550-62

Zeng H, Chattarji S, Barbarosie M, Rondi-Reig L, Philpot BD, et al. 2001. Forebrain-specific calcineurin knockout selectively impairs bidirectional synaptic plasticity and working/episodic-like memory. *Cell* 107:617-29

Zhou L, Martinez SJ, Haber M, Jones EV, Bouvier D, et al. 2007. EphA4 signaling regulates phospholipase Cgamma1 activation, cofilin membrane association, and dendritic spine morphology. *J Neurosci* 27:5127-38

Zhou Q, Homma KJ, Poo MM. 2004. Shrinkage of dendritic spines associated with long-term depression of hippocampal synapses. *Neuron* 44:749-57

Zisch AH, Kalo MS, Chong LD, Pasquale EB. 1998. Complex formation between EphB2 and Src requires phosphorylation of tyrosine 611 in the EphB2 juxtamembrane region. *Oncogene* 16:2657-70

Zisch AH, Pazzagli C, Freeman AL, Schneller M, Hadman M, et al. 2000. Replacing two conserved tyrosines of the EphB2 receptor with glutamic acid prevents binding of SH2 domains without abrogating kinase activity and biological responses. *Oncogene* 19:177-87

Zuo Y, Lin A, Chang P, Gan WB. 2005. Development of long-term dendritic spine stability in diverse regions of cerebral cortex. *Neuron* 46:181-9